Clinical Investigation and Genetic Characterization of Congenital Skeletal Dysplasia

By

AMJAD ALI

Faculty of Biological Sciences

Department of Biochemistry

Quaid-i- Azam University, Islamabad

Pakistan

2025

Clinical Investigation and Genetic Characterization of Congenital Skeletal Dysplasia

A dissertation submitted in the partial fulfillment of the requirements for the degree of

DOCTOR OF PHILOSOPHY

in

BIOCHEMISTRY/MOLECULAR BIOLOGY

By

AMJAD ALI

Faculty of Biological Sciences

Department of Biochemistry

Quaid-i- Azam University, Islamabad
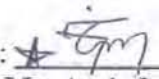
Pakistan

2025

Author's Declaration

I **Mr. Amjad Ali** hereby state that my PhD thesis, titled **"Clinical Investigation and Genetic Characterization of Congenital Skeletal Dysplasia"** is my own work and has not been submitted previously by me for taking any degree from

Department of Biochemistry, Faculty of Biological Sciences, Quaid-i-Azam University, Islamabad, Pakistan.

Or anywhere else in the country/world.

At any time if my statement is found to be incorrect even after my graduation, the University has the right to withdraw my Ph.D degree.
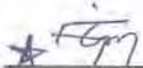
Student/Author Signature:

Mr. Amjad Ali

Date: *January 22, 2025*

Plagiarism Undertaking

I solemnly declare that research work presented in the PhD thesis, titled **"Clinical Investigation and Genetic Characterization of Congenital Skeletal Dysplasia"** is solely my research work with no significant contribution from any other person. Small contribution/help wherever taken has been duly acknowledged and that complete thesis has been written by me.

I understand the zero-tolerance policy of the HEC and **Quaid-i-Azam University, Islamabad,** towards the plagiarism. Therefore, I as an Author of the above titled thesis declare that no portion of my thesis has been plagiarized and any material used as reference is properly referred/cited.

I undertake that if I am found guilty of any formal plagiarism in the above titled thesis even after award of PhD degree, the University reserves the right to withdraw/revoke my PhD degree and that HEC and the University has the right to publish my name on the HEC/University website on which names of students are placed who submitted plagiarized thesis.
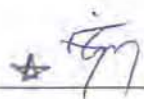
Student/Author Signature:

Mr. Amjad Ali
Date: *January 22, 2025*

Certificate of Approval

This is to certify that the research work presented in this thesis, entitled: "Clinical Investigation and Genetic Characterization of Congenital Skeletal Dysplasia" was conducted by **Mr. Amjad Ali** under the supervision of Dr. Imran Ullah.

No part of this thesis has been submitted anywhere else for any other degree. This thesis is submitted to the Department of Biochemistry, Faculty of Biological Sciences, Quaid-i-Azam University, Islamabad, Pakistan in partial fulfillment of the requirements for the **Degree of Doctor of Philosophy** in the field of Biochemistry from Department of Biochemistry, Faculty of Biological Sciences, Quaid-i-Azam University, Islamabad, Pakistan.

Mr. Amjad Ali   Signature: _____

Examination Committee:

1. **External Examiner:**   Signature: _____
   Dr. Shaheen Shahzad
   Assistant Professor
   Department of Bioinformatics & Biotechnology
   International Islamic University, Islamabad

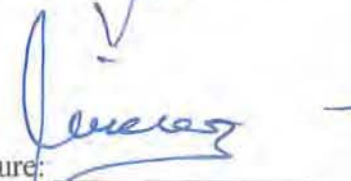2. **External Examiner:**   Signature: _____
   Dr. Muhammad Ramzan Khan
   Principal Scientific Officer
   National Agricultural Research Center
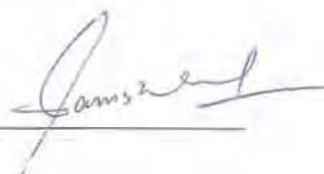   NARC, Islamabad

3. **Supervisor:**   Signature: _____
   Dr. Imran Ullah

4. **Chairperson:**   Signature: _____
   Prof. Dr. Samina Shakeel

Dated: _____   _____22-01-2025_____

SPECIAL DEDICATION

TO

THE GREAT BACHA KHAN

MY FATHER, KHAN TAREEN

MY MOTHER AND SISTER

MY BROTHER, FAROOQ ALI TANOLI

AND

ALL FAMILY MEMBERS

WHOSE LOVE AND SUPPORT LEAD ME TO SUCCESS AT

EACH STEP OF MY LIFE

Chapter 1

Chapter 2

Chapter 3

Chapter 4

Chapter 5

Chapter 6

Chapter 7

Chapter 8

Chapter 9

ACKNOWLEDGEMENT

List of Figures

List of Tables

Table No.	Title	Page No
Table 2.1	**List of Primers**	**39**

List of Abbrevations

AER	Apical Ectoderm Ridge
AJ	Ashkenazi Jewish
AMD	Acromesomelic Dysplasia
AMDG	Acromesomelic Dysplasia-Grebe type
AMDH	Acromesomelic Dysplasia-Hunter and Thompson type
AMDM	Acromesomelic Dysplasia- Maroteaux type
AMDP	Acromesomelic Dysplasia-PRKG2 type
AP	Anterior-posterior
ARSB	Arylsulphatase-B
BB	Basal Body
BBS	Bardet-Biedl Syndrome
BMP's	Bone morphogenetic factors
BMPR1B	Bone Morphogenetic Protein Receptor-1B
C6ST-1	Carbohydrate-6-O-sulfotransferase-1
CDMP1	Cartilage- derived morphogentic protein-1
CHD	Coronary Heart Disease
CHST3	Carbohydrate Sulphotransferase-3
CLS	Cenani-Lenz Syndactyly
cM	Centimorgan
CNP	C-type Natriuretic Peptide
CNS	Central Nervous System
COL2A1	Collagen type II-alpha 1
CS	Chondroitin Sulphate
DNA	Deoxy Ribonucleaic Acid
dNTP	Deoxy ribonucleo triphosphate
DS	Dermatan Sulphate

DVL	Dishevelled
EB	Elution Buffer
ECM	Extracellular Matrix
EDTA	Ethylene diamine tetra-acetate
ER	Endoplasmic Reticulum
EtBr	Ethidium Bromide
EVC	Ellis van Creveld disease
FBLN1	Fibulin-1
FGF	Fibroblast Growth Factor
FGFR	Fibroblast Growth Factor Receptor
Fgfr	Fibroblast Growth Factors Receptor
FMN1	Formin-1
FZ	Frizilled
GAG's	Glycosaminoglycans
GALNS	Galactosamine-6-Sulphate Sulphatase
GC	Guanylyl cyclase
GDF5	Growth Differentiation Factor-5
GJA1	Gap junction alpha-1
GLB1	Galactosidase-β1
GLI3	GLI-Kruppel family member-3
GME	Greater Middle East
gnomAD	Genome Aggregation Database
GNPTAB	N-acetylglucosamine (GlcNAc) -1-phosphotransferase-αβ
GNPTG	*N*-acetylglucosamine (GlcNAc)-1-phosphotransferase-γ
GUSB	β -Glucoronidase
HAND2	Heart- and neural crest derivatives-expressed protein-2
HGMD	Human Gene Mutation Database

HOX	Homeobox
HS	Heparin Sulphate
HYAL1	Hyaluronoglucosaminidase-1
IDS	iduronate-2-sulfatase
IDUA	α-1- iduronidase
IFT	Intraflagellar Transport
IHH	Indian Hedgehog
IRB	Institutional Review Board
ISS	Idiopathic Short Stature
KHD	Kinase Homology Domain
KPK	Khyber Pakhtunkhwa
KS	Keratin Sulphate
LMBR1	Limb region 1 protein homolog
Lmx-1	LIM- homeobox transcription factor-1
LRP4	low density lipoprotein receptor-related protein 4
LSD's	Lysosomal Storage Diseases
MAF	Minor Allele Frequency
MCOLN1	Mucolipin-1
Meis-1	Myeloid ectropic viral insertion site-1
ML	Mucolipidosis
MPS	Mucopolysaccharidosis
mTORC1	Mammalian Target of Rapamycin-1
NEU1	Neuroaminidase-1
NIH	National Institute of Health
NPRB	Natriueritc Peptide Receptor-B
NXN	Nucleoredoxin
OCD	Osteochondrdysplasia

ODDD	Oculodentodigital Dysplasia
OFDS	Orofacial Digital Syndrome
OMIM	Online Mendelian Inheritance in Man
PAGE	Polyacrylamide Gel Electrophrosis
PC	Procollagen
PCR	Polymerase Chain Reaction
PD	Proximal-distal
PK	Proteinase-K
PPCA	Protective protein/cathepsin A
PPD2	Preaxial Polydactyly type II
PZ	Polarizing Zone
RA	Retinoic Acid
ROR2	Receptor Tyrosine kinase-like Orphan receptor-2
RS	Robinow syndrome
SD	Syndactyly
SDS	Sodiaum dodecyl sulphate
SED	Spondyloepiphyseal dysplasia
SEDC	Spondyloepiphyseal dysplasia congenita
SEDL	*Sedlin*
SEDT	Spondyloepiphyseal dysplasia tarda
Sfrp's	Secreted frizzled related proteins
SHH	Sonic Hedgehog
SMO	Smoothened
SPD	Synpolydactyly
SRTDs	Short-rib Thoracic Dysplasias
TANGO1	Transport and Golgi Organization-1
TBE	Tris Boric EDTA

Tbx	T-box gene
TE	Tris-EDTA
TFEB	Transcription factor EB
TGF-β	Transforming Growth Factor-beta
TOPMed	Trans-Omics for Precision Medicine
TP-63	Tumor Protein-63
TRAPPC2	Trafficking protein particle complex subunit 2
TRP	Transient Receptor Potential
UV	Ultraviolet
VD	Ventral-Dorsal
WAD	Weyers acrodental dysostosis
WB	Washing Buffer
WES	Whole Exome Sequencing
WNT	Wingless-Integration-1
ZD	Zygodactyly
ZPA	Zone of Polarizing Activity
ZRS	ZPA Regulatory Sequence

Abstract

Human skeletal dysplasia is a heterogenous and complex group of congenital bone diseases, caused by mutations in genes involved in embryonic development of skeletogenesis. It affects axial, appendicular as well as craniofacial skeleton, both in terms of phenotypes and number of bones.

In the present research study, thirteen families, exhibiting various forms of congenital skeletal dysplasia were investigated at clinical and molecular level to identify diseases causing variants. All the families were sampled from district Swabi, Khyber Pakhtunkhwa, Pakistan. After getting informed consent, pedigrees were drawn and blood was collected in EDTA tubes. X-rays were then taken from affected family members in local hospital to assess disease phenotype. DNA was extracted from available family members using either Chloroform-Phenol method or commercially available kit. DNA of one affected member from each family (except family L &M) was proceeded for whole exome sequencing and identified pathogenic variant was segregated using Sanger sequencing. In family L & M, highly polymorphic microsatellite markers-based homozygosity mapping was performed and the linked genes were Sanger sequenced to identify disease causing variant.

Genetic analysis identified reported variants in *BBS5, EVC, IDUA, GALNS, CHST3, HOXD13, GJA1* and *NPR2* genes, while novel variants in *ROR2, GNPTG, NPR2* and *BMPR1B* genes. Sanger sequencing confirmed segregation of pathogenic variants in respective family members.

The identified variants expand mutational and clinical spectrum of congenital skeletal dysplasia in Pakistani families, which will further help in future diagnosis and genetic counseling.

The research work presented in thesis has been published in reputed scientific journals.

1. Sequence variants in different genes underlying Bardet-Biedl syndrome in four consanguineous families. **Ali, A,** Abdullah,....Wasim Ahmad* (2023). *Mol Biol Rep*

2. Clinical and Genetic Investigation of Fourteen Families with Various Forms of Short Stature Syndromes. Fati Ullah…….**Amjad Ali**…..Wasim Ahmad* (*Clinical Genetics*. 10.1111/cge.14550).

3. Phenotypic demarcation of a complex disorder in a family with a homozygous variant in EVC and a heterozygous variant in ROR2 gene. **Amjad Ali*,** Shabir Hussain, Petra Loid, Safeer Ahmad, Mari Muurinen, Imranullah, Wasim Ahmad, Outi Makitie (**Write up**).

4. Clinical and Molecular Characterization of Acromesomelic Dysplasia-Maroteaux Type in Pakistani Families. **Amjad Ali***,… Outi Makitie, Wasim Ahmad, Imran Ullah. (**Write up**).

5. Sequencing BMPR1B Gene in Consanguineous Pakistani Families Exhibiting Acromesomelic Dysplasia- Grebe Type. **Amjad Ali*,….** Imran Ullah. (**Write up**).

6. Clinical and Molecular Studies of Lysosomal Storage Diseases in Consanguineous families. **Amjad Ali**, Shabir Hussain, Wasim Ahmad, Imranullah. (**Write up**).

Introduction

The human skeleton is composed of bones, cartilage, ligaments, tendons and joints. Most of the adult human skeleton is composed of bone, hard, dense connective tissue composed of osteoblasts, osteoclasts, and osteocytes. On the other hand, cartilage is soft and flexible, made up of only chondrocytes. Bones and cartilage collectively give shape and form to the human skeleton (Waldmann *et al.,* 2022). The key function of the human skeleton is to act as a frame for body upright position, locomotion, and movement; however, it also provides protection to vital organs (lungs, heart, and brain). The skeleton is the repertoire for blood cells formation (Taichman. 2005; Lee and Karsenty. 2008), a storehouse for calcium and phosphorus that are involved in bone homeostasis and endocrine regulation (Blottner *et al.,* 2006).

The Human skeleton is derived from three different embryonic lineages; somites, lateral plate mesoderm, and neural crest. In the developing vertebrate embryo, ectoderm and mesoderm produce multipotent mesenchymal cells that migrate to particular parts of the body and begin the process of skeletogenesis (Erlebacher *et al.,* 1995). The mesenchymal cells continue to differentiate into three distinct cell types, chondrocytes, osteoclasts, and osteoblasts. The maturation and proliferation of chondrocytes and their replacement by bone is a highly regulated processes in the growth plate. The skeletogenic cells then initiate osteogenesis (the production of bones) through two processes: endochondral ossification and intramembranous ossification, which both involve the direct conversion of osteoblasts to the bone matrix (de Baat *et al.,* 2005). Endochondral ossification involves the replacement of chondrocytes by osteoblasts as a result of differentiation, proliferation, and hypertrophy (Kornak and Mundlos. 2003) and is responsible for the growth of long bones. Intra-membranous ossification involves the direct differentiation of mesenchymal cells into osteoblast cells of bones (Savarirayan and Rimoin. 2002). The bones of the craniofacial skeleton and some of the clavicle are generated by intramembranous ossification. Through these comprehensive mechanisms, a skeleton is formed as a result of a process of growth and remodeling (Zelzer and Olsen. 2003).

Human Skeleton

The Human skeleton is composed of 206 different bones (126 appendicular, 74 axials and 6 ossicle bones). Human skeleton has been divided into three types, i.e. axial skeleton, appendicular skeleton, and craniofacial skeleton (Savarirayan and Rimoin. 2002).

a. Axial Skeleton

Human axial skeleton consists of a vertebral column and rib cage (sternum, vertebrae, and ribs) (Tyl *et al.,* 2007). The vertebral column is composed of 24 vertebrae and the sacrum and coccyx, which support the upright position of the body and cushions the delicate and soft spinal cord. The rib cage comprises 12 rib pairs and a sternum that surrounds vital organs i.e. the heart, stomach, lungs, and other thoracic organs. The bones of the axial skeleton elements work together and form the structural framework to support the body, allow us to stand upright, and enable movement (Aguirre *et al*., 2014).

b. Appendicular Skeleton

The appendicular skeleton is comprised of upper and lower extremities, which include, hands and feet, pectoral girdle and pelvic girdle. The appendicular skeleton of an adult human is composed of 126 bones. The appendicular skeleton is important for the movement and support of the body. It allows us to walk, run, jump, and perform a wide range of other routine activities. Mechanical tensions are conveyed at pectoral and pelvis girdles connecting the axial and appendicular skeletons. The pectoral girdle contains a clavicle (collar bone) and scapula that connect both upper extremities to the thoracic cage of the axial skeleton, whereas pelvic girdle is made up of hip bones (ilium, ischium, and pubis), which further link the vertebral column to the lower extremities (Docherty. 2007).

The upper limb is made up of the pectoral girdle (scapula and clavicle), humerus, ulna, and radius, 8 carpals, 5 metacarpals, and 14 phalanges. Similarly, the lower extremity consists of the pelvic girdle, femur, patella (knee cap), tibia and fibula, 7-tarsals, 5 metatarsals, and 14-phalanges in the toes. The intricate anatomy of the foot,

ankle, and rest of the lower limbs work together to effectively support the body's weight and enable locomotion.

c. Craniofacial Skeleton

The human craniofacial skeleton is composed of a skull and facial bones. The human skull is an intricate structure, made up of 22 distinct bones, 20 deciduous bones, and 30 permanent teeth. The craniofacial skeletal tissues are derived from the neural crest, which develops from a cranial part of the neural plate during early embryogenesis. Various functions of neural crest cells include synchronization of diverse visceral activities, such as peripheral nervous system, protection of the body against external influences, and involvement in the development of craniofacial skeleton (Le Douarin *et al.,* 2004).

Human skull is made up of viscero-cranium, and neuro-cranium, derived from neural crest. Temporal, frontal, parietal, occipital, and sphenoid bones contribute to the development of the neurocranium, which covers and protects the brain and sense organs. Furthermore, the viscero-cranium consists of the maxilla, mandible, zygoma, and nasal bones, as well as the temporal, pharyngeal, palatal, and auditory bones.

Limb Development in Vertebrates

During embryonic development, mesenchymal cells of the mesoderm play a key role in skeletogenesis. Mesenchymal cells from lateral plate mesoderm, paraxial mesoderm, neural crest, and sclerotomes form cell aggregates at specific sites to make skeletal elements of the axial, appendicular, and craniofacial skeleton (Olsen *et al*., 2000).

Limb Bud Initiation

In vertebrates, limb bud formation is initiated by the localized proliferation of lateral plate mesodermal cells (Harrison. 1918). These cells interact with ectoderm and mesoderm through T-Box transcription factors, WNT's, retinoic acid, and FGF to form 3D patterning [anterior-posterior (AP), proximal-distal (PD), and ventral-dorsal (VD) axes] of limb buds (Zeller *et al*., 2009; Geetha-Loganathan *et al*., 2008; Duboc and Logan. 2011). Wolpert in 1969 showed that the appropriate position of fingers (thumb, middle finger, ring finger, and little finger) results from signaling cascades that are received by limb bud during development.

Apical Ectodermal Ridge (AER), polarizing zone (PZ), and ectoderm establish proximo-distal, anterio-posterior, and dorso-ventral axes in limb bud by receiving positional signals (Saunders. 1977; Tickle and Eichele. 1994), Different signaling molecules (fibroblast growth factors, Wnts, Hedgehogs and bone morphogenetic proteins) bind to cell surface receptors to induce the expression of developmental stage-specific genes (*HOX, TBX*, *MEIS*, *SPALT,* and *LMX1*). The three signaling centers that are key players in the 3D patterning of developing limb bud are as follows:

a. Polarizing Zone Signaling

Saunders (1977) for the first time showed the signaling properties of posterior rim of limb bud mesenchyme, known as the polarizing zone (PZ). Polarizing zone is enriched in retinoic acid (RA) (Thaller and Eichele. 1987), as these mesenchymal cells contain retinal dehydrogenase to convert retinal into retinoic acid (Swindell *et al.,* 1999). Retinoic acid causes patterning of proximal limb structures (humerus, femur, and girdles), because no limb bud outgrowth takes place in the presence of RA antagonists or by causing inactivation of the retinal dehydrogenase gene (Helms *et al*., 1996; Stratford *et al*., 1996; Niederreither *et al*., 1999). PZ also expresses sonic hedgehog (*SHH*) and bone morphogenetic proteins (BMPs), and together with retinoic acid constitute a signaling pathway. RA induces *SHH* expression, which then causes *BMP's* expression to form anterio-posterior patterning of the digits (Yang *et al*., 1997; Drossopoulou *et al*., 2000). It seems that the number of digits is determined by Shh (Capdevila and Belmonte. 2001) and digit identity by BMPs, as these convey positional information. RA, SHH and Bmp's pattern the proximal, middle and distal limb structures, as Shh null mice do not show any distal limb segments (Tucker *et al*., 1998). The sonic hedgehog (*SHH*) expression by mesenchymal cells adjacent to zone of polarizing activity (ZPA) is controlled by GLI-Kruppel Family Member-3 (*GLI3*) interaction with transcriptional regulators, *HOX* and *HAND2*. Shh induces *Fgf-4* expression in AER by blocking the effect of BMPs through *GREMLIN1 (GREM1)* and upregulating the AER-FGF signaling pathway (Niswander *et al*., 1994; Laufer *et al*., 1994; Zuniga *et al*., 1999; Zeller *et al*., 2009) to control anteroposterior polarity. The interaction between AER and PZ determines proximadistal polarity. Dorsoventral

polarity is determined by non-AER ectoderm signals, i.e., BMP's and Engrailed 1 from the ventral ectoderm while *Wnt7A* from the dorsal ectoderm.

b. Apical Ectodermal Ridge Signaling

The signals: specifically, *BMP4* signals from underlying mesenchymal cells induce ectoderm to elongate along anterior-posterior axis of limb bud to form AER, and its regulation (Benazet *et al*., 2009).

AER has a key role in maintaining limb bud outgrowth (Saunders. 1972) and the patterning along the proximal-distal axis (Saunders and Gasseling. 1968; Summerbell *et al*., 1973; Zeller *et al*., 2009; Towers and Tickle. 2009). The otic vesicles in the AER (Wilkinson *et al*., 1989) express fibroblast growth factors, *FGF's*, namely *FGF-4,8,9,10*, and *19* (Suzuki *et al*., 1992; Niswander and Martin. 1992), to induce the underlying mesenchymal cells near to AER in an undifferentiated, proliferating state (progress zone/PZ), while the proximal cells are in a differentiated state (Summerbell. 1973). The posterior mesenchymal cells of limb bud, known as ZPA, are destined for anterior-posterior polarity (Saunders and Gasseling. 1968).

Fibroblast growth factors expression in developing limb bud development is stage-specific, i.e., *FGF-8, FGF-10* are expressed at the early stage, while *FGF-4, FGF-9, and FGF-19* at the later stage in posterior structures to control the growth and morphogenesis of skeletal elements. Any sort of mutation in these signaling molecules and receptors may result in severe skeletal defects, for instance, a conditional knockout of *Fgf-8* affects anterio-proximal structures. Similarly, *Fgf-10* null mice and functionally inactivated *Fgfr2iiib* mice have either no limbs or are very short. Mutations in *FGFR1, FGFR2,* and *FGFR3* exhibit Pfeiffer syndrome, Apert syndrome, and achondroplasia, respectively (Sargar *et al*., 2017).

AER has a high concentration of *Tp63* for the maintenance of central limb rays, and any failure may lead to truncated skeletal elements; stylopod, zeugopod and autopod. It means that the sophisticated interaction between ZPA and AER is essential for the growth and coordinated patterning of developing limb bud (Vogel and Tickle, 1993) along with the downstream patterning genes (Laufer *et al*., 1994).

c. Ectodermal Signaling

Wnt-signaling proteins are expressed in the ectoderm as well as in the mesenchyme, just like FGF's, and are responsible for the dorso-ventral polarity of limbs. Recent research suggests that *FGF's* are expressed by *WNT's,* expressed in mesenchyme (Kawakami *et al*., 2001). *WNT5A* knockout mice have severely affected distal structures, with the absence of distal phalanges in digits (Yamaguchi *et al*., 1999), while *WNT7A* knockout mice show a double ventral phenotype in paws (Parr and McMahon. 1995). Secreted frizzled related proteins (Sfrp's) control the morphogenetic gradients/ zones of Wnt signaling activity (Lee *et al*., 2000), and are necessary for normal elongation of the anterior-posterior axis and somitogenesis (Satoh *et al*., 2006). Sfrp's acting as an inhibitor of apoptosis by blocking Wnt-dependent activation of BMP-mediated apoptosis (Lee *et al*., 2000; Satoh *et al*., 2008).

Despite this intricate network of signaling in developing limbs, any type of mutation/alteration in transcription factors, RNA processing machinery, cellular transporters, extracellular matrix proteins, ion channels, enzymes, signaling molecules, and cilia result in skeletal dysplasia, which includes, syndactyly, polydactyly, dwarfism, spondyloepiphyseal dysplasia, etc.

Congenital Skeletal Dysplasia

Skeletal dysplasia (also known as osteochondrodysplasia) is group of genetically inherited complex and heterogeneous disorders, affecting growth, maintenance, and development of human skeletal elements. Congenital skeletal dysplasia is characterized by dysmorphology in skeletal elements, caused by mutations in genes involved in chondrogenesis and/or osteogenesis. These mutations may either lead into osteochondrodysplasia and dysostosis. Skeletal dysplasias are associated with dysmorphology of the axial and appendicular skeleton, its size, and its arrangement. Osteodysplasia results from defects in bone mineralization; i.e., osteoporosis and osteopenia (Hurst *et al*., 2005). On the other side, chondrodysplasia is due to defects in cartilaginous components of skeleton (Mortier. 2001). Skeletal disorders are either non-syndromic (isolated) or syndromic (complex syndromes) and inherited in

autosomal dominant, recessive, X-linked, or *de novo* forms (Abbas *et al.,* 2023; Baldridge *et al.,* 2010).

According to the latest Nosology classification (2023), 771 bone disease have been identified and characterized, caused by pathogenic mutations in 552 genes. These skeletal disorders have been re-categorized into 41 different groups (Unger *et al.,* 2023) as compared to the previous classification; 42 groups.

Ciliopathies

Ciliopathies are rare genetic disorders characterized by structural or functional abnormalities in the primary cilium, a sub-cellular organelle ubiquitously found on the surface of all types of cells (Turan *et al*., 2023). The primary cilium plays a crucial role as a cellular hub in the cilia due to the remarkable intricacy of their interconnected signaling pathways. The cilium is a hair-like organelle with a microtubule backbone known as an axoneme, along with a basal body (BB) that provides the base to dock the cilium in the cell. The intraflagellar transport (IFT) molecules are also present, which are regulated in a bidirectional fashion along the microtubule backbone and carry out the essential proteins for ciliogenesis (Quadri & Upadhyai. 2023). These particles play a significant role in cilia-mediated signaling pathways. Ciliopathies are classified into two main types: namely motile ciliopathies which include pulmonary disease, and infertility, while primary ciliopathies, encompass diverse diseases, ranging from organ-specific disorders to multiorgan involvement (Wheway *et al*., 2019). Ciliopathies exhibit significant clinical and genetic heterogeneity, with the alteration of genes resulting in varied involvement of various organs, including the kidneys, retina, central nervous system (CNS), skeleton, and liver (Waters & Beales. 2011).

Classification of Ciliopathies

Ciliopathies have been classified into following sub-groups, depending upon organ involvement.

- Retinal ciliopathies
- Renal ciliopathies
- CNS-related ciliopathies
- Ciliopathies with skeletal involvement

Ciliopathies with skeletal involvement

The category of disorders is distinguished by its varying severity, which ranges from moderate to severe or even deadly characteristics. It has been divided into two groups: major skeletal system involvement, which includes craniofacial, thoracic cage, and long bones involvement, identified as short-rib thoracic dysplasias (SRTDs), with/without polydactyly or ciliary chondrodysplasia, and OFDS, with milder skeletal involvement. IFT and Hh pathways play major role in the intricate process of skeletogenesis. Indian hedgehog (IHH) signaling disruption in the chondral primary cilia impacts chondrocyte development during ossification (Quadri & Upadhyai. 2023). As a result, there may be a variety of skeletal anomalies, such as polydactyly, reduction of the rib or extended bones, and craniofacial abnormalities. On the other hand, a lack of proper regulation of IFT can reduce the transportation of transmembrane SMO receptors, which can cause chondrocytes to differentiate prematurely and reduce proliferation, which may lead to SRTDs and abnormalities in long bone growth plates. The milder abnormalities include Ellis-van-Creveld syndrome (EVC; MIM, 2255000), identified by ectodermal abnormalities, polydactyly, short ribs, and disproportionately short limb dwarfism; Weyers acrodental dysostosis (WAD; MIM, 193530); with moderate short stature, postaxial polydactyly, nail and dental anomalies, and Sensenbrenner syndrome (MIM, 218330); incolving skeletal abnormalities, and ectodermal anomalies along with kidney and liver failure (Pei & Chung, 2022).

Bardet-Biedl Syndrome

Bardet-Biedl Syndrome (BBS) is very rare (1:13,500-160,000) and heterogeneous disease in terms of molecular diagnosis and clinical phenotypes (Forsythe and Beales, 2013). Laurence and Moon (1866) for the first time reported clinical and phenotypic features of BBS (obesity, mental retardation, and retinitis pigmentosa). Later on, Georges Bardet (1995) and Arthur Biedle (1995) separately described the aforementioned phenotypes along with post-axial polydactyly.

Due to its pleiotrophic nature, there is phenotypic variation at the intra and inter-familial level (Riise *et al*., 1997; Water & Beales. 2003). The prevalence frequency varies among various geographical regions (Klein & Ammann. 1969). In Europe and

North America, prevalence rate is 1/120,000 to 1/160,000 in live birth, respectively (Beales *et al*., 1997). BBS is most common in communities where consanguinity is high, i.e., isolated Arab population of Kuwait (1/36,000), 1/6900 in district Jahara, Bedouins (1/13,500) (Farag & Teebi. 1989), 1/18000 in island of Newfoundland (Moore *et al*., 2005), and 1/3700 in Forae Islands (Hjortshøj *et al*., 2009). BBS is inherited in autosomal recessive form, but can also show triallelic pattern (Katsanis *et al*., 2001; Chen *et al*., 2011).

Clinical phenotypes of BBS have been characterized into primary and secondary features. Primary phenotypes may include postaxial polydactyly, truncal obesity, hypogonadism, rod-cone dystrophy, cognitive impairment, and renal abnormalities (renal cystic dysplasia, anatomical malformation) (Putoux *et al*., 2012). Secondary features include diabetes mellitus, delayed growth, speech impairment and psychomotor delay, hearing loss, liver abnormality, strabismus, cardiac malformations, and dental abnormality.

To date 25 causative genes have been reported to cause BBS, accounting for about 80% of BBS diagnosis (Dehani *et al*., 2021; Gupta *et al*., 2022). These genes are involved in the formation (assembly and maintenance) or functioning of cilia, which is the reason why clinical features of BBS patients overlap with other ciliopathies, i.e., McKusick-Kaufmann syndrome, Joubert syndrome, Alstrom syndrome, Senior-Løken syndrome, Mainzer-Zaldino syndromes, and Meckel-Gruber syndrome (Wheway *et al*., 2019).

BBS proteins are involved in proper formation of BBsome, chaperonin, and other proteins. The BBsome is comprised of 8 proteins (BBS1, BBS2, BBS4, BBS5, BBS7, BBS8, BBS9 and BBS18/BBIP10). BBSome is essential for anterograde and retrograde transportation of vesicular components and molecular cargo along the primary cilium (Nachury *et al*., 2007; Loktev *et al*., 2008; Wei *et al*., 2012).

Besides BBsome, there is a chaperonin homology complex comprised of three BBS proteins (BBS6, BBS10, BBS12), necessary for assembly and stability of BBsome and other BBS proteins (Seo *et al*., 2010). While the remaining BBS proteins interact to these complexes and are involved in ciliary targeting of BBSome and recognition of BBSome cargo (Novas *et al*., 2015), for instance, BBS17 regulates entry of

BBsome into cilia when it is recruited by BBS3. BBS7 is initially stabilized by BBS chaperonins to assemble the BBsome core complex. In cilia, BBSome passes through transition zone/ control barrier, where different protein complexes, i.e., cep290 (NPH5), stabilizes integrity of BBSome. BBS phenotypes arise from defects in any subunit(s) of BBsome, chaperonin homology complex and/or other regulatory/related proteins (Barbelanne *et al*., 2013).

Ellis-van Creveld Syndrome

Ellis-van Creveld syndrome (EvC)/mesoectodemal dysplasia/chondrectodermal dysplasia, is rare congenital skeletal disease. The characteristic clinical features include short stature due to rhizomelic shortening of the upper and lower limbs, congenital heart defects, thoracic cage defects, digits and nail defects, leg and foot defects, and spine defects. (Baker & Beales. 2009; Alves Pereira, Berini-Aytés & Gay-Escoda; Niceta *et al*., 2009; Jan *et al*., 2018; Lauritano *et al*., 2019). The craniofacial abnormalities may include hypoplastic zygomatic bone, frontal bossing, low set ears, dysmorphic philtrum, and tooth abnormalities/hypodontia (Tuna *et al*., 2016; Lauritano *et al*., 2019; Peña-Cardelles *et al*., 2019).

EVC is inherited in autosomal recessive fashion, with a prevalence rate of 7/1,000,000 in general population (Stoll *et al*., 1989), but has a high incidence rate (5/1,000) in the eastern Pennysylvania Amish population (Kamal *et al*., 2013). EvC shares clinical phenotypes (skeletal and cardiac defects) with other syndromes (Smith-Lemli-Opitz syndrome, Hydrolethalus syndrome), and, hence, is sometimes misdiagnosed (Parilla *et al*., 2003; Witters *et al*., 2008; Schramm *et al*., 2009).

EvC is caused by disease-causing mutations in *EvC* and *EvC2* genes, located at chromosomal position 4p16.2, separated by a 2.6Kb genomic region (Ruiz-Perez *et al*., 2000; Galdzicka *et al*., 2002). The *EvC* gene has 21 exons, encoding protein of 992 amino acids, that interact with its homologue EVC2 head-to-head. Both gene products encode type1 transmembrane proteins (Al-Fardan & Al-Qattan, 2017), expressed in bones, lungs and heart (Aziz *et al*., 2016), transducing extracellular signals towards nucleus via hedgehog signaling pathway (Caparrós-Martín *et al*., 2013; Pusapati *et al*., 2014). Both proteins form a complex, called the EvC zone, in primary cilium responsible for intramembranous and endochondral ossification (Dorn *et al*.,2012).

EvC patients have pathogenic variants mostly in *EvC* as compared to *EvC2* (D'Asdia *et al*., 2013). To date, 105 and 124 different pathogenic variants have been reported in *EvC* and *EvC2,* respectively.

Robinow Syndrome

Robinow syndrome (RS) is rare genetic disease, involving short stature, mesomelic shortening of both limbs, facial dysmorphism, congenital heart defects, brachydactyly, vertebral anomalies, and genital defects (Afzal & Jeffery. 2003). The disease was clinically reported for the first time in a multi-generational non-consanguineous family (Robinow *et al*., 1969).

RS is heterogeneous disorder, inherited in autosomal dominant and recessive forms, which can be caused by genes such as *ROR2, DVL1, WNT5A, DVL3, FZD2,* and *NXN* (Zhang *et al*., 2022)*.* Variants in *ROR2* gene cause recessive form of Robinow syndrome. The *ROR2* gene is involved in various basic cellular processes (Afzal and Jeffery. 2003). All the reported genes for RS have functions in non-canonical WNT/Planer Cell Polarity (PCP) signaling pathway (White *et al*., 2018).

RS diagnosis is very challenging as patients exhibit molecular and allelic heterogeneity (White *et al*., 2018; Zhang *et al*., 2021). For instance, AR-RS is caused by loss-of-function mutation in *ROR2* (Oishi *et al*., 2003, Minami *et al*., 2010) and *NXN* (Funato *et al*., 2006, 2008), but some deletion mutations have also been reported (Mazzeu & Brunner. 2020; Zhang *et al*., 2021). On the other hand, AD-RS and sporadic cases of RS are caused by *DVL1/3* (White *et al*., 2018, Bunn *et al*., 2015; White *et al*., 2015; White *et al*., 2016).

Lysosomal Storage Diseases

Lysosomal storage diseases (LSDs) comprises group of about 70 different monogenic inherited metabolic diseases, with an incidence rate of 1/7,700 live births (Hoffmann & Mayatepek. 2005). LSDs are inherited either in autosomal recessive or X-linked recessive form. These are caused by defective lysosomal degradation of glycosaminoglycans, lipids and cholesterol resulting in accumulation. Pathogenic mutation in lysosomal glycosidases, integral membrane proteins, proteases, enzyme modifiers and activators and transporters, resulting in deficiency/malfunctioning of lysosomal enzymes.

LSDs have been further subclassified on the basis of the biochemical nature of the stored molecule, i.e., sphingolipidosis, mucopolysaccharidosis, lipid storage diseases, glycogen storage diseases, post-translational modification defects, integral membrane protein disorders, neuronal ceroid lipofuscinosis, and lysosomal related organelles (Schröder *et al*., 2007; Sleat *et al*., 2009; Palmieri *et al*., 2011; Chapel *et al*., 2013; Di Fruscio *et al*., 2015; Szklarczyk *et al*., 2015). LSDs are heterogeneous both phenotypically and genotypically but share some overlapping characters visceromegaly/ spleeno-hepatomegaly and neurodegeneration (Parenti *et al*., 2015).

Mucopolysaccharidosis

Mucopolysaccharidosis (MPS) is genetic disorder, caused due to defective breakdown of glycosaminoglycans (GAGs), composed of repeating subunits of sulfated galactose and hexosamine. Their primary function is the formation of bone, cartilage, skin, connective tissues, and corneas. These GAGs may include four types of mucopolysaccharides; heparin sulphate (HS), keratin sulphate (KS), chondroitin sulphate (CS) and dermatan sulphate (DS). Lysosomal enzymes have key role in GAGs degradation and, hence, help in normal functioning. Any type of genetic defect in these lysosomal enzymes disturbs the normal degradation of GAGs and their accumulation in lysosomes, affecting normal function of cells, tissues, and organs. These accumulated GAGs are then moved into the bloodstream and, with the help of urine, move out of the body (Khan *et al*., 2017). High levels of GAGs cause developmental defects in bones and cartilage and bone ossification. These disruptions then lead to a unique structural dysplasia. The overall incidence rate of MPS is 1 out of 25,000 live births (Tomatsu *et al*., 2019**).**

Classification of Mucopolysaccharidosis

Mucopolysaccharidosis is inherited either in recessive fashion; may be either autosomal or X-linked. Based upon the genetic defects in particular genes, their associated clinical phenotypes, and their severity, MPS is further divided into seven types; MPSI, MPSII, MPSIII, MPSIV, MPSVI, MPSVII and MPS IX. In Pakistan, MPS I is present most frequently, then MPS IV and MPS III, while MPS II is very rare (Cheema *et al*., 2017). Most of the clinical features of MPS subtypes overlap with each other; i.e., dwarfism, short trunk, coarse face, kyphosis, scoliosis, pectus

carinatum, joint contractures, corneal clouding, mental and growth retardation, and macrocephaly (Neufeld. 2001; Muenzer. 2004). (Fesslova *et al.*, 2009; Stapleton *et al.*, 2017).

MPS Type I is due to mutation in *IDUA* gene, located at 4p16, codes for α-1-iduronidase (IDUA) enzyme. MPS1 is further divided into three different syndromes; Hurler (MPS1-H), Hurler-Scheie (MPS1-HS), and Scheie (MPS1-S) (Ganesh *et al.*, 2013). MPS type II (Hunter syndrome) occurs due to a mutation in *IDS* gene at Xq28; encoding iduronate-2-sulfatase (I2S). MPS II shows an X-linked inheritance pattern, affecting mostly males (Tomatsu *et al.*, 2019). MPS type III (Sanfilippo syndrome) is caused by mutations in heparan-N-sulfatase, α-N-acetyl glucosaminidase, α-glucosaminidase-acetyltransferase, and N-acetyl-glucosamine-6-sulfatase (Ozkinay *et al.*, 2021).

MPS type IV (Morquio syndrome) is divided into two subtypes (MPS-IVA and MPS-IVB) caused by mutations in *GALNS* and *GLB1*gene, respectively. MPS type VI is rare lysosomal storage disorder caused by mutational defects in *ARSB* (chromosomal position 5q11) (Ganesh *et al.*, 2013). MPS type VII (Sly syndrome) is a heterogeneous and rare GAGs storage disorder. MPS VII is caused by mutation in *GUSB* gene (chromosomal position7q11) (Ganesh *et al.*, 2013). MPS IX (Natowicz syndrome) occurs due to mutational defects in the *HYAL1* gene (cytogenetic position 3p21) (**Ganesh *et al.*, 2013**). Only four cases of MPS IX have been reported in literature so far.

Mucolipidosis

Mucolipidosis (ML) is a lysosomal storage disease, characterized by coarse face, bulbous nose, gingival hyperplasia (Sprigz *et al*, 1978), prominent forehead, puffy eyelids, epicanthus, a flat nasal bridge, anterverted nostrils, and macroglossia (Nishimura *et al*, 2002). ML patients have either not enough enzymes or harbor genetic defects, producing abnormal enzymes, and, hence, materials are stored in organs (brain, bones, visceral organs, muscle cells), causing skeletal deformity, mental retardation and abnormal functions of liver, heart, spleen and lungs (https://www.ninds.nih.gov/Disorders/Patient-Caregiver-Education/Fact-Sheets/Mucolipidoses-Fact-Sheet (accessed on 29 July 2020).

ML is further divided into four subtypes; ML-I, II, III, and IV, on the basis of the genes (enzymes) involved. ML-1/ Sialidosis, is rare, autosomal recessive lysosomal disease (1/250,000-1/2,000,000 live births) (Loren *et al*., 2005). ML-I is caused by deficiency of neuroaminidase-1, encoded by *NEU1* gene, resulting in sialylated glycoconjugates accumulation (Schiff *et al*., 2005). ML-1 is further classified into normomorphic type-1 and dysmorphic type-II. Sialidosis type-I phenotypes (myoclonus, visual impairment, gait abnormality, seizures, and cerebellar ataxia), while Sialidosis type-2 is usually diagnosed either at birth or in early infancy due to the severity of clinical features (coarse faces, skeletal dysplasia) along with aforementioned phenotypes (d'Azzo *et al*., 2015).

Mucolipidosis-II/Inclusion Cell Disease (Leroy & DeMars. 1967) or MLII α/β (Cathey *et al*., 2008) is the most severe form of ML. MLII is caused by mutation in *GNPTAB*, encoding α/β subunit of N-acetylglucosamine (GlcNAc) -1-phosphotransferase (Tiede *et al*., 2005). ML-II is clinically characterized by different skeletal deformities, i.e., craniosynostosis, rickets, kyphosis, thoracic deformity, hip dysplasia, dysplasia of long tubular bones, joint contractures, and clubfeet. Additional features include osteopenia, dystosis multiplex, which results in oar-shaped ribs, bullet shaped phalanx, iliac flaring, metacarpal pointing (David- Vizcarra *et* al., 2010; Velho *et al*., 2019; Ammer *et al*., 2020; Dogterom *et al*., 2021; Ammer *et al*., 2022), hepato and spleenomegaly, gingival hyperplasia, cardiac and respiratory complications.

MLII patients develop signs both at prenatal and neonatal stages. The prenatal symptoms include short and/or curved bones and, sometimes, bone fractures (Yuksel, Kayserili & Gungor 2007; Heo *et* al., 2012; Aggarwal *et al*., 2014; Alegra *et al*., 2014; Yang *et* al., 2017; Costain *et al*., 2018; Velho *et al*., 2019). Children with MLII usually fail to thrive and develop at neonatal stages, with a median age of death of 1.8 years (Dogterom *et al*., 2021), due to cardiac and respiratory complications. The symptoms become more evident at postnatal stages (1-2 years), where patients develop corneal clouding and short truck dwarfism. MLII patients have an IQ below 85 (Cathey *et al* 2010), mental disabilities, and delayed development of cognitive functions (Kollmann *et al* ., 2012; Idol *et al* ., 2014; Shibazaki *et al*., 2016; Velho *et al*., 2019; Favret *et al*., 2020; Dogterom *et al*., 2021; Di Lorenzo *et al*., 2021).

Mucolipidosis-III (ML-III)/pseudo-Hurler polydystrophy (Spranger & Wiedemann. 1970), ML-IIIA, ML-IIIC/ MLIIIα/β, and MLIIIγ (Cathey *et al*., 2008) is milder form of ML-II as the clinical features of patients are less severe. ML-III is caused by mutation in *GNPTG*, encoding for *N*-acetylglucosamine-1-phosphotransferase (GlcNAc-1-phosphotransferase). Characteristic phenotype, may include skeletal dysplasia, short stature, joint stiffness, waddling gait, spinal deformity and pain in hands, shoulder and hip, corneal clouding, mental retardation, and learning disability (Spranger & Wiedemann. 1970; Velho *et al*., 2019). Additional features may include cardiopulmonary complications, e.g., pneumonia, bronchitis, otitis media and cardiac valvular diseases (Spranger & Wiedemann. 1970; Liu *et al*., 2016; Oussoren *et al*., 2018; Tüysüz *et al*., 2018).

Human N-acetylglucosamine (GlcNAc) -1-phosphotransferase consists of six subunits (α2β2γ2) (Kudo *et al*., 2005; Tiede *et al*., 2005). *GNPTAB* (Chr 12q23.3) (Kudo *et al*., 2005) encodes for αβ subunits, while *GNPTAG* (Chr 16p13.3) (Raas-Rothschild *et al*., 2000) encodes for γ-subunit. Mutations in *GNPTAB* (catalytic domain) cause MLII & MLIIIA, and *GNPTG* (substrate recognition and sorting) cause MLIIIC. MLII patients have a complete or near complete deficiency of GlcNAc-1-phosphotransferase, while MLIIIA and MLIIIC has reduced activity (Kornfeld & Sly.1985).

Unlike other lysosomal enzymes, which are involved in a single catabolic pathway, MLII & III cause the mis-sorting, secretion and accumulation of about 70 different types of acid hydrolases in extracellular spaces. Consequently, glycosaminoglycans, cholesterol, and lipids remained stored in lysosomes, causing tissue damage (Velho *et al*., 2019).

Mucolipidosis IV is rare lysosomal storage disease, clinically characterized by progressive neurodegeneration, delayed psychomotor functions (motor and speech), intellectual disability, corneal clouding, gradual vision loss due to retinal degeneration, achlorhydria, and a short life span (Amir *et al*., 2013; Schiffmann *et al*., 2014). MLIV patients reveal high gastrin levels, neuronal demyelination, and a reduction in corpus callosum in brain biopsy, while skin biopsy shows accumulation of amphiphilic lipids, and water-soluble substances (Wakabayashi *et al*., 2011; Schiffmann *et al*., 2014).

MLIV is caused by a mutation in *MCOLN1* (Chr 19p13.2-13.3) (Bargal *et al.*, 2000). *MCOLN1* has 14 exons, coding for the 580 amino acid protein (65Kd), mucolipin-1 (also known as TRPML-1), a vesicular Ca^{+2} releasing channel belongs to transient receptor potential (TRP) superfamily (Bargal *et al.*, 2000; Bassi *et al.*,2000; Cantiello *et al.*, 2000), involved in endocytosis. TRPML-1 expression is high in brain, spleen, heart, kidney and liver, where it is confined to the surfaces of late endosomes and lysosomes (Cheng *et al.*, 2010). Any sort of dysfunction in TRP family members leads into accumulation of lysosomal substrates to the cytoplasm (LaPlante *et al.*, 2006), aberrant trafficking of endosomes and autophagosomes and, hence, autophagy, abnormal regulation of lysosomal exocytosis, mammalian Target of Rapamycin-1/Transcription factor EB (mTORC1-TFEB) signaling and heavy metal homeostasis (Boudewyn & Walkley. 2019).

MLIV disease was reported for the first time in a young male Ashkenazi Jewish (AJ) infant in 1974, having corneal clouding and storage bodies (Berman *et al.*, 1974). About 70-80 of MLIV patients belong to either Ashkenazi Jewish or Ashkenazi Polish ethnicity (Bach. 2001), while the remaining 20-30% are of non-AJ origin (Wakabayashi *et al.*, 2011). The AJ population has a carrier frequency of 1/100 (Bach. 2001) and a prevalence rate of 1/42,000 (Hantash *et al.*, 2006). In 1999, linkage analysis of 13 AJ families mapped the disease causing gene at 19p13.3-13.3 and identified two founder haplotypes/variants, called major AJ and minor AJ variant, in population (Slaugenhaupt *et al.*, 1999). In AJ families with MLIV history, 95% have the founder mutations, major AJ variant (splice site mutation in intron 3, c.416-2A>G, causing premature termination of ML-1 protein), or a 6434 bp deletion, c.1-788del (first 6 exons and starting 12bp of exon 7) (Minor AJ variant). Among these 95% families, major and minor AJ variants account for 72% and 23% of MLIV patients respectively (Bargal *et al.*, 2000; Edelmann *et al.*, 2002), while the remaining 5% are due to other types of mutations (Bargal *et al.*, 2000;). Till now, 35 different mutations have been reported in *MCOLN1* (HGMD Professional, 31 May, 2020).

Spondyloepiphyseal dysplasia

Spondyloepiphyseal dysplasia (SED) is a multisystemic skeletal disorder, characterized by dwarfism, bone deformities, auditory and visual problems. Based on mode of inheritance and age of onset, SED has been classified into two types: SED congenita and SED tarda. The other rare forms of SED have also been reported in the literature with slightly different clinical features.

Spondyloepiphyseal Dysplasia Tarda

Spondyloepiphyseal dysplasia tarda (SEDT) is inherited in X-linked pattern (Maroteaux *et al.* 1957) and the clinical symptoms resembles to SED. SEDT symptoms appear later in life (6-8 years of age) when spine growth becomes slow, while legs and arms keep expanding, resulting in disproportionate stature. Females are carriers and hence asymptomatic but can pass the defective X chromosome to their son. SEDT is caused by mutation in *SEDL* or *TRAPPC2 (*Xp22.2-22.1) (Szpiro-Tapia *et al.*,1988). The prevalence of SEDT is 1:150,000- 200,000 (Wynne-Davies, Gormley. 1985).

TRAPPC2 (Trafficking protein particle complex subunit 2)/SEDL belongs to a family of multi-subunit tethering factors, encodes a 140-amino acid protein, showing homology to yeast protein Trs20, suggesting the conserved evolutionary function of proteins (Sacher *et al* 2008). *TRAPPC2* was directly linked to cause SEDT (Gedeon *et al.*, 1999). Up till now, 58 pathogenic variants (32 insertions or deletions, 9 nonsense variants, and 10 splice site variants) in *TRAPPC2* have been reported (Sacher *et al.* 2019). Although TRAPPC2/Sedlin is found to be expressed in tissues throughout the body, it is abundantly present in endoplasmic reticulum and Golgi apparatus. TRAPPC2/Sedlin transports a large amount of procollagen (PC) from endoplasmic reticulum to the Golgi apparatus for processing, which are further processed to form mature collagen proteins that are used by skin, cartilage, ligaments, tendons and bones for strengthening. Mutations in this gene primarily affect cartilage. It has been showed that TANGO1 recruited Sedlin, is defective in spondyloepiphyseal dysplasia tarda, and the Sedlin is essential for the ER export of PC. It has been

discovered that this gene has mutations that ultimately influence the availability of collagen to the bones and cartilage (Venditti *et al.* 2012).

Major phenotype associated with SEDT

Since the disease phenotypes appeared at 6-8 years of age, when spine starts to grow more slowly and upper and lower limbs keep expanding, the body becomes disproportionate. Consequently, the chest becomes rounded and bulges outwards, hence called a barrel-shaped chest. Short stature and short trunk are clinical features of SEDT, with a final height of 137-163 cm. (Whyte *et al.*, 1999). Other major phenotypes include platyspondyly (due to mutation in *COL2A1* gene), Kyphosis and Hyperlordosis and osteoarthritis.

Minor phenotype associated with SEDT

In addition to major clinical symptoms, SEDT patients have some minor features, i.e., middle-face protrusion, motor and cognitive development.

Spondyloepiphyseal dysplasia Congenita

Spondyloepiphyseal dysplasia congenita (SEDC) is one of the rare skeletal disorders. The word 'congenita' refers to the condition in which symptoms are noticeable at birth and persist throughout adulthood. Spranger (1966) described spondyloepiphyseal dysplasia congenita and later in 1970 explained it as "heritable dysplasia manifested at birth with the smallness of stature and retarded ossification of the vertebral bodies, extremities, and pelvis." Major phenotypes are dwarfism, skeletal deformities and problems with vision and hearing. It is an extremely rare, autosomal dominant inherited chondrodysplasia, that affects vertebral bodies (spondylo-) and proximal epiphyseal centers (Spranger & Langer, 1970). Over 40 clinical subtypes and 450 different conditions have been characterized based on radiological, molecular, and biochemical criteria. (Panda *et al.*, 2014).

Inheritance pattern

SEDC inherits in autosomal dominant form. Both males and females are at equal risk of developing SEDC. Despite being autosomal dominant, the disease is frequently

acquired by individuals due to a *de novo* mutation with no previous family history. The prevalence is approximately 3.4 per million (Wynne-Davies & Hall. 1982). Several studies have correlated the *COL2A1* gene with SEDC. Another study suggested that mutations in the *CHST3* gene have been linked with SEDC (Unger *et al*., 2010).

COL2A1

The *COL2A1* (collagen type II alpha 1 chain) is present on the long arm of chromosome 12 (12q13.1-q13.2), having 54 exons spanning a region of about 31.5kb. *COL2A1* codes for type II collagen, which is a 134.4 kDa (1487- amino acid) protein. (Anderson *et al*., 1990). Type II collagen is the major component of cartilage in the extracellular matrix, plays essential role in endochondral bone formation, growth and development, and proper joint functioning. Type II collagen is also found in vitreous humor, cartilage, and nucleus pulposus, which functions as shock absorber present between spinal bones. Mutation in *COL2A1* gene alters the normal levels of functional type II collagen resulting in skeletal abnormalities leading to SEDC.

CHST3

CHST3 gene, located on chromosome 10q22.1, encodes the 6-O-sulfotransferase-1 or C6ST-1 enzyme, which belongs to a family of carbohydrate sulfotransferase (also known as chondroitin-6-sulfotransferase 3) family of 15 enzymes that are involved in transfer of Sulphur group to carbohydrate moieties of glycolipids and glycoproteins (Tsutsumi *et al*., 1998). The C6ST-1 enzyme is essential for sulfation of proteoglycan; chondroitin, found in the cartilages of the extracellular matrix. A loss of function mutation in *CHST3* results in chondrodysplasia with severe spinal damage. C6ST-1 enzyme plays critical role in the development and preservation of skeleton (van Roij *et al*., 2008).

Rajab *et al*. (2004) made the first differential diagnosis of SED and in the same year, Thiele *et al*. (2004) linked *CHST3* with SED. To date, 48 different types of mutations have been reported in *CHST3* (www. Hgmd.cf. ac. uk accessed May, 2022).

CHST3-type SEDC patients are short in stature (84-128cm)**,** short limbs, short trunks and neck, kyphosis and lordosis, and respiratory complications **(**Tracheolaryngomalacia and other respiratory problems are common in affected individuals due to an extremely underdeveloped rib cage) (Terhal *et al*., 2015). Other clinical symptoms include flat face, cleft palate, kyphoscoliosis, heart valve anomalies, muscle hypotonia, clubfoot, myopia, and bilateral sensorineural deafness (Tuysuz *et al*., 2009; Waryah *et al*., 2016).

Syndactyly

Syndactyly is a heterogeneous genetic disorder of the limbs, involving the fusion of adjacent digits (fingers and toes) in upper and lower limbs (Malik 2012). It is caused by the failure of apoptosis to occur between the mesenchyme of adjacent digits at the 7th and 8th weeks of gestation, when limb development occurs (Kozin, 2001; Canale and Beaty, 2008).

Syndactyly may either exist in isolated or syndromic form. Isolated syndactyly is further divided into nine different types (SD I-IX) (Malik *et al*., 2005), while syndromic form is associated with more than 300 other genetic abnormalities (Malik 2012). These may include apert-syndrome (FGFR2), carpenter syndrome (RAB23), Pfeiffer syndrome (FGFR1, FGFR2), Saethre-Chotzen syndrome (TWIST1, FGFR2) and Bardet-Biedl-syndrome (BBS1-26).

Epidemiology of Isolated Syndactyly

Syndactyly is the second most common congenital limb anomaly after polydactyly, with an incidence rate of 1/2000-2500 live births. Castilla (1980) reported that out of 10,000 live births, 2.2 are born with isolated syndactyly. Feet syndactyly is four times more prevalent than upper limb syndactyly (Castilla, 1980). In SD, a familial pattern of inheritance is seen in 10-40% of the cases (Green *et al*., 2005; Netscher and Baumholtz, 2007) with variable expressivity and penetrance, predominantly affecting males (Green *et al*., 2005; Canale and Beaty, 2008), while the remaining cases are sporadic. Syndactyly is two times more prevalent in males than in females due to incomplete penetrance (Jordan *et al*., 2012; Malik. 2012).

Classification of Isolated Syndactyly

Isolated syndactyly has been classified into simple or mild/complicated or severe, complete/incomplete, isolated/complex, unilateral, bilateral, symmetrical, asymmetrical types (Malik 2012). Simple syndactyly, also known as cutaneous syndactyly, involves only the fusion of the skin, while complex syndactyly involves bony fusion. In complete syndactyly, digits are fused all the way up to nails, and in incomplete syndactyly, partial fusion is found. The complicated syndactyly occurs in conjunction with other malformations, while in isolated syndactyly, other anomalies don't occur. Unilateral syndactyly involves only fusion of either the right hand and feet or vice versa, while in bilateral syndactyly both hands/feet are affected. Similarly, in symmetrical syndactyly, same fingers/toes may be affected.

Inheritance Pattern:

Syndactyly is inherited in autosomal dominant form (Eaton & Lister. 1990), autosomal recessive: SD-7& 9 (Malik 2012) and X-linked recessive fashion, SD-5 (Lonardo *et al*., 2004). Autosomal dominant forms of SD exhibit less severity, incomplete penetrance and variable expressivity.

Types of Isolated Syndactyly

Nine classes of isolated syndactyly/non-syndromic have been described by Malik (2012) based on genotype-phenotype co-relation and clinical diagnosis, which are caused by mutations in eight different genes and eleven loci (Deng & Tan. 2015)

Syndactyly Type-1

Syndactyly type-1 (SD-1) involves webbing of $3^{rd}/4^{th}$ fingers and/or $2^{nd}/3^{rd}$ toes. It is further divided into four subgroups (Malik *et al.,* 2005), as mentioned below:

Weidenreich Type/ Syndactyly Type 1-a

Weidenreich (1923) for the first-time reported syndactyly type 1-a (SD-1a), also called 2/3 toes syndactyly or zygodactyly. It inherits in an autosomal dominant fashion, and exhibits clinical features of bilateral and symmetrical cutaneous webbing of $2^{nd}/3^{rd}$ toes without affecting fingers (Stiles and Hawkins, 1946). The prevalence rate is 4:1,000 live births (Schurmeier, 1922; Castilla *et al*., 1980). Weidenreich syndactyly is regarded as the most prevalent form of toe syndactyly (Temtamy and

McKusick, 1978; Mondolfi. 1983). Weidenreich type accounts for 70% of overall isolated cases of 2/3 toe syndactyly (Castilla *et al*., 1980, Malik 2012). In some severe cases, fusion of adjacent toes may reach up to nails, causing varus inclination of second toe (Malik *et al*., 2005). Syndactyly type 1-a was mapped to ZD-1 locus on chromosome 3p21-31 in a Pakistani family for the first time (Malik *et al*. 2005).

Syndactyly type 1-b/Lueken type

Syndactyly type1-b (SD1-b) involves bilateral cutaneous webbing or bony fusion at the phalangeal tips of 3/4 fingers and 2/3 toes (Lueken, 1938). It is inherited in autosomal dominant form. In severe cases, fusion of all fingers (2-5) and toes (1-5) may occur. Lueken type syndactyly was mapped at chromosomal locus 2q34-q36, also known as SD1 locus, in German and Iranian families (Bosse *et al.,* 2000, Ghadami *et al*., 2001), but no disease-causing genes have been identified yet.

Syndactyly type 1-c/ Montagu Type

Montagu Type (SD-1c) is a rare form that inherits in autosomal dominant fashion, characterized by bilateral or unilateral cutaneous or bony fusion of 3/4 fingers (but occasionally 4/5 fingers) without affecting feet (Montagu, 1953). Hsu reported a Chinese family of Montagu type, with phenotypic variability (Hsu, 1965). Dai *et al*., 2014 linked SD-1c to the chromosomal locus chr2q31-q32 in two Chines families and found mutations (p.R306Q, p.R306G) in the *HOXD-13*gene.

Syndactyly Type 1-d/Castilla Type

Syndactyly type 1-d (SD1-d) has bilateral webbing of 4/5 toes. It is the second most common type of isolated toes syndactyly (Castilla *et al*., 1980) and inherited in autosomal dominant form.

Syndactyly type II/Synpolydactyly

Syndactyly type-2 (SD-2) is a very rare form of syndactyly, inherited in an autosomal dominant pattern. The affected individuals show not only fusion of 3/4 fingers and 4/5 toes, but also duplication of digits (postaxial polydactyly) in the fused region (Temtamy, 1969), showing phenotype variability and incomplete penetrance (86%-97%) (Winter and Tickle 1993; Sayli *et al*., 1995; Goodman *et al*., 1997).

Depending upon the variation in phenotypes (~18 clinical variants), SPD has been categorized into three subclasses: (a) SPD1, or Vordinborg type, exhibiting typical SPD features (b) SPD2/Debeer type includes minor variants and (3) SPD3/Malik type having unusual/unique phenotypes (Malik and Grzeschik, 2008). SPD has been mapped to three chromosomal loci; chr2q31.1, chr22q13.31, and chr14q11.2-13 (Akarsu *et al*., 1996; Muragaki *et al*., 1996; Debeer *et al*., 2002; Malik *et al*., 2006).

The variable phenotypic expressivity and penetrance of SPD1 is due to a mutation in polyalanine tract of the first exon of *HOXD13*, an expanding normal 15-residue polyalanine tract, encoded by imperfect trinucleotide repeats, as reported in American and Turkish families (Winter and Tickle, 1993; Muragaki *et al*., 1996; Akarsu *et al*., 1996). The alanine tract expansion is proportional to disease penetrance, severity, and involvement of the upper and lower limbs in SPD patients (Winter and Tickle, 1993; Muragaki *et al*., 1996). There is no penetrance in small families, while 86% (in case of 7-alanine expansion) and 97% (9-alanine expansion) exist in large families (Akarsu *et al*., 1996; Goodman *et al.,* 1997). Similarly, the involvement of both upper and lower limbs is highly significant with tract expansion (*p = 0.012* for upper limbs; *p<0.00005* for lower limbs) (Goodman *et al*., 1997). The studies performed by Dolle *et al*., 1993; Davis and Capecchi, 1996, suggested that the expansion of the trinucleotide repeat results in gain of function of the mutant protein. This was further supported by Zákány and Duboule, 1996, which showed that mutant protein have a dominant negative effect on expression of normal counterpart allele as well as *HOXD11* and *HOXD12*.

de Smet *et al*. (1996) reported SPD2 in a Belgian family (father and daughter) and later on in a second daughter (Debeer *et al*., 1998), characterized clinically and radiologically by complex 3/3'/4 syndactyly and synostosis of tarsals, metatarsals, and metacarpals. SD2 inherits in autosomal dominant form (Debeer *et al*., 1998). SPD2 is caused by chromosomal translocation between 12 and 22; t(12;22) (p11.2;q13.3) (de Smet *et al*. 1996; Debeer *et al*., 1998a,b; Debeer *et al*., 2000). Further studies showed that SPD2 is due to the translocation of last exon of the Fibulin-1 (*FBLN1*) gene isoform D (Debeer *et al*., 2002).

Synpolydactyly type-3 (SPD-3) was mapped at the chr14q11.2-13 locus (Malik *et al.*, 2006), in large Pakistani family with variable and diverse clinical features, i.e., bony and cutaneous fusion of 3rd/4th fingers, symphalangism, clinodactyly, and campodactyly.

Syndactyly type III/Johnston-Kirby type

Syndactyly type III (SD3) is inherited in autosomal dominant form with incomplete penetrance (Malik *et al.*, 2012). Lohmann (1920) for the first time reported the phenotype of SD-3, also known as oculodentodigital dysplasia (ODDD); i.e., developmental defects in craniofacial features, ocular anomalies, and limbs. But, later on, in a number of studies, a detailed clinical spectrum were described; i.e., facial abnormality, bilateral 4th/5th fingers syndactyly (but occasionally 3/4/5 fingers syndactyly), campodactyly, enamel hypoplasia, and micropthalmia (Johnston and Kirby. 1955; Meyer-Schwickerath. 1957; Temtamy and McKusick, 1978; Gladwin *et al.*, 1997).

The genomic location of SD3/ODDD was identified by Gladwin *et al.* 1997 at chromosomal location 6q22-24, which was further refined to 1.9 cM interval (Boyadjiev *et* al., 1999). Later, the connexin-43 encoding gene, *GJA1*, was identified to cause both ODDD and isolated SD3 (Paznekas *et al.*, 2003; Richardson *et al.*, 2004).

Syndactyly type IV/ Haas type Synpolydactyly

Haas (1940) for the first-time reported syndactyly type IV (SD4) in a family showing complete cutaneous syndactyly of all fingers, giving hands a cup-shaped appearance due to flexion of all fingers. In its severe form, there is a complete fusion of variable number of toes along with fingers and polydactyly (Haas. 1940; Anderson and Hansen. 1990; Dai *et al.*, 2013). The prevalence rate of type IV syndactyly is 1 out of 300,000, with autosomal dominant inheritance (Castilla *et al.*, 1980).

Syndactyly type IV is caused by a mutation in ZRS region, present in intron 5 of *LMBR1* at chromosome 7q36.3. ZRS acts as a limb-specific enhancer of *Shh,* located downstream at 1Mb (Lettice *et al.*, 2002, 2003; Sagai *et al.*, 2004). Mutations in ZRS have been reported in other limb anomalies, collectively known as ZRS-associated limb malformations. These may include triphalangeal thumb polysyndactyly (Sun *et al.,* 2008; Klopocki *et al.*, 2008), preaxial polydactyly type II/PPD2 (Lettice *et al.*,

2002, 2003; Li *et al*., 2009), Haas syndactyly (Klopocki *et al*., 2008; Sun *et al* ., 2008; Wu *et al.*, 2009; Furniss *et al .,* 2009; Wieczorek *et al* ., 2010), Triphalangeal thumb polysyndactyly syndrome (Klopocki *et al*., 2008; Sun *et al*., 2008; Wu *et al*., 2009; Furniss *et al*., 2009; Wieczorek *et al*., 2010), Werner mesomelic syndrome (Wieczorek *et al.*, 2010; Cho *et al*., 2013; Girisha *et al.,* 2014; Norbnop *et al.,* 2014), Laurin-Sandrow syndrome (Lohan *et al*., 2014) and PPD2 with radial deficiency (Al-Qattan *et al*., 2012).

Syndactyly type V/Dowd type

Dowd (1896) for the first time described the clinical phenotypes of syndactyly type V (SD-5) as cleft hand, since the affected individual had fusion of 4/5 metacarpals. Later on, Temtamy and McKusick (1978) classified it as a subclass of isolated syndactyly (SD-5). The affected individuals also exhibit additional symptoms, ranging from second to fifth finger ulnar deviation, fifth finger campodactyly, third and fourth fingers having interdigital cleft, short distal phalanges, and absence of distal interphalangeal creases. In case of foot involvement, hyperplasia of the first metatarsal and metatarsal hypoplasia from the second to fifth finger have been observed. As a result, there is varus deviation in metatarsals and valgus deviation in phalange (Robinow *et al*., 1982; Malik. 2012).

In 2005, Kjaer *et al*. suggested that polyalanine tract expansion is responsible for SD-5. But, however, Zhao *et al*. (2007) found a missense variant in *HOXD13* to cause SD-5 in large Han Chines family. SD-5 is a rare form of isolated syndactyly and is inherited in autosomal dominant form (Zhao *et al*., 2007).

Syndactyly type VI/ Mitten type

Syndactyly type VI (SD-6) is a rare phenotype of syndactyly, reported for the first time by Temtamy and McKusick (1978), The affected individuals experience unilateral webbing of 2/5 fifth fingers and 2/3 toes. SD-6 is inherited in autosomal dominant form with reduced penetrance and variable expressivity (Malik 2012).

Syndactyly type VII/Cenani-Lenz Syndactyly

Syndactyly type VII (SD-7) is a rare type of isolated syndactyly. Cenani and Lenz (1967) and Elçioglu *et al.* (1997) reported that the affected individuals exhibit synostosis of the carpals, metacarpals, and phalanges (spoon-shaped hands), fused,

hypoplastic/rudimentary ulna and radius. SD-7 is inherited in autosomal recessive form, affecting the upper and lower limbs similarly.

Up to now, nephrological, enamel dentation abnormalities, nail aplasia/hypoplasia, and craniofacial features have been rarely reported in some patients (Cenani & Lenz. 1967; Temtamy *et al*., 2003; Li *et al*., 2010).

Harpf *et al*. (2005) subdivided SD-7 into two groups on the basis of phenotypes; i.e., Cenani-Lenz Sydrome (CLS)/spoon-hand type and oligodactyly type. Li *et al*. (2010), for the first time, showed that CLS is caused by mutation in *LRP4* (Chr:11p11.2), encodes for co-receptor of the frizilled (fz) receptor, that is involved in Wnt-β catenin pathway. It is inherited in autosomal recessive form. Similarly, mutation/rearrangement in *GREM1-FMN1* genes at chromosome 15q13.3 result in an oligodactyly type phenotype accompanied by hearing loss, renal defects, non-syndromic oligodactyly, and autosomal, dominant mode of inheritance (Dimitrov *et al*., 2010). The functional annotation of *GREM1-FMN1* genes in limb development has also been studied in limb deformity (*ld*) mouse model (Kleinebrecht *et al*., 1982), and chicken limb primordia (Capdevila *et al*., 1999; Merino *et al*., 1999), resulting in shortening of digit rays, absent fibulae, complete radioulnar synostosis, and kidney abnormalities.

Syndactyly type VIII/Orel-Holmes type

Syndactyly type VIII (SD-8) is an X-linked recessive limb anomaly (Orel. 1928; Lerch 1948; Holmes *et al*., 1972), characterized by partial/complete webbing of 4/5 metacarpals, vivid separation of 4/5 metacarpals at distal ends, and little finger exhibiting ulnar deviation. There is fifth finger hypoplasia and the absence of tri-radii c and d (Holmes *et al*., 1972; Anneren and Amilon, 1994).

Jamsheer *et al*. (2013) performed whole exome sequencing of probands in Polish and German families with SD-8 and found a homozygous nonsense mutation in *FGF16*, located on chromosome Xq21.1. It has been further divided into two subclasses on the basis of inheritance; Orel-Holmes type (X-linked recessive) and Lerch type (autosomal dominant).

Syndactyly type IX; Malik-percin Type:

Syndactyly type IX, an autosomal recessive disorder (Malik S *et al*., 2005), shows characteristic features of bony fusion of 3rd/4th fourth metacarpals, malformed thumbs, hypoplasia and clinodactyly of 5th finger and mesoaxial reduction of fingers. Additional features may include preaxial webbing of toes with terminal phalangeal hypoplasia of all toes. Percin *et al.,* 1998 and Malik *et al*., 2004 separately described syndactyly type-IX in Pakistani and Turkish families respectively, and mapped the locus at chromosome 17p13.3 (Malik *et al*., 2005), but no causative gene has been identified yet.

Acromesomelic Dysplasia

Acromesomelic dysplasias (AMD)/osteochondrodysplasias (OCD) is characterized by disproportionate shortening/growth of the appendicular skeleton elements, predominantly affecting middle (mesomelia; forearms and forelegs) and distal segments (acromelia; hands and feet). AMDs exist either in isolated or syndromic form, which is linked to respiratory, genital, cardiac, and nervous system disorders (Khan *et al*., 2016; Mustafa *et al*., 2020). Acromesomelic dysplasia inherits in autosomal recessive form.

To date, six types of acromesomelic dysplasia have been identified; acromesomelic dysplasia-Grebe type (OMIM #200700) (Grebe. 1952); acromesomelic dysplasia-Maroteaux type (AMDM, OMIM #602875) (Maroteaux, 1971); acromesomelic dysplasia-Hunter and Thompson (AMDH, OMIM #201250) (Hunter & Thompson. 1976), acromesomelic dysplasia Osebold-Remondini type (OMIM #112910); (Osebold *et al*., 1985), fibular hypoplasia and complex brachydactyly type (Du pan, OMIM #228900) and recently discovered novel type, acromesomelic dysplasia PRKG2 type (AMDP) (OMIM #609441) (Díaz-González *et al*., 2022).

Acromesomelic Dysplasia Grebe Type

Clinical manifestations of acromesomelic dysplasia-Grebe type (AMDG) include dwarfism, severe micromelia, and acromesomelia, restricted mostly to appendicular skeleton (Grebe. 1952). Other features may include short hands with toe-like fingers

and valgus deformity (Thomas *et al.*, 1997), ulnar hypoplasia, fusion of carpals, metacarpals, tarsals, and metatarsals and missing of proximal and middle phalanges, short nick, absence of tibia, and diaphysis of fibula (Costa *et al.*, 1998; Faivre *et al.*, 2000). The afflicted individuals have normal intelligence and face (Martinez-garcie *et al.*, 2016; Khan *et al.*, 2016).

According to the literature, AMDG is caused by mutation in *CDMP1* (2q11.22) (Thomas *et al.*, 1997; Faiyaz-Ul-Haque *et al.*, 2002; Al-Yahyaee *et al.*, 2003; Basit *et al.*, 2008; Martinez-Garcia *et al.*, 2015) and *BMPR1B* (4q22.3) (Graul-Neumann *et al.*, 2014).

CDMP1 encodes Growth Differentiation Factor-5 (GDF5), a member of secreted signaling molecule superfamily of transforming growth factor-beta (TGF-β), mostly expressed in cartilaginous tissues of growing long bones and appendicular skeleton. GDF5 is involved in limb patterning, joint development, and the growth of distal bones by stimulating the early stages of chondrogenesis. It further increases cellular adhesion and then chondrocytic proliferation. Biallelic sequence variants in bone morphogenetic protein receptor-1b (*BMPR1B*), receptor of GDF5, also causes AMDG (Martinez-garcie *et al.*, 2016; Ullah *et al.*, 2018).

The *BMPR1B* gene encodes for a cell surface receptor, Bone Morphogenetic Protein Receptor-1B, comprising 502 amino acids, consist of three domains: namely extracellular ligand binding, transmembrane, and intracellular protein kinase domains. The extracellular domain binds to GDF5, activating p38MAP kinase and SMAD-dependent pathways, and, hence, contributing to bone formation (Gilboa *et al.*, 2000; Nohe *et al.*, 2002; von Bubnoff and Cho. 2001).

Acromesomelic dysplasia Maroteaux type

AMDM patients have short stature (<-5 SD height; below 120 cm), bowed forearms, shortening of distal and middle skeletal elements, and widening of metacarpals and phalanges (Kant *et al.*, 1998). The phenotypic severity increases in the proximo-distal direction; i.e., hands and feet are severely affected (either brachydactyly or rudimentary fingers). X-ray radiographs show short ulnas with hypoplastic distal ends. Usually, AMDM patients exhibit dolichocephaly, a short trunk, and lower

vertebral height without any facial dysmorphism (Langer & Garrett. 1980). AMDM patients reveal normal mental growth but delayed motor functions and puberty.

Kant *et al*. (1998) mapped AMDM on chromosome 9 (p21-p12), later Bartels *et al*. (2004), reported NPR2 as the causative gene underlying the disease. The NPR2 gene encodes for a homodimeric transmembrane receptor (NPR-B) (Potter *et al*., 2006). The secreted peptide product of the natriuretic peptide precursor gene (NPPC, OMIM# 123830), CNP, binds to NPR-B to initiate cascades of signaling pathways in chondrocytes, endothelial cells, and female reproductive organs to produce cGMP (Schulz. 2005; Potter *et al*., 2006). This binding results in differentiation and hypertrophy of growth plate chondrocytes and an increase in bone matrix synthesis (Krejci *et al*., 2005).

The phenotypic variability among AMDM patients is due to specific loss-of-function mutations (homozygous, compound heterozygous or heterozygous) in NPR2. Homozygous mutations cause only AMDM (Wang *et al*., 2015; Umair *et al*., 2015; Jacob *et al*., 2018). Additionally, some other compound heterozygous mutations result in idiopathic short stature with/without involvement of other skeletal elements (Olney *et al*., 2006; Amano *et al*., 2014).

Acromesomelic dysplasia Hunter–Thompson type

Acromesomelic dysplasia Hunter–Thompson type (AMDH, MIM 201250), is caused by a mutation in *GDF5* (Khan *et al*., 2016; Umair *et al*., 2017). Clinical features include limb shortening, especially in the lower limbs as compared to the upper limbs. Upper limbs have hands with a short phalanges and metacarpals, a short humerus, and curved radius and an ulna, while lower limbs have short femurs, tibias, fibulas, and dislocated ankles.

Acromesomelic dysplasia DuPan type

Acromesomelic dysplasia DuPan type/ fibular hypoplasia and complex brachydactyly, is characterized by mild shortening of limbs. Affected individuals have normal radius, ulna, femur, carpals, metacarpals, and phalanges while tarsals, metatarsals, and phalanges of toes are mildly affected by impalpable fibulae. Du Pan type is caused by bi-allelic variants in *GDF5* and *BMPR1B* genes (Stange *et al*., 2015). In AMDD

patients, genital anomalies, namely hypoplasia of uterus and premature ovarian failure have also been reported, leading to hypogonadotropic hypogonadism. Demirhan *et al*. (2005) reported 8-bp deletion (c.361_368del8) in *BMPR1B*, causing AMDD in a Turkish family. AMDD differs from AMDG because of the presence of genital anomalies and distinct limb phenotype.

Acromesomelic dysplasia Osebold-Remondini type

The Osebold-Remondini syndrome is inherited in autosomal dominant form (Osebold *et al.,* 1984). Clinical features of affected members include short stature, radial deviation due to a short radius and long ulna in hands, mesomelic shortness of hands and feet, absent/hypoplastic middle phalanges in both upper and lower limbs, short and broad digits.

Aacromesomelic dysplasia PRKG2 type (AMDP)

Aacromesomelic dysplasia PRKG2 type (AMDP) is clinically characterized by disproportionate short stature, mild acromesomelic shortening of limbs, platyspondyly, and metaphyseal dysplasia of long bones. AMDP is caused by homozygous mutation in *PRKG2*, located downstream of the NPR-B receptor gene (Dîaz-Gonzalez *et al*., 2022). It encodes for cGMP-dependent kinase II (cGKII), a membrane-bound serine-threonine kinase, consists of a cGMP binding domain and a C-terminal catalytic domain (Pfeifer *et al*., 2005).

Previous studies using animal models; cGKII null mice (Pfeifer *et al*., 1996; Kawasaki *et al*., 2008), *prkg2*-deleted KMI rats (Tsuchida *et al*., 2008) and homozygous mutations in American Angus cattle (Koltes *et al*., 2009), also supported the clinical phenotypes of human probands (Dîaz-Gonzalez *et al*., 2022)

Aims and Objectives

Current research study has the following aim and objectives:

- ➢ Clinical and genetic analysis of congenital skeletal dysplasia in Pakistani Families
- ➢ Mapping and mutational screening of disease-causing genes/loci using highly polymorphic microsatellite markers and whole exome sequencing
- ➢ Establishing genotype-phenotype correlation

- ➤ Clinical assessment in disease diagnosis
- ➤ Genetic counseling of families having consanguineous marriages

Materials and Methods

Study Approval

The present research was approved by the Institutional Review Board of Quaid-i-Azam University, Islamabad, Pakistan. Family elders were initially briefed about the purpose and nature of the research study and written consent was taken from family members.

Study Subjects

In the present research study, thirteen families of Pakistani origin, exhibiting various forms of congenital skeletal dysplasia were sampled from different regions of District Swabi, Khyber Pakhtunkhwa province, Pakistan. The respective families were visited in their hometowns to collect information regarding their family history, and pedigree drawing, and to observe the clinical features of affected members in detail by taking photographs and radiographs.

Pedigree Drawing

The standard method proposed by Bennet *et al*. (2008) was used for the construction of the pedigrees of all the recruited families. In pedigree, normal male and female is shown by empty square and circle respectively while affected by filled square and circle. Double lines between two individuals (male and female) indicate consanguinity, while cross symbols represent deceased individuals. Arabic numerals represent individuals within a generation, while Roman numerals represent each generation.

Blood Sample Collection

The blood samples were collected at a local medical clinic from normal and affected individuals. Venous blood sample of about 5 ml was collected using sterilized syringe (BD 0.8 mm × 38 mm, 21 G, 1 ½ TW, Franklin Lakes, USA). Fresh blood samples were then transferred into EDTA-vacutainers (BD, 10 ml vacutainer containing K3-EDTA, (Franklin lakes, USA) and stored at 4^0C.

Genomic DNA Extraction

The stored blood samples were incubated at room temperature for half an hour to extract genomic DNA. The following method was used for genomic DNA extraction:

1   Kit method (commercially available) (Thermo-Scientific, Washington, USA).

Kit-based DNA Extraction

Extraction of DNA using a commercial Kit for high-quality rapid DNA isolation was carried out according to the recommended protocol (Gene JET Genomic-DNA purification, Thermo-Scientific, Washington, USA).

• 200 blood 20µl of protein kinase (PK) and 400µl of lysis solution were taken together in an Eppendorf tube and put on incubation for 10-20 minutes at 56-70°C and vortexed after an interval of 5 minutes.

• 200 ethanol (100%) was added and slightly vortexed. The entire content was transferred to a silica spin column and centrifuged at 8,000rpm for one minute.

• The flow-through was discarded, and DNA was washed with 500µl washing buffer1 (WB1) and washing buffer2 (WB2) and centrifuged at 8,000rpm and 14,000rpm, respectively for 1-3 minutes.

• An empty spin was executed at 13,000rpm for one minute to elute the residual washing buffers.

• After washing, the DNA was eluted in 100-150µl elution buffer (EB) by centrifuging at 14000rpm for three minutes and subsequently stored at 4°C.

Agarose Gel Electrophoresis

Agarose gel electrophoresis was carried out to check the integrity/quality of extracted DNA and to make dilutions from the stock DNA for the future. Normally 1% agarose gel is used for this purpose.1 g agarose is added in 100ml volume (90ml distilled water, 10ml 10X TBE) and allowed to heat in a microwave oven for 45-60 seconds to completely dissolve the agarose. 2-4 µL ethidium bromide (EtBr) (0.5µg/mL) was then added into agarose and gently shaken for complete dissolution. The gel was then

poured into agarose gel tank and allowed for solidification for 25-30 minutes at room temperature.

After gel solidification, the combs were removed and 3 μL loading dye (0.25% Bromophenol Blue, 40% sucrose) was mixed with 3 μL genomic DNA and was loaded into the wells. The agarose gel was run in 1X TBE buffer at 120V for 20-30 minutes. Visualization of genomic DNA bands was made by exposing the gel to a UV transilluminator (Biometra, Gottingen, Germany), and the images were captured using a digital camera EDAS 290 (Kodak, New York, USA).

Linkage Analysis and Homozygosity Mapping

Linkage analysis and homozygosity mapping was performed using gene-specific, highly polymorphic microsatellite markers. Rutger's Combined Physical Map and Online UCSC Genome Browser provided the required information to find physical distances between known genes/loci and microsatellite markers flanking within these loci. For a given gene/locus, 4-6 microsatellite markers of a different centimorgan (cM) were used for the identification of homozygosity and heterozygosity in affected and normal family members, respectively.

Genotyping PCR

Genotyping PCR is usually performed for the amplification of microsatellite markers to identify homozygous and heterozygous regions in normal and affected family members. To run a PCR reaction, 200 μL PCR tubes were taken, containing a reaction mixture of 25 μL. The reaction mixture was composed of 2.5 μL 10X PCR buffer (750 mM Tris HCl pH 8.8, 200 mM Ammonium Sulphate, and 1% Tween-20), 2 μL MgCl$_2$ (25 mM), 0.5 μL dNTP's (10 mM), 0.5 μL of forward and reverse primers (0.2 μg/μL), 1 unit of Taq polymerase (0.2 μL) (Perkin-Elmercetus, Fermentas, Burlington, Canada), 2 μL DNA dilution and 18 μL PCR water. The reaction mixture was spun at 3000 rpm for 30 seconds and assembled in Thermocycler (Biometra, Gottingen, Germany).

The following conditions were kept during the steps of the PCR reaction:

Step 1: Denaturation of genomic DNA at 96^{0}C for 7 minutes.

Step2: 40 cycles of amplification, encompassing the following three sub-steps:

Sub-step a: Denaturation of template DNA (96^0 C for 1 minute).

Sub-step b: Annealing of primers to template DNA (54^0C for 1 minute) for the amplification of microsatellite markers.

Sub-step c: Elongation of DNA strands (72^0C for 1 minute) by Taq Polymerase.

Step3: Final elongation of remaining DNA strands by Taq Polymerase (72^0C for 8-10 minutes).

Polyacrylamide Gel Electrophoresis (PAGE)

To search for linkage analysis and homozygosity mapping, amplified PCR products were run on an 8% polyacrylamide gel. Initially, PCR products were mixed with 6 μL of loading dye (0.25% bromophenol blue, 40% sucrose) and loaded into wells, followed by electrophoresis at 130-145 V for 2-3 hours. Following completion of electrophoresis, the gel was stained with washing dye (Ethidium Bromide; 10 mg/mL), placed under a UV transilluminator (Biometra, Gottingen, Germany) for band visualization, and the image was captured by the digital camera EDAS290 (Kodak, New York, USA). The band pattern reveals linkage and homozygosity. In case of linkage between a particular microsatellite marker and a disease-associated gene/locus, Sanger sequencing PCR is performed to find a variant.

Whole Exome Sequencing

DNA of one affected member in families (A-K) was subjected to whole exome sequencing (WES). Exome library preparation was performed using SureSelect Human All Exon V6 kit (60.45 MB). Barcoded libraries were pooled, and paired-end sequencing was performed on Illumina HiSeq. The reads were processed with FastQC (v0.11.9) and TrimGalore (Version 0.6.8dev) tools with default parameters for quality control and adapter trimming. Reads were aligned to GRCh37/Hg19 using the Burrows-Wheeler Aligner (BWA-MEM) (Li H & Durbin R. 2009). SAM file processing, duplicate removal, quality recalibration, single nucleotide variant calling, and small indel detection were performed using Samtools, Picard, and the Genome Analysis Toolkit (GATK) (McKenna *et al.*, 2010). Variants were annotated using ANNOVAR (Wang, Li & Hakonarson. 2010).

The following criteria was used for gene/variant identification:

Selection of variants affecting the structure of exons and splice sites (+/- 12 bp); homozygous and compound heterozygous variants in case of recessive inheritance; MAF =<0.1% in the Genome Aggregation Database (gnomAD) database and the Greater Middle East Variome Project (GME); CADD Phred score =>15. Bioinformatics predictions of their impact obtained from ANNOVAR databases dbnsfp35a and dbscSNV1 and OMIM genes for skeletal dysplasia were used to aid in determining a list of variants for segregation analysis using Sanger sequencing.

Bioinformatical Analysis

Several human databases, including Trans-Omics for Precision Medicine (TOPMed) Bravo database (Kowalski *et al.*, 2019), gnomAD v3.1.2 (Karczewski *et al*., 2020), All of Us research program data (Lyles *et al*., 2018), Human Gene Mutation Database (http://www.hgmd.cf.ac.uk/ac/validate.php), and ClinVar (ncbi.nlm.nih.gov/clinvar/) were searched for the disease-causing variants. The pathogenicity of the identified variants was analyzed using online bioinformatics tools such as PolyPhen-2 (http://genetics.bwh.harvard.edu/pph2/), MutPred2 (http://mutpred.mutdb.org/), Mutation Taster (mutationtaster.org), and Varsome (Varsome.com).

Candidate Genes Sequencing

The candidate-linked genes and screened variants, identified through WES were sequenced and validated for segregation in respective family members through Sanger sequencing.

The *BMPR1B* gene showed linkage in two families exhibiting chondrodysplasia and was Sanger sequenced, while the remaining families were subjected to WES and shortlisted variants in different genes (*BBS5, IDUA, CHST3, BMPR1B, NPR2, EVC, ROR2, HOXD-13, GJA1, GALNS, GNPTG*) were further validated for segregation.

Primer Designing

To confirm disease-causing pathogenic variants in linked genes and those shortlisted in the WES file, primers were designed using online tools (Primer3plus; https://www.bioinformatics.nl/cgi-bin/primer3plus/primer3plus.cgi) and Primer blast (https://www.ncbi.nlm.nih.gov/tools/primer-blast/). During primer designing, annealing temperature difference between forward and reverse primer, GC-contents, annealing, and dimer formation were kept in mind. The primers were then optimized, and the amplified PCR products were run on 2% agarose gel.

Sanger Sequencing PCR

Sanger sequencing PCR was performed to find out which exon of a gene has pathogenic variant. Both exons were Sanger sequenced to find any disease-causing variant. All the exons of a particular linked gene, along with their flanking intronic regions, in the affected member were amplified using region-specific primers. The amplified products were purified with the commercially available kit (Fermantas, USA) and then sequenced by Automated DNA Sequencer, ABI prism 310 (Applied Biosystem, USA), using its Big Dye Terminator version 3.1 cycle sequencing kit. Bioedit (version 7.2) was used for the analysis of Sanger chromatograms. The primer sequences along with their respective melting temperatures have been mentioned in Table 2.2.

Sequencing PCR

For the amplification of exons, sequencing PCR with a volume of 50 µL in a 200 µL PCR tube was carried out. The reaction mixture contained 2.5 µL (20 ng/µL) genomic DNA, 2.5 µL forward and reverse primer, 5 µL PCR buffer, 4 µL of 25 mM $MgCl_2$, 1 µL of 10 mM dNTP's (MBI Fermentas, UK), 1 unit (0.7 µL) Taq Polymerase (MBI Fermentas, UK), and 38.1 µL PCR water. The PCR tubes were assembled into thermocycler (Biometra, Gottingen, Germany), and the reaction was performed as described above. For confirmation of exon amplification, PCR products were analyzed on 2% agarose gel.

Purification of Amplified Exons

The amplified exons were then purified to avoid any damage to amplified products using a Gene Jet PCR Purification Kit (Fermentas, USA) according to the following protocol:

- PCR buffer A (130 µL) was added into PCR tube containing 50 µL of amplified PCR product and mixed thoroughly by proper vertexing.

- The whole mixture was then transferred into purification column and allowed to centrifuge for 1 minute at 13,000 rpm. The flow-through liquid was discarded.

- 600 µL wash buffer was added to column to remove Taq Polymerase, buffer, dNTPs, and unused primers. Centrifugation at 13,000 rpm for 1 minute was done. The flow-through liquid was discarded, and the above step was repeated with 400 µL wash buffer.

- After washing, empty spin at 13,000 rpm for 2-3 minutes was given to remove the wash buffer from the column.

- The purification column was then transferred into another Eppendorf, and 30 µL elution buffer (10 mM Tris HCl with pH 8.8, 0.1 mM EDTA) was added to the center of column and kept at room temperature for 10 minutes.

- The purification column was again centrifuged for 3 minutes at 13,000 rpm and finally the purified product was collected into Eppendorf tube.

- The purified product was once again checked on 2% agarose gel.

Table 2.1: List of Primers used to amplify gene (s)

S.No	Gene Name	Oligo Name	Sequence (5'-3')	Tm (ºC)
1	*IDUA1*	IDUA1-F	GGGGTTCCAGGGAGGTCT	61.3
		IDUA1-R	CCTCAGGGTTCTCCAGGGG	64.3
2	*BBS5*	BBS5-F	CCTCGCATCTCAAATCGGCT	64.9
		BBS5-R	CTACAGGGTTGAAGATCCCTCG	62.2
3	*BMPR1B*	BMPR1B-1F	TGCGTGATACTTAGCAAGTACC	57.2
		BMPR1B-1R	GTGGTGAGAAACACTAACAGGC	58.8
4	*BMPR1B*	BMPR1B-2F	TTTATCCTGTGTCGAGCCTGTT	61.0
		BMPR1B-2R	TGGGTAGTTTTGAAGTCTGAAGC	59.8
5	*CHST3*	CHST3-F	TCTCTTGTCCCTGAGCGAG	59.2
		CHST3-R	TTGACGAAGGGCGTACAGA	60.4
6	*NPR2*	NPR2-F	GCCTATTTGTCCATGTCCTGCT	62.6
		NPR2-R	TATGCGTAGCCTCAGCTGGT	61.0
7	*NPR2*	NPR2-2F	CATCGCATGGGAGTCTCAAGT	62.5
		NPR2-2R	GTTGGGTCCGGTCAATGCTT	64.4
8	*EVC*	EVC-F	ATGCACAATCCTAGCAAGCAGG	63.7
		EVC-R	GCTGCAATTGGGCACAAGA	63.3
9	*ROR2*	ROR2-F	TGGCAAAATGAAGCGGAGTT	62.9
		ROR2-R	GAGGTGGAGAGTGGGTTGGTAG	62.2
10	*HOXD13*	HOXD13-F	TGGGCTTACAGCAGAATGCG	64.4
		HOXD13-R	TAACCCTGGTCACGTGTGGA	62.4
11	*GJA1*	GJA1-F	AGAAATACGTGAAACCGTTGGT	59.8
		GJA1-R	CAGTTTGGGCAACCTTGAGT	60.1

12	*GALNS*	GALNS-F	CAGGACACAGGCAGACAAG	**57.9**
		GALNS-R	ACAGCAGATGCAGGCAAG	**58.6**
13	*GNPTG*	GNPTG-F	TATGAGTTCTGCCCGTTCCA	**61.6**
		GNPTG-R	GTGAGCAAACCTTTCAGCCT	**59.5**

Ciliopathies

Ciliopathies are heterogenous and rare genetic diseases, affecting the skeleton, kidneys, retina, CNS, and liver (Waters & Beales. 2011). Ciliopathies are caused by mutations in primary cilium (Turan *et al*., 2023). Cilium is a hair-like projection with a microtubule backbone (axoneme) and a basal body (BB) that provides a base to anchor the cilium in the cell. The cilium regulates the bidirectional flow of cargo molecules along the microtubule backbone via intraflagellar transport (Quadri & Upadhyai. 2023). These cargo molecules play important roles in cilia-mediated signaling pathways. Ciliopathies are classified into primary and motile ciliopathies (Wheway *et al*., 2019).

Bardet-Biedl Syndrome

Bardet-Biedl Syndrome (BBS) is rare and heterogeneous congenital disease (Riise *et al*., 1997; Water & Beales. 2003; Forsythe and Beales, 2013). BBS inherits in autosomal recessive form, but there are some studies showing its triallelic inheritance pattern (Katsanis *et al*., 2001; Chen *et al*., 2011).

Primary clinical phenotypes of BBS include postaxial polydactyly, truncal obesity, hypogonadism, rod-cone dystrophy, cognitive impairment, and renal abnormalities (renal cystic dysplasia, anatomical malformation) (Putoux *et al*., 2012). BBS patients sometimes develop secondary features as well, i.e., diabetes mellitus, delayed growth, speech impairment and psychomotor delay, hearing loss, liver abnormality, strabismus, cardiac malformations, dental abnormality, brachydactyly/syndactyly (Abbas *et al*., 2023).

To date, 25 causative genes have been reported to cause BBS, which accounts for about 80% of BBS diagnoses (Dehani *et al*., 2021; Gupta *et al*., 2022). These genes are involved in assembly, maintenance and functioning of cilia which is the reason why clinical features of BBS patients overlap with other ciliopathies i.e., McKusick-Kaufmann syndrome, Joubert syndrome, Alstrom syndrome, Senior-Løken syndrome, Mainzer-Zaldino syndromes and Meckel-Gruber syndrome (Wheway *et al*., 2019).

Ellis van-Creveld Syndrome

Ellis-van Creveld Syndrome (EvC) is rare congenital skeletal disease The affected members have short stature due to rhizomelic shortening limbs, congenital heart defects, thoracic cage defects, digits and nails defects, leg and feet defects, and spine defects. (Baker & Beales. 2009; Alves Pereira, Berini-Aytés & Gay-Escoda; Niceta *et al*., 2009; Jan *et al*., 2018; Lauritano *et al*., 2019). While the craniofacial features may include hypoplastic zygomatic bone, frontal bossing, low-set ears, dysmorphic philtrum, and tooth abnormalities/hypodontia (Tuna *et al*., 2016; Lauritano *et al*., 2019; Peña-Cardelles *et al*., 2019). Due to overlapping clinical phenotypes with other syndromes, EvC is sometimes misdiagnosed (Parilla *et al*., 2003; Witters *et al*., 2008; Schramm *et al*., 2009).

EvC is caused by mutation in *EvC* and *EvC2* (4p16.2), separated by a 2.6Kb genomic region (Ruiz-Perez *et al*., 2000; Galdzicka *et al*., 2002). Both proteins form a complex, called EvC zone, in primary cilium, responsible for endochondral and intramembranous ossification (Dorn *et al*.,2012). EvC patients have mostly pathogenic variants in *EvC* gene than *EvC2* (D'Asdia *et al*., 2013). A total of 105 and 124 different pathogenic variants have been reported in *EvC* and *EvC2* respectively.

Robinow Syndrome

Robinow syndrome (RS) is rare genetic disease, characterized by short stature due to mesomelic shortening of limbs, facial dysmorphism, congenital heart defects, brachydactyly, vertebral anomalies, and genital defects (Afzal & Jeffery. 2003). The disease was clinically reported for the first time in a multi-generational non-consanguineous family (Robinow *et al*., 1969).

RS is heterogeneous disorder, inherited in autosomal dominant and recessive form, which can be caused by genes such as *ROR2*, *DVL1*, *WNT5A*, *DVL3, FZD2,* and *NXN* (Zhang *et al*., 2022). Variants in *ROR2* gene causes recessive form of Robinow syndrome. The *ROR2* gene is involved in various basic cellular processes (Afzal and Jeffery. 2003). All the reported genes for RS have functions in non-canonical WNT/Planer Cell Polarity (PCP) signaling pathway (White *et al*., 2018).

In the present chapter, two consanguineous families showing clinical features of ciliopathies were recruited and subjected to WES for disease-causing gene identification.

Family A

Family A belongs to district Swabi, Khyber Pakhtunkhwa Province, Pakistan. They willingly provided information regarding family history and facilitated pedigree drawing. The pedigree shows an autosomal recessive pattern of inheritance. It encompasses four generations, including two affected siblings (Fig. 3.1). The affected members show characteristic features of BBS (postaxial polydactyly, clinodactyly, retinitis pigmentosa) (Fig. 3.2).

Clinical Features

Affected male member (V-1) of family A manifests strabismus (Fig. 3.2a), bilateral $5^{th}/6^{th}$ fingers clinodactyly in hands (Fig. 3.2b), bilateral postaxial polydactyly in hands (Fig. 3.2b) and bilateral postaxial polydactyly in feet (Fig. 3.2c). Affected member (IV-3) has bulging eyes (Fig.3.2d), 5th & 6th finger clinodactyly in left hand (Fig. 3.2e), and bilateral postaxial polydactyly in hands and feet (Fig. 3.2 e, f).

Genetic Analysis

DNA of the affected male member (IV-1) of family A was subjected to whole exome sequencing (WES). Analysis of WES data identified homozygous missense variant [(c. T2A; p.M1K)] in *BBS5* in family A (Fig. 3.3). Sanger sequencing validated segregation of the identified variant in other family members (Fig. 3.3).

Family B

Family B belongs to district Swabi, Khyber Pakhtunkhwa (KPK), Pakistan. Information regarding family history and pedigree was collected from the family elders. The family shows first and second-cousin consanguinity and, hence, autosomal recessive pattern of inheritance. The pedigree consists of four generations including two affected members (Fig. 3.4). The clinical phenotypes of patients match best with Ellis-van Creveld Syndrome (EvC) and Robinow syndrome, i.e., short stature,

mesomelic shortening of limbs, facial dysmorphism, abnormal genitalia, hypodontia (Fig. 3.5).

Clinical Features

Affected members (V-1&2) of family B exhibit hypodontia, genu valgum, rhizomelic shortening of limbs, bilateral postaxial polydactyly and brachydactyly, lock elbow and knee joints and anonychia (Fig. 3.5 a-f). Affected male (V-1) has abnormal genitalia, a characteristic feature of Robinow Syndrome.

Genetic analysis

WES of the affected male member (V-1) of family B was performed. WES data analysis identified a previously reported homozygous splice site variant (c.1886+1G>T) in exon 13 of *EVC* gene and a novel heterozygous stopgain variant (c.C1204T: p.Q402X) in exon 8 of *ROR2* gene in family B (Fig. 3.6). Sanger sequencing confirmed segregation of the identified variant in other family members (Fig. 3.6).

Discussion

The present chapter highlighted clinical and genetic investigation of two consanguineous families (A&B) of Pakistani origin, exhibiting characteristic features of ciliopathies. WES of the affected member (IV-1) in family A identified a previously reported missense variant (c. T2A; p.M1K) in *BBS5*. BBS5 protein functions in ciliogenesis (contains two pleckstrin-homology domains to bind phosphoinositides), ciliary trafficking, and sonic hedgehog signal transduction regulation (Yuan *et al*., 2017). *BBS5* variants account for 2% of total BBS families from different populations (Hjortshoj *et al*., 2008). *BBS5* knockout mouse model has impaired glucose homeostasis, obesity and retinal morphology (Meehan *et al*., 2017). To date, three pathogenic variants have been identified in *BBS5* in Pakistani population including the variant in the present study (Khan *et al*., 2019). Variant (c. T2A; p.M1K) is assumed to disrupt gene function by leading to the creation of an aberrant initiation codon or preventing the normal initiation of BBS5 protein synthesis (Shao *et al*., 2022).

In family B, both affected members (V-1, V-2) exhibit clinical features of EVC, i.e., short stature, bilateral postaxial polydactyly and brachydactyly, anonychia, hypodontia. Since, the clinical features of EVC overlap with Robinow syndrome, the affected member (V-1) was further evaluated for confirmation of some additional clinical features, i.e., reproductive system development. Exome analysis of the affected member (V-1) identified previously reported homozygous splice site variant (c.1886+1G>T) in exon 13 of *EVC* and a novel heterozygous stop gain variant (c.C1204T:p.Q402X) in exon 8 of *ROR2* gene. Both variants are segregated in all available family members. The *EVC* variant is segregated in a recessive fashion, while the *ROR2* variant is presumed to exert its effects through the digenic way of inheritance.

EVC encodes for 992 amino acids protein that has a transmembrane, a coiled-coil, and multiple disordered regions. It is part of the EVC-EVC2 complex which is tethered to the base of primary cilia by EFCAB7 and IQCE (Pusapati *et al.*, 2014). It controls hedgehog (HH) signaling in chondrocytes by regulating Sufu/Gli3 interaction and Gli3 transport into primary cilia (Caparrós-Martín *et al.*, 2013). HH pathway, being a multipurpose process, also plays essential role in regulating cardiac development (Thomas *et al.*, 2008) and ectodermal structures (Hosoya *et al.*, 2020; Zheng *et al.*, 2019).

ROR2 encodes a 943 aa protein that has four domains (Ig-like C2-type, Frizzled, Kringle, Protein kinase) and a few regions of compositional bias and intrinsic disorder. ROR2 has been shown to act as a receptor for WNT ligands (Bainbridge *et al.*, 2014; Morioka *et al.*, 2009) to contribute to a noncanonical (WNT/ROR2) axis of WNT signaling (Si *et al.*, 2022). It also modulates the activity of canonical WNT signaling possibly by acting as a WNT co-receptor (Winkel *et al.*, 2008).

WNT signaling and cilia are interlinked (Niehrs *et al.*, 2024). The biogenesis of primary cilia is controlled by a WNT-PP1 axis (Zhang *et al.*, 2024). Primary cilium seems to be a converging point for *ROR2* and *EVC* functions. This is also evident from the overlapping features of Ellis-van Creveld syndrome and Robinow syndrome caused by variations in two genes (Figure 3). Both conditions in the affected individuals display distinct features which should be explained with recessive

inheritance. However, we have a heterozygous variant in *ROR2*, requiring a second variant to comply with a recessive inheritance. We hypothesize that the *ROR2* variant might be impactful in the presence of a homozygous *EVC* variant, fulfilling a recessive pattern with digenic inheritance. The digenic potential of *ROR2* and *EVC* is based on their functional proximity, phenotypic similarity, and prediction by ORVAL software that classified the digenic pair of variants as disease-causing.

The present study is peculiar in the sense that it presents a complex case with dual diagnosis as well as digenic inheritance. The distinct features of the two syndromes lead to dual diagnosis, whereas the dependence of the *ROR2* heterozygous variant on the *EVC* homozygous variant implies a digenic triallelic inheritance for the features of Robinow syndrome. Although rare, digenic triallelic inheritance has previously been reported in ciliopathies (Katsanis *et al*., 2001; Katsanis *et al*., 2002). In conclusion, we report two new variants in *EVC* and *ROR2* genes in a consanguineous family with Ellis-van Creveld syndrome and features of Robinow syndrome with a digenic inheritance pattern.
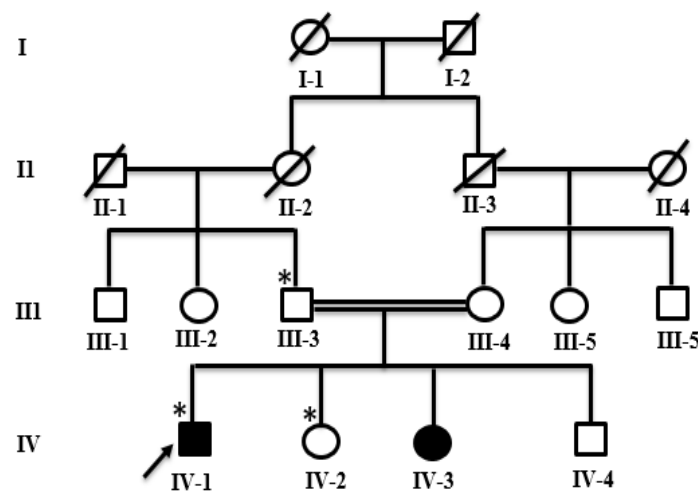
Fig. 3.1. Family A pedigree. Squares and circles indicate males and females. Empty and filled shades indicate normal and affected members. Double lines show consanguinity, while single lines indicate no consanguinity. Crossed lines over each square and circle indicate deceased individuals. The asterisk sign (*) indicates participated members, while the arrow shows a member subjected to WES.

Fig. 3.2. Clinical features of family A: Affected member (IV-1) manifesting strabismus (a), bilateral postaxial polydactyly in feet (b) and bilateral 5th/6th fingers clinodactyly and bilateral postaxial polydactyly in both hands (c). Affected member (IV-3) presenting bulging eyes (d), bilateral postaxial polydactyly in both feet and hands (e, f) and 5th/6th fingers clinodactyly in left hand (f).
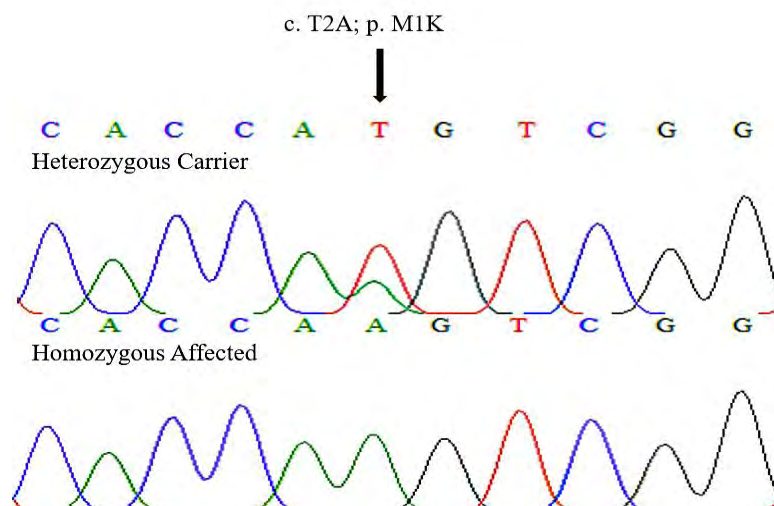
Fig 3.3. Sanger sequencing results of family A. The upper and lower panels show heterozygous carrier and homozygous affected member.
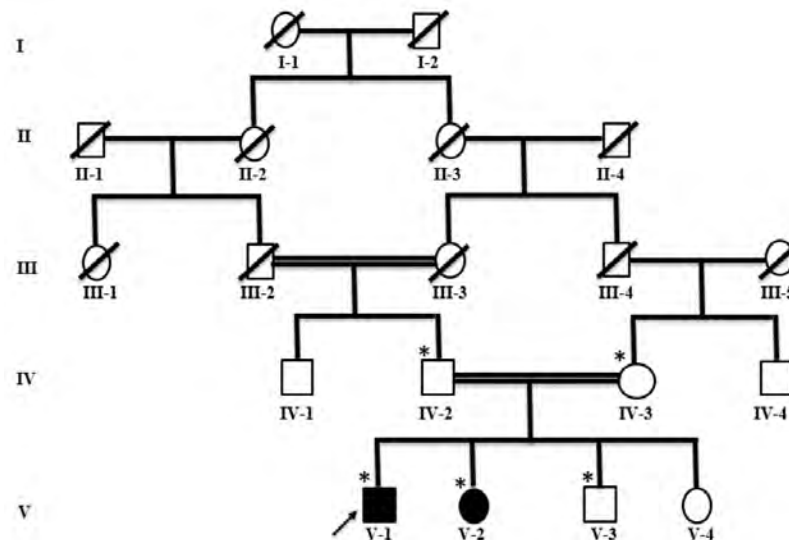
Fig. 3.4. Pedigree of family B. Squares and circles indicate males and females. Empty and filled shades indicated normal and affected members. Double lines show consanguinity, while single lines indicate no consanguinity. Crossed lines over each square and circle indicate deceased individuals. The asterisk sign (*) indicates members participated in the current research study, while the arrow shows a member subjected to WES.

Fig. 3.5. Clinical phenotypes of family B: Affected members (V-1) exhibiting hypodontia (a), genu valgum (b), rhizomelic shortening of feet and hands (b & c), bilateral postaxial polydactyly and brachydactyly in both upper and lower limbs (b & c), anonychia (b & c). X-ray radiographs of feet (d), knee joints (e) and hands (f).
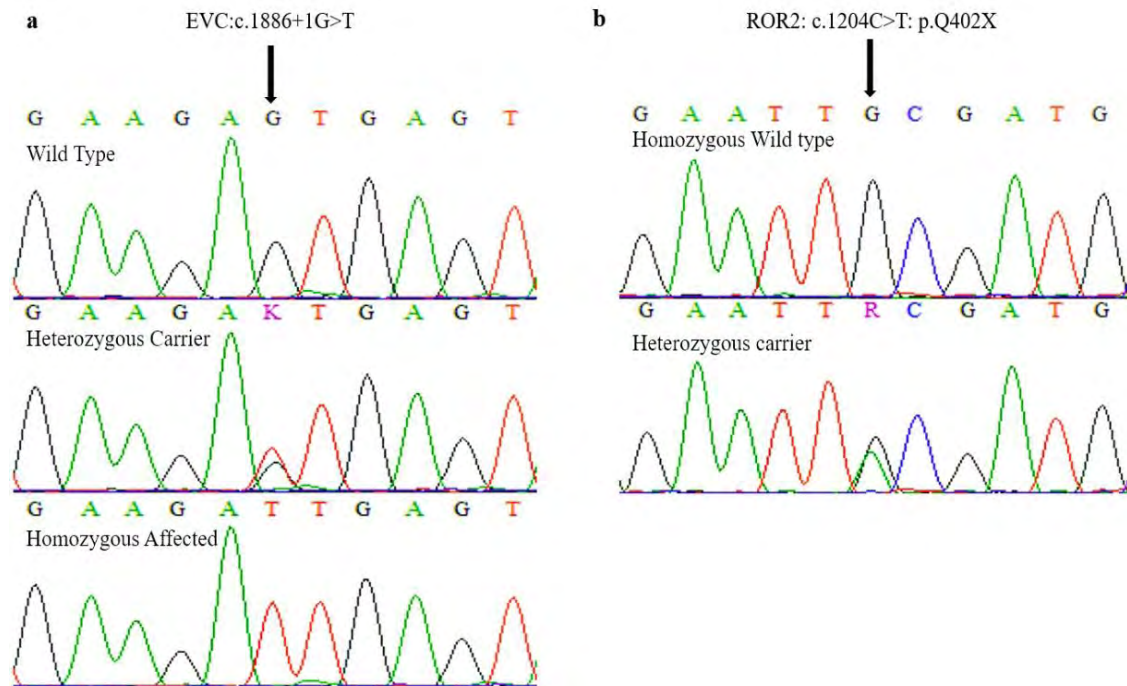
Fig. 3.6. Sanger sequencing results of family B. **(a)** Upper, middle, and lower panels show segregation of *EVC* variant (c.1886+G>T) in wildtype, heterozygous carrier and homozygous affected members. **(b)** The upper and lower panels show segregation of the *ROR2* variant (c.C1204T; p. Q402X) in wild type and heterozygous carrier.

Lysosomal Storage Diseases

Lysosomal storage diseases (LSDs) are metabolic diseases, caused by deficiency/malfunctioning of lysosomal enzymes involved in the degradation of glycosaminoglycans, lipids, and cholesterol. Disease-causing mutation in lysosomal enzymes results in LSDs have been further subclassified based on the biochemical nature of stored molecules, i.e., sphingolipidosis, mucopolysaccharidosis, glycogen storage diseases, lipid storage diseases, post-translational modification defects, integral membrane protein disorders, neuronal ceroid lipofuscinosis, and lysosomal related organelles (Schröder *et al*., 2007; Sleat *et al*., 2009; Palmieri *et al*., 2011; Chapel *et al*., 2013; Di Fruscio *et al*., 2015; Szklarczyk *et al*., 2015). LSDs are heterogenous both phenotypically and genotypically but share some overlapping characteristics visceromegaly/ spleenohepatomegaly and neurodegeneration (Parenti *et al*., 2015).

Mucopolysaccharidosis

Mucopolysaccharidosis (MPS) is clinically characterized by dwarfism, short trunk, coarse face, kyphosis, scoliosis, pectus carinatum, corneal clouding, joint contractures, mental retardation and macrocephaly (Neufeld. 2001; Muenzer. 2004). (Fesslova *et al*., 2009; Stapleton *et al*., 2017). In MPS, glycosaminoglycans (GAGs) accumulation cause developmental defects in bones and cartilage and bone ossification. These disruptions then lead to unique structural dysplasia. MPS is further divided into seven types: MPSI, MPSII, MPSIII, MPSIV, MPSVI, MPSVII, and MPS IX. In Pakistan MPS I is present most frequently, then MPS IV, MPS III, while MPS II is very rare (Cheema *et al*., 2017).

Mucolipidosis

Mucolipidosis (ML) is clinically characterized by coarse face, bulbous nose, gingival hyperplasia (Sprigz *et al*, 1978), prominent forehead, epicanthus, flat nasal bridge, anteverted nostrils, and macroglossia (Nishimura *et al*, 2002). ML patients have either not enough enzymes or harbor genetic defects, producing abnormal enzymes, and, hence, materials are stored in organs (brain, bones, visceral organs, muscle cells), causing skeletal deformity, mental retardation, and abnormal functions of liver, heart,

spleen and lungs, (https://www.ninds.nih.gov/Disorders/Patient-Caregiver-Education/Fact-Sheets/Mucolipidoses-Fact-Sheet (accessed on 29 July 2020).

ML is further divided into four subtypes; ML-I, II, III, and IV, based on the genes involved. Mucolipidosis-III (ML-III) is caused by mutation in *GNPTG*, encoding *N*-acetylglucosamine-1-phosphotransferase (GlcNAc-1-phosphotransferase). The characteristic phenotype may include skeletal dysplasia, short stature, joint stiffness, waddling gait, spinal deformity and pain in hands, shoulder, and hip, corneal clouding, mental retardation, and learning disability (Spranger & Wiedemann. 1970; Velho *et al*., 2019). Additional features may include cardiopulmonary complications, e.g., pneumonia, bronchitis, otitis media, and cardiac valvular diseases (Spranger & Wiedemann. 1970; Liu *et al*., 2016; Oussoren *et al*., 2018; Tüysüz *et al*., 2018).

In present chapter, three families (C, D & E) showing clinical phenotypes of LSDs were included. Affected members of family C & D exhibit MPS phenotypes i.e. short stature, joint contracture, macrocephaly, and genu valgum, while that of family D have Mucolipidosis exhibiting short stature, coarse face, genu valgum, pectus excavitum, short neck, corneal clouding, elbow and knee joint contractures, and stiffness.

Family C

Family C belongs to district Swabi, Khyber Pakhtunkhwa (KPK), Pakistan. Information regarding family history and pedigree was collected from the family elders. The family pedigree shows consanguinity. Family pedigree has five generations including four affected members (Fig. 4.1). The affected members (V-1 & 5) show characteristic features of Mucopolysaccharidosis type I (Hurler type) (Fig. 4.2).

Clinical Features

The affected members (V-1 & V-5) show short stature, macrocephaly, coarse face, full cheek, full lips, enlarged tongue, short neck, claw-hand deformity, umbilical hernia, joint stiffness, and contracture (Fig.4.2a, b & c).

Genetic Analysis

WES data analysis of affected male member (V-1) identified missense variant (c. T1073C; p. L358P) in exon 9 of *IDUA* in family C (Fig. 4.3). Sanger sequencing validated segregation of identified variant within the available family members (Fig. 4.3).

Family D

Family D belongs to district Swabi, Khyber Pakhtunkhwa (KPK), Pakistan. Information regarding family history and pedigree was collected from family elders. The family pedigree consists of two loops, having first cousin marriage. The pedigree has six generations including four affected members (Fig. 4.4). The affected members show characteristic features of Mucopolysaccharidosis type IV-A (Morquie type) (Fig. 4.5).

Clinical Features

In family D, affected members (VI-2, VI-4 & VI-10) show characteristics features of Mucopolysaccharidosis type IV-A i.e., short stature, genu valgum, pectus excavitum, short neck (Fig. 4.5a). Affected member (VI-9) shows normal height, but extended belly, pectus excavatum and joint contracture (Fig. 4.5b, c).

Genetic Analysis:

DNA of the affected member (VI-10) was subjected to WES. Analysis of WES data identified missense variant (c. C1259; p. P420R) in exon 12 of *GALNS* in family D (Fig. 4.6). Sanger sequencing confirmed segregation of identified variant within the family (Fig. 4.6).

Family E

Family E belongs to district Swabi, Khyber Pakhtunkhwa (KPK), Pakistan. Information regarding family history and pedigree was collected from family elders. The family pedigree shows consanguinity. The pedigree consists of eight generations including four affected members (Fig. 4.7).

Clinical Features

In family E, affected member (VI-1) show characteristics features of Mucolipidosis type-III, exhibiting short stature, coarse face, genu valgum, pectus excavitum, short neck, corneal clouding (Fig.4.8 a, b), elbow and knee joint contractures, and stiffness (Fig.4.8 c, d).

Genetic Analysis

WES data analysis of affected member (VI-1) identified a novel frameshift insertion variant (c. 477-478insGTAG; p. A160Vfs*39) in exon 7 of *GNPTG* in family E (Fig. 4.9). Sanger sequencing of available family members validated segregation of identified variant within family (Fig. 4.9).

Discussion

IDUA gene was mapped at chromosomal location 4p16.3 (Scott *et al*., 1990), spanning about 19kb genomic region, encompassing 14 exons and codes for 653 amino acids containing enzyme; α-L-iduronidase (Taylor *et al*., 1991; Scott *et al*., 1991 & 1992). The protein structure has three main domains; i.e., β/α$_8$ triose phosphate isomerase barrel domain, β sandwich domain and immunoglobulin-like domain (Saito *et al*., 2014). The α-L-iduronidase enzyme breaks complex polysaccharides/ glycosaminoglycans into simple subunits of dermatin and heparin sulfate. Malfunctioning/ absence of α-L-iduronidase enzyme causes partial/ complete non-decay of GAGs, resulting in their accumulation and consequently multiple organ damage.

The homozygous missense variant (c. T1073C; p. L490P) identified in exon 9 of *IDUA* in family C was earlier reported by Tieu *et al*., 1995, in patient-derived cell line (GM 00512) of Asian-Indian origin. Cos-1 cells transfected with cDNA containing T1073C showed no expression of gene product. The affected female, aged 15, exhibited clinical features of Hurler-Scheie type with deficient IDUA activity. A total of 221 different mutations (128 missense and nonsense, 16 insertion, 35 deletion, 36 splicing site variants, 1 mutation in regulatory region, 1 gross insertion-deletion, 1 indel, insertion-duplication, and three complex rearrangements) have been reported in

IDUA gene (http://www.hgmd.cf.ac.uk/ ac/gene.php?gene=IDUA. Accessed on 15-04-2019).

The *GALNS* gene (16q24.3) spans over the genomic region of 50kb, encompasses 14 exons, coding for a 60kDa glycopeptide, lysosomal enzyme; N-acetylgalactosamine-6-sulfate sulfatase, consists of 522 amino acids (Tomatsu *et al*., 1991; Masue *et al*., 1991; Masuno *et al*., 1993). GALNS is a homodimeric glycoprotein (Pshezhetsky & Potier. 1996) consists of two domains; domain-1(28-379 aa's) is the N-terminal domain that forms the hydrophobic core of enzyme, containing active site, domain-2 (380-481 aa's) consists of surface residues, forming antiparallel β-strands and C-terminal meander (482-510 aa's), which twist back towards N-terminal domain and form active site (Rivera-Colón *et al*., 2012). Homology modeling reveals the structural identity of GALNS protein to human arylsulfatase A (36%) and arylsulfatase B (28%) (Bond *et al*., 1997; Lukatela *et al*., 1998; Sukegawa *et al*., 2000). Due to the unique geometry of the active site, lysosomal sulfatases, especially GALNS, are capable of interacting with a variety of substrates containing sulfate groups *in vitro*, but this redundancy is lost *in vivo*, where each sulfatase interacts with the specific substrate (Rivera-Colón *et al*., 2012).

GALNS is found as a multiportion complex with other lysosomal enzymes (sialidase-1, β-galactosidase and protective protein/cathepsin-A (PPCA)) (Pshezhetsky & Potier. 1996; Adzhubei *et al*., 2010) and primarily involved in breakdown of GAGs, keratin sulfate and chondroitin-6-sulfate (Peracha *et al*., 2018). Biallelic variants in *GALNS* result in autosomal recessive metabolic disorder, MPS-TypeVI-A (Morquio disease) (Matalon *et al*., 1974; Nakashima *et al*., 1994). The homozygous missense variant (c. C1259G; p. P420R) mutation identified in the present study was previously reported (Morrone *et al*., 2014a). The mutation lies in domain 2 of GALNS, necessary for proper intermolecular contacts and protein folding. So, we can say that MPS IV-A is a protein-folding disease, resulting from disruption in protein folding. According to the HGMD database, 333 types of variants have been identified in the *GALNS*, including 248 missense/nonsense, 32 splice site variants, 32 small deletions, 5 small insertions, 3 complex rearrangements, and 2 small indels (http://www.hgmd. org, accessed on 21st October 2021).

GNPTG gene located at 16p13.3, spanning a genomic region of 11kb, containing 11 exons, encoding for γ-subunit of human *N*-acetylglucosamine-1-phosphotransferase (GlcNAc-1-phosphotransferase) (Raas-Rothschild *et al*., 2000). GNPTG is involved in substrate recognition and sorting, so any type of mutation causes MLIIIC, having reduced enzymatic activity (Kornfeld & Sly 1985). γ-subunit of GlcNAc-1-phosphotransferase consists of mannose-binding domain, destined for substrate selection (Lee *et al*., 2007; Van Meel *et al*., 2016) and proper transportation of lysosomal hydrolases (Lee *et al*., 2007; Qian *et al*., 2010; Di Lorenzo *et al*., 2018). GNPTG enzyme has a signal peptide (Raas-Rothschild *et al*., 2000), mannose-6-phosphate receptor homology domain (MRH) (Munro.2001; D'Alessio & Dahms.2015) and DMAP-1 interaction domain (Van Meel *et al*., 2016). MRH domain binds to the glycan moiety of the substrate to direct them towards the enzyme active site (Qian *et al*., 2010; Van Meel *et al*., 2016), while the DMAP-1 interaction domain binds to lysosomal hydrolases (Van Meel *et al*., 2016).

A total of 66 different types of mutations (31 missense/nonsense, 14 small deletions, 9 splicings, 9 small insertions, and 3 gross deletions) have been reported (HGMD. last accessed. April 2024). No mutation has been identified in exon 2 & 10. About 80% of mutations results in premature stop codon, causing non-sense mediated mRNA decay and, hence, deficiency or absence of enzyme.
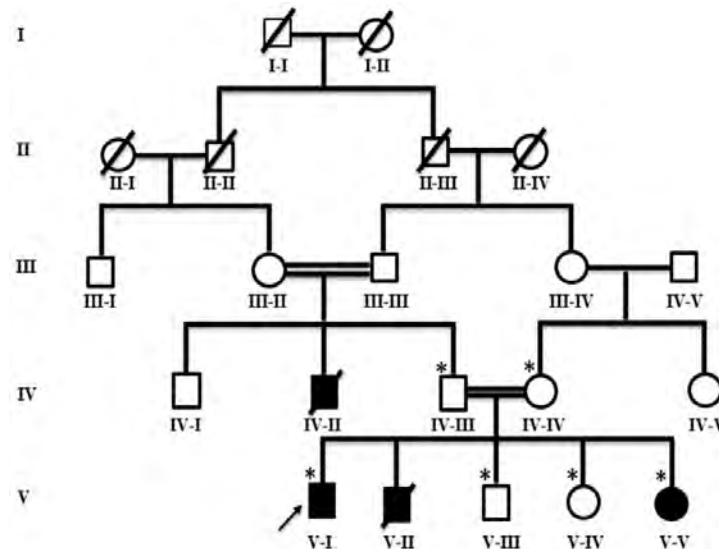
Fig. 4.1. Family C pedigree. Squares and circles indicate males and females, while empty and filled indicate normal and affected members. Double lines show consanguinity, while single lines indicate no consanguinity. Crossed lines over each square and circle indicate deceased individuals. The asterisk sign (*) indicates participated members, while the arrow shows a member subjected to WES.

Fig. 4.2. Clinical pictures of affected members (V-1 &5). The affected members (V-1) show short stature, macrocephaly, coarse face, full cheek, full lips, enlarged tongue, short neck, claw-hand deformity, broad nasal tip, umbilical hernia, joint stiffness, and contracture (a,b). Affected member (IV-5) also exhibits the same clinical features (c).
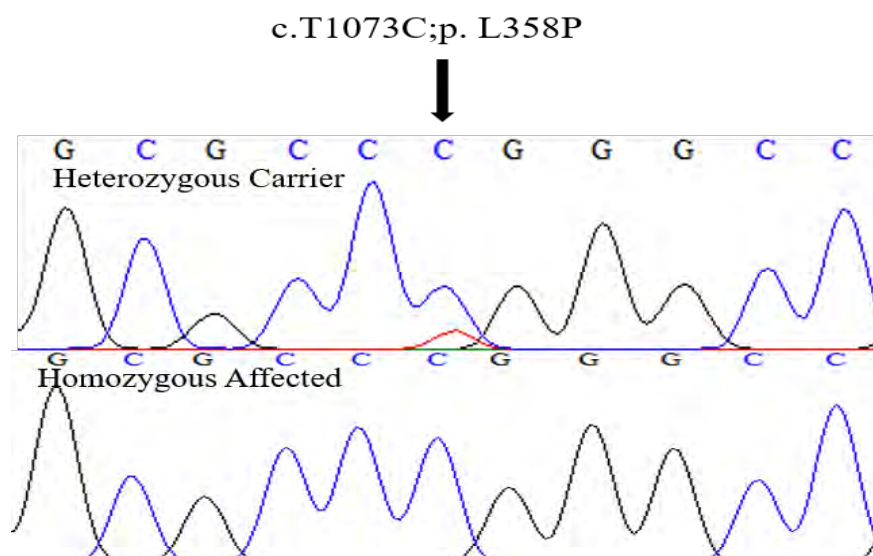
Fig. 4.3. Sanger Sequencing chromatogram. The upper and lower panels show heterozygous carrier and homozygous affected.
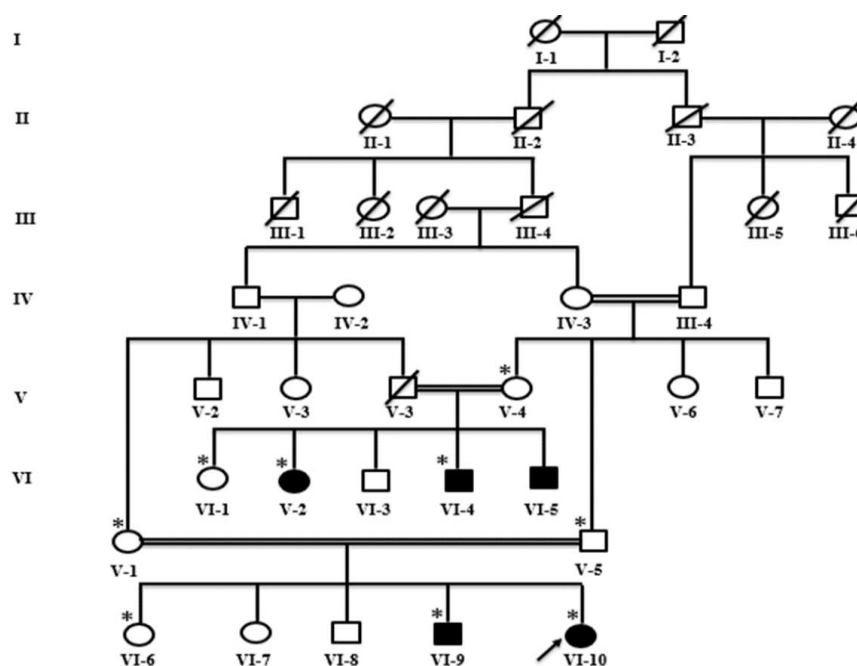
Fig. 4.4. Family D pedigree. Squares and circles indicate males and females, while empty and filled shades indicate normal and affected members. Double lines show consanguinity, while single lines indicate no consanguinity. Crossed lines over each square and circle indicate deceased individuals. The asterisk sign (*) indicates participated members, while the arrow shows member subjected to WES.

Fig. 4.5. Clinical phenotypes of affected members (VI-2, VI-4 & VI-10) of family D. short stature, genu valgum, pectus excavitum, broad mouth, short neck (Fig.4.5). Affected member (VI-4) show kyphosis and lordosis. Affected member (VI-9) shows normal height, but extended belly, pectus excavatum and joint contracture.
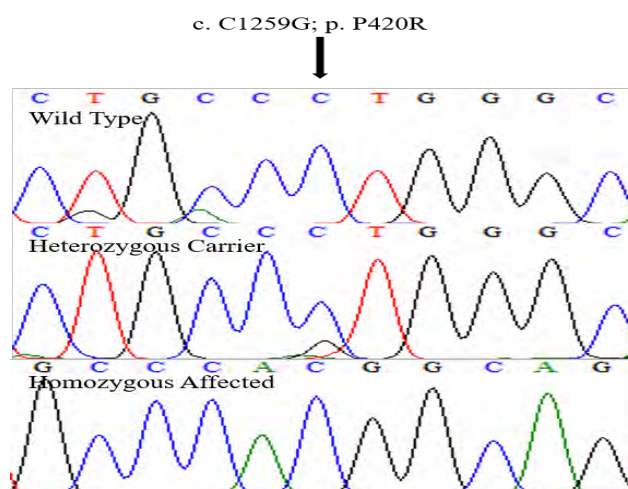
Fig. 4.6. Sanger sequencing chromatogram. Upper, middle, and lower panels show wild type, heterozygous carrier, and homozygous affected member respectively.
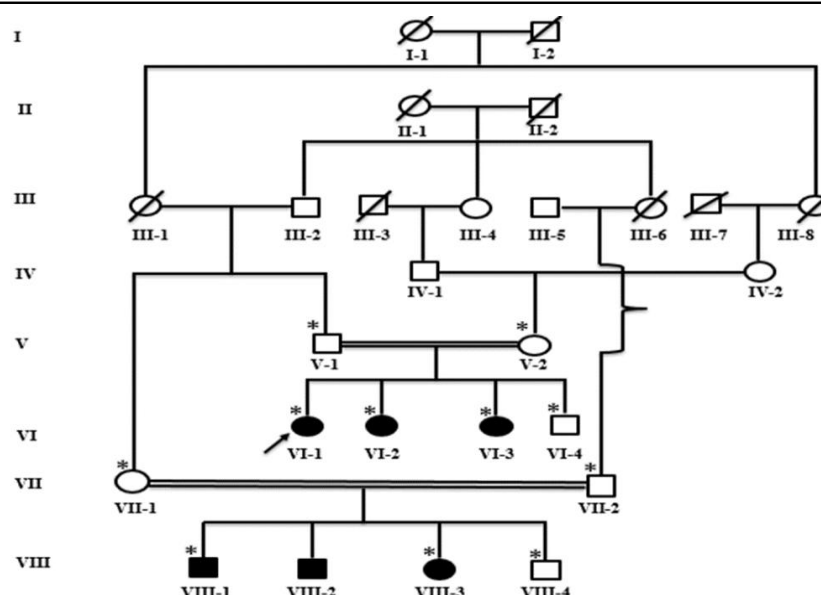
Fig. 4.7. Family E pedigree. Squares and circles indicate males and females. Empty and filled shades indicated normal and patients. Double lines show consanguinity, while single lines indicate no consanguinity. Crossed lines over each square and circle indicate deceased individuals. The asterisk sign (*) indicates members participated in the current research study, while the arrow shows a member subjected to WES.

Fig. 4.8. Clinical phenotypes of affected member (VI-1) of family E. The affected members show characteristics features of Mucolipidosis type-III, short stature, coarse face, pectus excavitum, short neck, mental retardation, corneal clouding (a), full mouth, large tongue and hypodontia (b), genu valgum, elbow and knee joint contractures and stiffness (c,d).

GNPTG
c. 477-478insTAGG; p. A160Vfs*39
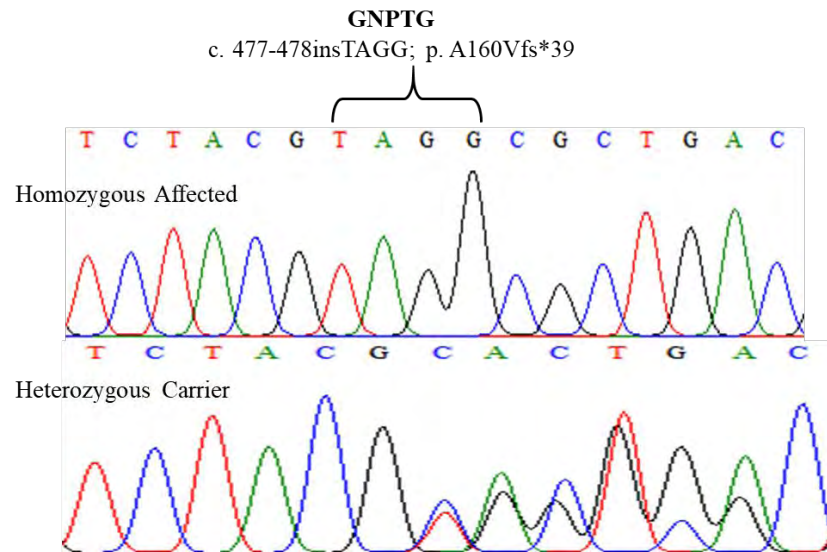
Fig. 4.9. Sanger sequencing results of family E. The upper and lower panels show homozygous affected and heterozygous carrier respectively.

Spondyloepiphyseal Dysplasia

Spondyloepiphyseal dysplasia (SED) is a multisystemic skeletal disorder, characterized by dwarfism, skeletal deformities (club feet, joint dislocations, platyspondyly, end plate irregularities, increased interpedicular distance, kypo-scoliosis, irregular epiphysia,), problems with vision and hearing, and cardiac involvement (Tuysuz *et al*., 2009; Unger *et al*., 2010). Based on mode of inheritance and age of onset, SED has been classified into two types: SED congenital (SEDC) and SED tarda (SEDT). SEDC inherits in autosomal dominant and recessive form but can also be caused by *de novo* mutation in *COL2A1* and *CHST3* gene (Unger *et al*., 2010). CHST3-type SEDC is an autosomal recessive, and progressive skeletal deformity. The clinical symptoms start to appear in infancy and fully develop in adulthood (Rajab, Kunze & Mundlos. 2004). SEDT is X-linked (Maroteaux *et al*., 1957) and caused due to mutation in *SEDL* or *TRAPPC2* (Szpiro-Tapia *et al*.,1988).

In the present study, family F was recruited, exhibiting features of SEDC (short stature, joint contracture, pectus excavatum, clubfeet), was subjected to WES followed by Sanger sequencing.

Family F

Family F belongs to district Swabi, Khyber Pakhtunkhwa (KPK), Pakistan. Information regarding family history and pedigree was collected from family elders. The family history shows no consanguinity. The pedigree consists of two generations (Fig. 5.1). The affected members show clinical features of spondyloepiphyseal dysplasia (Fig. 5.2).

Clinical Features

Both affected members (II-3 & 4) of family F show severe short stature, deformed and dislocated joints, pectus excavatum, short neck, hunched shoulders, joint dislocation, elbow and knee joint stiffness, and club feet (Fig. 5.2 a, b).

Genetic Analysis

DNA of the affected member (II-4) was subjected to WES. Analysis of WES data revealed previously reported duplication (c. 528dupG; p.A179Rfs*141) in exon 3 of *CHST3* (Fig. 5.3). Sanger sequencing of available family members validated segregation of identified variant (Fig. 5.3).

Discussion

CHST3 gene, located on chromosome 10q22.1, encodes 6-O-sulfotransferase-1 or C6ST-1 enzyme, which belongs to a family of carbohydrate sulfotransferase (also known as chondroitin-6-sulfotransferase 3) family of 15 enzymes which are involved in transfer of sulfate group from 3′-phospho-5′-adenylyl sulfate (PAPS) to position-6 carbohydrate moieties of glycolipids and glycoproteins (Tsutsumi *et al*., 1998). C6ST-1 enzyme is essential for the sulfation of proteoglycan; chondroitin, found in cartilages of extracellular matrix. Loss of function mutation in the *CHST3* gene results in chondrodysplasia with severe spinal damage. C6ST-1 enzyme plays critical role in the development and preservation of skeleton (van Roij *et al*., 2008).

The identified variant (c. 528dupG; p.A179Rfs*141) has been previously reported in an Indian family (Srivastava *et al*., 2017), where the patients exhibit abnormal knee epiphyses (epiphyses of lower end of femora are triangular with deep intercondylar notch), larges and squared metacarpals epiphyses, mild sclerosis around cranial sutures. The reported variant lies in a highly conserved PAPS-binding site, essential for the transfer of the sulfate group. To date, 62 patients have been reported with C6ST-1 enzyme deficiency (Duz & Topak. 2020; Kauser *et al*., 2022). To date, 48 variants have been reported in *CHST3* (www. Hgmd. cf. ac. uk accessed May 2022).
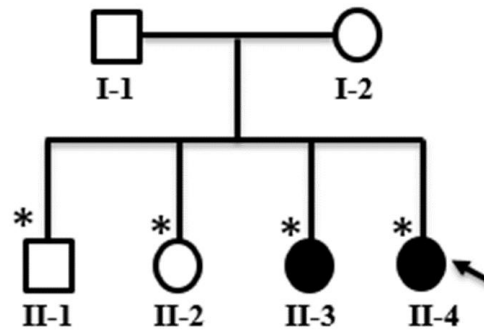
Fig. 5.1. Pedigree of Family F. Squares and circles indicate males and females. Empty and filled shades indicated normal and affected members. Single line between parents indicates no consanguinity. The asterisk sign (*) indicates participated members while arrow shows a member subjected to WES.

Fig. 5.2. Phenotypes of family F. Both affected members (II-3 &4) show severe short stature, deformed and dislocated joints, pectus excavatum, elbow and knee joint stiffness, and club feet (a, b).

c. 528dupG;p.A179Rfs141
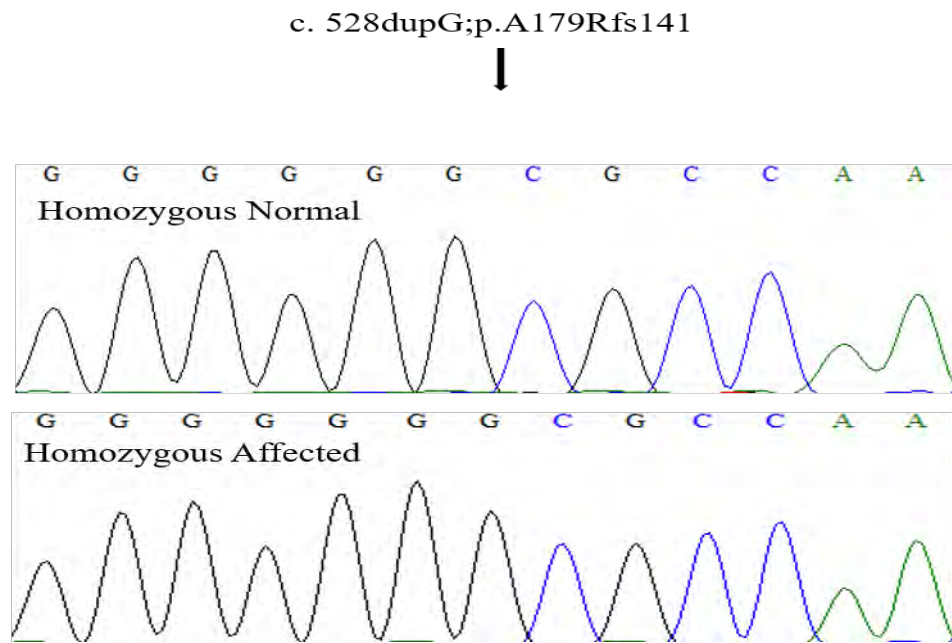
Fig. 5.3. Sanger sequencing results of family F. The upper and lower panels show homozygous wild type and affected members, respectively.

Syndactyly

Syndactyly involves the fusion of adjacent digits (fingers and toes) in the upper and lower limbs (Malik 2012). Syndactyly may either exist in isolated or syndromic form (Chopra *et al*., 2013). Isolated syndactyly is further divided into nine different types (SD I-IX) (Malik *et al*., 2005), while the syndromic form is associated with more than 300 other genetic abnormalities (Malik 2012). Isolated syndactyly has been classified into simple or mild/complicated or severe, complete/incomplete, isolated/complex, unilateral/ bilateral, and symmetrical/asymmetrical types (Malik 2012). Syndactyly is inherited in autosomal dominant form (Eaton & Lister. 1990), autosomal recessive; SD-7 & 9 (Malik 2012), and X-linked recessive fashion; SD-5 (Lonardo *et al*., 2004). Autosomal dominant forms of SD exhibit less severity, incomplete penetrance, and variable expressivity. In SD familial pattern of inheritance is seen in 10-40% of the cases (Green *et al*., 2005; Netscher and Baumholtz, 2007) with variable expressivity and penetrance, predominantly affecting males (Green *et al*., 2005; Canale and Beaty, 2008), while remaining cases are sporadic. In scientific literature, mutations in different genes (*HOXD13, GJA1, FBLN1, ZRS/LMBR1, FGF16*) and several loci (*GREM1-FMN1*15q13.3, 2q34-q36, 14q11.2-q13, 17p13.3) have been reported. Recently, mutations in two additional genes: *SEMA3D* and *ALDH1A2*, have been documented to cause non-syndromic syndactyly (Elsner *et al*., 2021).

In the present two families (G & H) exhibiting syndactyly were recruited, subjected to WES followed by Sanger sequencing.

Family G

Family G belongs to district Swabi, Khyber Pakhtunkhwa (KPK), Pakistan. Information regarding family history and pedigree was collected from family elders. The pedigree shows the autosomal dominant nature of inheritance. The pedigree consists of six generations (Fig. 6.1). The affected members show varying degrees of syndactyly, and synpolydactyly (Fig. 6.2).

Clinical Features

Affected member (V-3) shows synpolydactyly in the right hand only (Fig. 6.2 a, b), while affected member (V-1) has complete cutaneous syndactyly in the left hand and camptodactyly of 5th finger (Fig. 6.2 c, d).

Genetic Analysis

Analysis of WES data of the affected member (V-3) identified previously reported stop gain variant (c. c.C742T; p.Q248X) in exon 1 of *HOXD13* (Fig. 6.3). Sanger sequencing validated segregation of identified variant (Fig. 6.3).

Family H

Family H belongs to district Swabi, Khyber Pakhtunkhwa (KPK), Pakistan. Information regarding family history and pedigree was collected from family elders. The family history shows consanguinity. The pedigree consists of five generations, including three affected females (Fig. 6.4). The affected members show syndactyly type IV-A (Fig.6.5).

Clinical Features

All the affected members (IV-4, V-1, V-2) show 4/5th complete cutaneous syndactyly in both hands only (Fig. 6.5 a-c).

Genetic Analysis

WES of the affected female member (IV-4) was performed. Analysis of WES data revealed previously reported missense variant (c.C226T; p.R76C) in exon 1 of *GJA1*(Fig. 6.6). Sanger sequencing of all available family members validated segregation of identified variant within the family (Fig. 6.6).

Discussion

HOXD13 gene belongs to a large family of genes, called the *HOX* gene family, grouped into four major types, i.e., *HOXA*-D, comprising of 39 genes. All these gene clusters are located in 3′-5′ direction on chromosomes 2q31, 12q13, 7p14, and 17q21

(Deng *et al*., 2015). During early developmental stages, 3′ genes are expressed only, while 5′ genes are expressed in later stages (Zhou *et al*., 2013; Brison *et al*., 2014).

In family G, affected members show heterogenous phenotypes of syndactyly, i.e., unilateral synostotic synpolydactyly, unilateral complete cutaneous syndactyly, bilateral complete synostotic syndactyly in both hands and feet, campodactyly. *HOXD13* gene is ubiquitously expressed in limb buds, genital tubercle, and trunk and consists of two exons encoding 343 amino acid protein. The functional domain has 45bp trinucleotide repeats in the first exon encoding 15 alanine amino acids tract, also known as polyalanine tract. The protein also has a conserved homeobox domain in exon 2 and a C-terminal DNA-binding motif.

Three types of mutations (missense, truncation, and polyalanine tract expansion), have been reported in *HOXD13* (Dai *et al*., 2014). Expansion or retraction in the polyalanine tract leads to the retention and aggregation of distorted protein in the cytoplasm. This phenomenon acts in a dominant negative fashion in association with other polyalanine-containing proteins (HOXA13, RUNX2) (Albrecht *et al*., 2004). Loss of function mutations (frameshift & nonsense) affects DNA binding ability, while missense mutation impairs transcriptional activation of the targeted gene. Clinical phenotypes of homozygous mutations in *HOXD13* are more severe than heterozygous mutations (Muragaki *et al*., 1996; Ibrahim *et al*., 2016).

In family H, all the affected females (IV-4, V-1 & V-2) have bilateral 4th /5th fingers complete cutaneous syndactyly in both hands, while toes are unaffected. Exome data analysis of the affected member (VI-4) revealed previously reported heterozygous, missense variant (c.C226T; p. R76C) in exon 2 of *GJA1*.

GJA1 encodes for gap junction α-1 protein, Connexin-43 (Cx43), which belongs to connexin protein family having 21 members (Paznekas *et al*., 2003). Six connexin proteins polymerize to form a hemichannel/connexon on the cell surface, which combine with another hemichannel on an adjacent cell forming a complete gap junction, allowing neighboring cells to exchange ions, secondary messengers, and other molecules having a molecular weight below 1KDa (Söhl & Willecke. 2004). This cell-cell communication is necessary both in normal physiology and embryonic

development; i.e., trophoblast cell differentiation, cell proliferation, and apoptosis (Levin. 2002; Cheng *et al*, 2015).

Mutations in *GJA1* causes typical/atypical ODDD, isolated SD3, and Hallermann-Streiff/ODDD phenotypes (Vitiello *et al*., 2005). Among syndactyly patients, 43% have isolated SD3 (Gladwin *et al*., 1997), while 25% of ODDD patients have additional features of toe syndactyly (Paznekas *et al*., 2009). SD3 is inherited in autosomal dominant form, due to dominant negative effect of *GJA1*, resulting in defective channel formation. The missense mutation (c.C226T; p. R76C) reported in the current study has been previously reported in patients, experiencing ODDD phenotypes, pulmonary atresia, and coronary heart disease (CHD) (Izumi *et al*., 2013). The patients in the present family experience no other anomaly (craniofacial, ocular, and dental abnormality) except SD3. The same clinical phenotypes (bilateral 4/5 finger syndactyly) have also been reported in a Chinese family (You *et al*., 2016). All these depict the heterogeneous clinical spectrum of *GJA1* mutation.

Another study also confirmed the association of ODDD with CHD, especially pulmonary stenosis in Cx43 in null mice (Reaume *et al*., 1995). Although missense mutations in mice didn't develop any signs of cardiac malformations (Flenniken *et al*., 2005; Kalcheva *et al*., 2007; Dobrowolski *et al*., 2008), arrhythmia and abnormal cardiac conduction were observed, as reported in OCD patients (Paznekas *et al*., 2003).
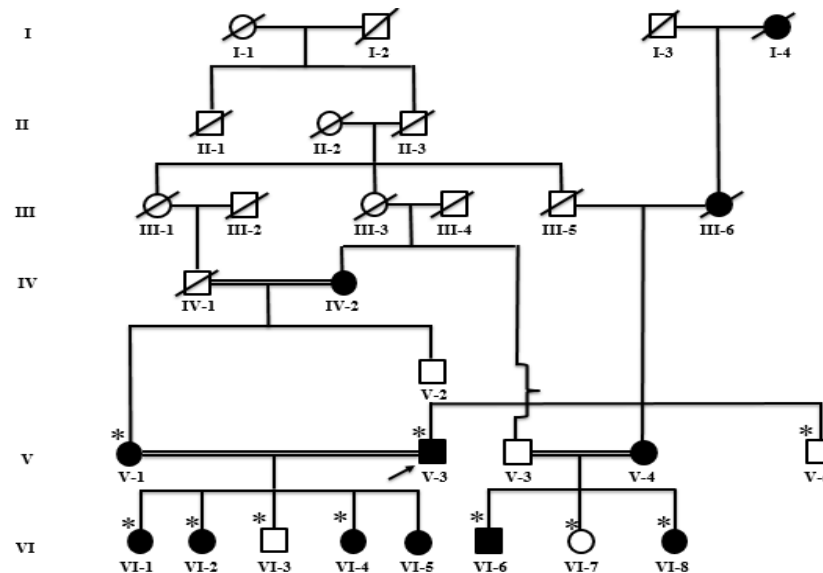
Fig. 6.1. Family G pedigree. Squares and circles indicate males and females. Empty and filled shades indicate normal and affected members. Double lines show consanguinity, while single lines indicate no consanguinity. Crossed lines over each square and circle indicate deceased individuals. The asterisk sign (*) indicates participated members, while arrow shows affected member subjected to WES.

Fig. 6.2. Clinical Phenotypes of Family G. Affected member (V-3) shows synpolydactyly in the right hand only (a,b), while affected member (V-1) has complete cutaneous syndactyly in the left hand and camptodactyly of 5th finger (c,d).
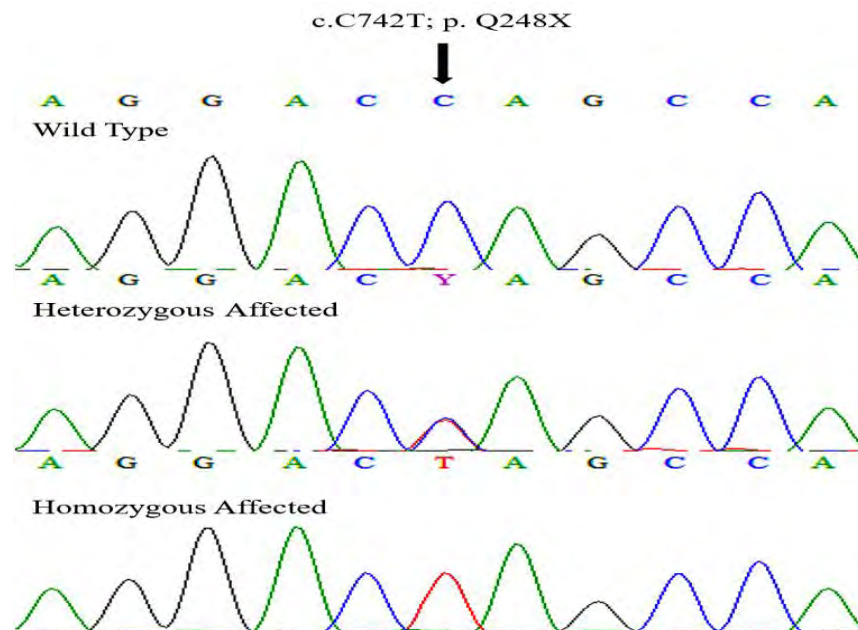
Fig. 6.3. Sanger sequencing results of family G. Upper, middle, and lower panels show wild type, heterozygous affected, and homozygous affected members.
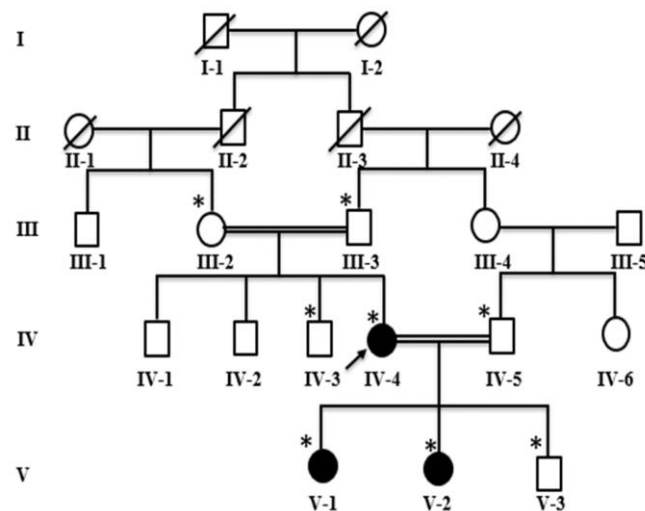
Fig. 6.4. Family H pedigree. Squares and circles indicate males and females. Empty and filled shades indicate normal and affected members. Double lines show consanguinity, while single lines indicate no consanguinity. Crossed lines over each square and circle indicate deceased individuals. The asterisk sign (*) indicates participated members, while arrow shows patient subjected to WES.

Fig. 6.5. Phenotypes of family H. All affected members (IV-4, V-1, V-2) show 4/5th complete cutaneous syndactyly in both hands.
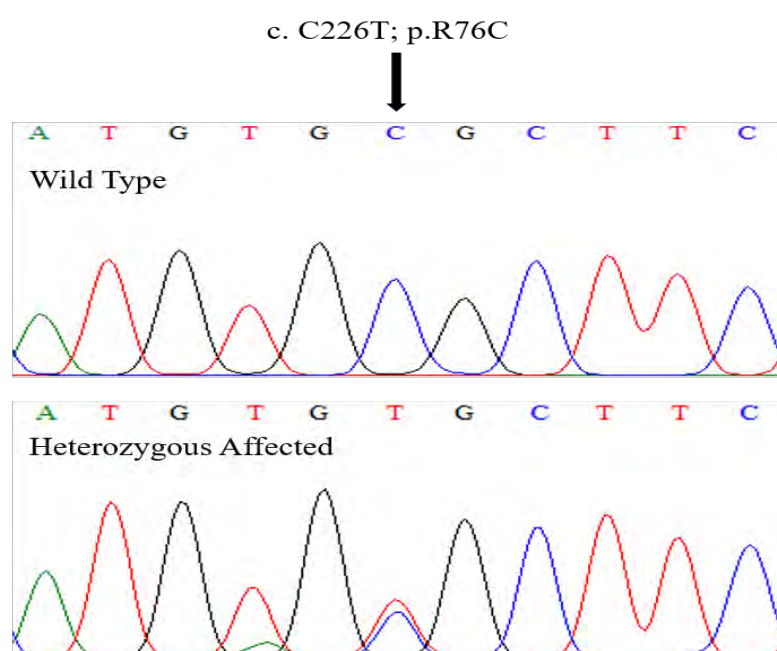
Fig. 6.6. Sanger sequencing results of family H. Upper and lower panels show homozygous normal and heterozygous affected members respectively.

Acromesomelic Dysplasia

Acromesomelic dysplasias (AMDs), also known as osteochondrodysplasias (OCD) is a group of congenital skeletal dysplasia, mainly affecting appendicular skeleton and, hence, affected members have disproportionate dwarfism. Acromesomelic dysplasia inherits in autosomal recessive fashion. AMDs has been further divided into six different types, namely AMD-Grebe type/AMDG (Grebe. 1952), AMD-Maroteaux type/AMDM (Maroteaux. 1971); AMD- Hunter and Thompson type/AMDH (Hunter & Thompson. 1976), acromesomelic dysplasia Osebold-Remondini type (Osebold *et al*., 1985), fibular hypoplasia and complex brachydactyly type /Du pan dysplasia (Mortier *et al*., 2019) and recently discovered novel type, acromesomelic dysplasia PRKG2 type (AMDP) (Dîaz-Gonzalez *et al*., 2022).

Acromesomelic Dysplasia- Maroteaux type:

Acromesomelic dysplasia-Maroteaux type (AMDM) is sub-group of AMD, where the affected member has disproportionate short stature due to defective development of middle and distal skeletal elements of appendicular skeleton, and a dolichocephalic head without any facial or mental abnormalities (Umair *et al*., 2015). In AMDM patients, there is also involvement of axial skeletal elements; and wedging of vertebral bodies (dorsal margins being shorter than ventral).

AMDM is inherited in autosomal recessive pattern and caused by mutation in *NPR2* which encodes natriuretic peptide receptor 2. Natriuretic peptide receptors (NPRs) are specific cell surface receptors that binds to natriuretic peptide hormones and regulate different physiological processes, i.e., heart development, axonal pathfinding, and endochondral ossification (Kishimoto *et al*., 2001; Tamura *et al*., 2004; Langenickel *et al*., 2006).   There are three distinct types of NPRs, namely NPR-A, B & C, expressed on surfaces of different types of cells (Kishimoto *et al*., 2001). For example, NPR-B is expressed on the surface of different cells; i.e., chondrocytes, blood vessels, heart, uterus, and brain (Pagel-Langenickel *et al*., 2007) and acts as a receptor (homodimeric transmembrane receptor) for C-type natriuretic peptide (CNP) (Koller and Goeddel. 1992), acting in autocrine and paracrine manner in variety of tissues (Schulz. 2005). CNP binding causes the generation of cytoplasmic cGMP from

GTP in chondrocytes via guanylyl cyclase activity (Lincoln and Cornwell. 1993), which in turn activates type-II cGMP-dependent protein kinase (Vasques *et al*., 2014) stimulating chondrocytes differentiation into bone-forming cells, hypertrophy and matrix synthesis (Schulz. 2005; Potter *et al*., 2006; Miura *et al*., 2014; Vasques *et al*., 2014).

Acromesomelic Dysplasia-Grebe type:

Acromesomelic dysplasia-Grebe type (AMDG) is clinically characterized by dwarfism and severe micromelia and acromesomelia (Grebe. 1952). Other features may include short hands with toe-like fingers and valgus deformity (Thomas *et al*., 1997), ulnar hypoplasia, the fusion of carpals, metacarpals, tarsals, and metatarsals and missing proximal and middle phalanges, short nick, absence of tibia and diaphysis of fibula (Costa *et al*., 1998; Faivre *et al*., 2000). The afflicted individuals' intelligence and facial traits are not affected (Martinez-Garcie *et al*., 2016; Khan *et al*., 2016). AMDG is caused due to mutations in *CDMP1* gene (2q11.22) (Thomas *et al*., 1997; Faiyaz-Ul-Haque *et al*., 2002; Al-Yahyaee *et al*., 2003; Basit *et al*., 2008; Martinez-Garcia *et al*., 2015) and *BMPR1B* gene (4q22.3) (Graul-Neumann *et al*., 2014).

In the present chapter, two consanguineous families (I & J) showing AMDM phenotypes (dwarfism, joint contracture, dolichocephalic head) and three families (K, L & M) showing AMDG phenotypes (disproportionate dwarfism, brachydactyly, and shortened long bones) were included.

Family I

The family I belong to district Swabi, Khyber Pakhtunkhwa (KPK), Pakistan. Information regarding family history and pedigree was collected from family elders. The family pedigree shows consanguinity and hence autosomal recessive mode of inheritance. The pedigree consists of four generations (Fig. 7.1). The affected members show acromesomelic dysplasia-Maroteaux type (Fig. 7.2).

Clinical Features

Affected member (IV-1) shows short stature, dolichocephalic head (Fig. 7.2a), bowed legs (Fig. 7.2 a, b), dislocation and stiffness of elbow joints (Fig. 7.2 c, d), and severe bilateral brachydactyly of both hands (Fig.7.2 c, d) and feet (Fig.7.2 e, f).

Genetic Analysis

Analysis of the WES data of the affected member (IV-1) revealed a previously reported stop gain variant (c.C2761T:p.R921X) in exon 19 of *NPR2* (Fig. 7.3). Sanger sequencing of all available family members validated segregation of the identified variant within the family (Fig. 7.3).

Family J

Family J belongs to district Swabi, Khyber Pakhtunkhwa (KPK), Pakistan. Information regarding family history and pedigree was collected from family elders. The family history shows consanguinity. The pedigree consists of six generations (Fig. 7.4). The affected members show acromesomelic dysplasia-Maroteaux type (Fig. 7.5).

Clinical Features

All the affected members (IV-1) show short stature, dolichocephalic head (Fig. 7.5a), dislocation and stiffness of elbow joints (Fig.7.5 b, c, e, f), and bilateral brachydactyly of both hands (Fig. 7.5b) and feet (Fig. 7.5 a, d).

Genetic Analysis

WES of the affected member (VI-1) identified a novel stop gain variant (c.A2059T; p. K687X) in exon 14 of *NPR2* in family J (Fig. 7.6). Sanger sequencing confirmed segregation of identified variant within the family (Fig. 7.6).

Family K

Family K belongs to district Swabi, Khyber Pakhtunkhwa (KPK), Pakistan. Family elder provided information regarding history and pedigree. The family history shows

no consanguinity. The pedigree consists of three generations (Fig. 7.7). The affected members show acromesomelic dysplasia-Grebe type (Fig. 7.8).

Clinical Features

Affected member (II-1) shows disproportionate short stature (Fig. 7.8a), severe bilateral brachydactyly in both hands (Fig. 7.8b) and feet (Fig. 7.8d), delocalized elbow joints (Fig. 7.8c), bowed and short hummer, fibula and patella (Fig.7.8 d, e).

Genetic Analysis

WES data analysis of the affected member (II-1) identified a novel four-base deletion (c. 398-401del; p. C135Vfs*28) in exon 5 of *BMPR1B* in family K (Fig. 7.9). Sanger sequencing of all available family members validated segregation of identified variant (Fig. 7.9).

Family L

Family L belongs to district Swabi, Khyber Pakhtunkhwa (KPK), Pakistan. Family members provided information regarding family history and pedigree. The family history shows consanguinity. The pedigree consists of four generations (Fig. 7.10). The affected members show acromesomelic dysplasia-Grebe type (Fig. 7.11).

Clinical Features

Affected member (IV-1) show short stature (Fig. 7.11a), severe bilateral brachydactyly in both hands (Fig. 7.11b) and feet (Fig. 7.11c), bowed and short fibula and patella (Fig.7. 11c). The affected member (Fig. 7.11, IV-2) also exhibits short stature, bilateral brachydactyly in both the upper and lower limbs (Fig. 7.11 d, e), and bowed feet (Fig. 7.11e).

Genetic Analysis

Homozygosity mapping using microsatellite markers show linkage to *BMPR1B*. All the coding exons were Sanger sequenced. Sequencing data analysis identified a novel four-base deletion (c. 398-401del; p. C135Vfs*28) in exon 5 of *BMPR1B* in family K (Fig. 7.12). Sanger sequencing of other available family members validated segregation of identified variant (Fig. 7.12).

Family M

Family M belongs to district Swabi, Khyber Pakhtunkhwa (KPK), Pakistan. Family elders provided information regarding family history and pedigree was drawn, showing consanguinity. The pedigree consists of four generations (Fig. 7.13). The affected members show acromesomelic dysplasia-Grebe type (Fig. 7.14).

Clinical Features

Affected member (IV-1) shows disproportionate short stature (Fig. 7.14a), severe bilateral brachydactyly in both hands (Fig. 7.14b) and feet (Fig. 7.14 c, d), delocalized elbow joints (Fig. 7.14c), bowed and short humer, fibula and patella (Fig. 7.14 c, d).

Genetic Analysis

Microsatellite-based homozygosity mapping established linkage to *BMPR1B*. Sanger sequencing of affected member (IV-1) revealed a novel four-base deletion (c. 398-401del; p. C135Vfs*28) in exon 5 of *BMPR1B* in family M (Fig. 7.15). Sanger sequencing of all available family members validated segregation of identified variant within the family (Fig.7.15).

Discussion

In the present research study, WES of Family I & J identified one previously reported (c.C2761T:p.R921X), and one novel variant (c.A2059T; p. K687X) in *NPR2* respectively. In families (K, L & M) a novel homozygous variant (c. 398-401del; p. C135Vfs*28) was identified and has successfully segregated in all family members.

Human *NPR2* gene comprises a genomic region of 16.5kb, having 22 exons encoding for 1047 amino acids protein (Kant *et al.,* 1998). The encoded natriuretic peptide receptor-2 has an extracellular ligand binding domain (450 aa's), a single transmembrane hydrophobic domain (20 aa's), and intracellular domain (570 aa's) (Potter *et al*., 2006). The intracellular domain is further divided into three domains, namely kinase homology domain/KHD (250-260 aa's), coiled-coil dimerization domain (40aa's), and C-terminal guanylyl cyclase domain/GC (250aa's) (Tamura & Garbers. 2003). Both NPR-A & B exert their effects through the GC domain.

The reported variant, c.C2761T:p.R921X, in the family I is present in homozygous form in affected members, and lies in C-terminal guanylyl cyclase domain, resulting in loss of function of protein due to premature truncation codon. The identified variant was previously reported in AMDM patients in compound heterozygous condition by Wang *et al*., 2015 in a non-consanguineous family, and in heterozygous form in a mother and her daughter afflicted with short stature and skeletal dysplasia by Jacob *et al*., 2018. In contrast to the previous study, where the AMDM patient's height was 123cm (Wang *et al*., 2015), the mother (146cm) and daughter (117.5cm), in the present family, the heights of both affected members are 106.68 c, 93.878 cm respectively, indicating the fact that homozygous variant has more drastic effects than compound heterozygous/heterozygous variant. Wang *et al*., 2015 showed weak CNP/NPR2 signaling as indicated by increased serum NT-proCNP level (21.72±0.31pmol/L), no cGMP response (showing loss of function), co-localization with ER marker (pointing defective trafficking from ER to Golgi bodies).

In family J, the novel identified variant (c.A2059T; p. K687X) lies in KHD and is predicted to affect protein folding by altering highly interactive residues in the kinase domain. KHD of NPRs is highly conserved across different species, but show no kinase activity. Hachiya *et al*., 2007 demonstrated the involvement of the Kinase domain in endochondral ossification by inducing cGMP production in the presence of CNP ligand binding *in vivo*. There is a marked impairment in cGMP production in AMDM patients exhibiting mutation (p.L658F) in KHD.

Some other *in vitro* studies suggest that in the absence of KHD, there is constitutive activation of GC, even in absence of ligand (Chinkers & Garbers. 1989). Although ATP binding motif (^{519}LXGXXXG^{525}) and phosphorylation sites (S513, T516, S518, S523, S526) are indispensable for receptor sensitization (Tamura & Garbers, 2003; Potter & Hunter. 1998), but it is the KHD that induces ligand binding conformational changes in NPRs and GC activation (Potter *et al*., 2006).

BMPR1B gene (4q22.3) comprises 1509 bp and encodes for a cell surface receptor, bone morphogenetic protein receptor-1B/BMPR1B, comprising 502 amino acids. BMPR1B belongs to type-I BMP receptors, which bind to secreted BMP ligands, dictating spatiotemporal aspects of vertebrate embryonic development (Hogan. 1996).

In the canonical BMP pathway, binding of GDF5 to extracellular domain of BMPRs (type-I or type-II), activates BMPR1B via transphosphorylation. The phosphorylated BMPR1B, then activate p38MAP Kinase and transcription factor, R-Smads, recruiting Smad-4, and the whole complex is translocated into nucleus to transcribe target genes, and, hence, contribute to bone formation (Gilboa *et al.*, 2000; von Bubnoff and Cho. 2001; Nohe *et al.*, 2002).

Pathogenic mutations in *BMPR1B* have been shown to cause various forms of skeletal dysplasia; i.e., AMDG (Graul-Neumann *et al.*, 2014), AMD-Hunter and Thompson type (Ullah *et al.*, 2018), AMD-du Pan type (Stange *et al.*, 2015), brachydactyly and complex digital malformations (Yıldırım *et al.*, 2018). In the present study, analysis of WES and linkage analysis revealed a novel four-base deletion (c. 398-401del; p. C135Vfs*28) in exon 5 of *BMPR1B* in family K, L & M. The mutation lies in transmembrane domain of protein. This is the first case in which a pathogenic variant in transmembrane domain causes chondrodysplasia. Structural analysis shows the hydrophilic nature of BMPR1B which favors its secretory nature. There is also N-terminal signal peptide sequence of 30 amino acids, important for the secretion of target protein into the extracellular environment. BMPR1B has four domains: extracellular ligand binding activin-receptor domain (30-110 aa's), transmembrane domain (126-148 aa's), GS motif (174-204 aa's), and STYKc protein kinase (204-486aa's) (Eivazi & Modarresi. 2014). All the three families (K, L & M) belongs to same ancestry/tribe and are living in same region, so it is inferred that the inheritance of common pathogenic variant in all families is because of the common ancestors.

The activin-receptor domain belongs to the receptor serine/threonine kinase family, rich in hydrophilic cysteine residues (for ligand binding), containing a cysteine box of nine amino acids with consensus sequence CCX {4-5} (Attisano and Wrana, 1996); i.e., CCTERNECN in BMPR1B. An additional unique feature of BMPR1B is the conserved spacing of 10 cysteine amino acids in the extracellular domain. GS motif has 30 aa's region with helix-loop-helix domain, showing phosphorylation activity (Massagué, Attisano & Wrana. 1994), while STYKc protein kinase domain has two kinase inserts and exhibit phosphotransferase activity (Eivazi & Modarresi. 2014).
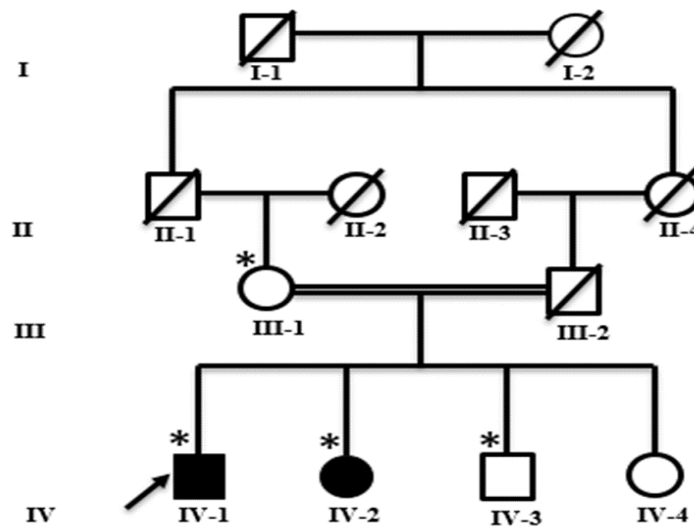
Fig. 7.1. Family I pedigree. Squares and circles indicate males and females. Empty and filled shades indicate normal and affected members. Double lines show consanguinity, while single lines indicate no consanguinity. Crossed lines over each square and circle indicate deceased individuals. The asterisk sign (*) indicates participated members, while the arrow shows member subjected to WES.

Fig. 7.2. Phenotypes of family I. Affected member (IV-1) shows short stature, dolichocephalic head (a), bowed legs (a, b), dislocation and stiffness of elbow joints (c, d), and severe bilateral brachydactyly of both hands (c, d) and feet (e, f).

c.C2761T; p. R921X
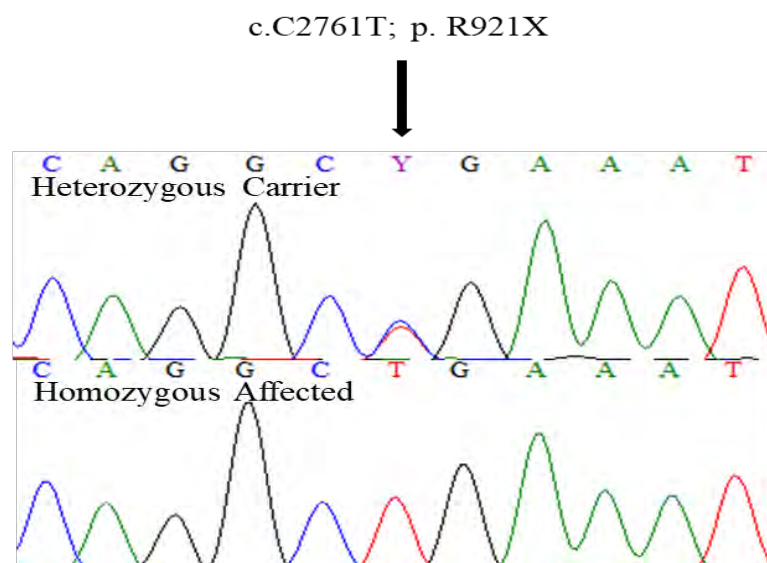
Fig. 7.3. Sanger sequencing results of family I. The upper and lower panels show heterozygous carriers and homozygous affected members.
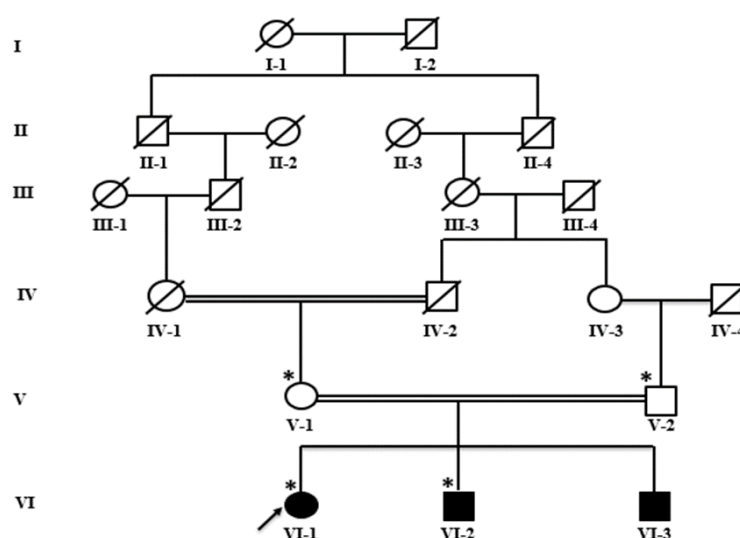
Fig. 7.4. Family J pedigree. Squares and circles indicate males and females. Empty and filled shades indicate normal and affected members. Double lines show consanguinity, while single lines indicate no consanguinity. Crossed lines over each square and circle indicate deceased individuals. The asterisk sign (*) indicates members participated in the current research study, while the arrow shows a member subjected to WES.

Fig. 7.5. Clinical phenotypes of family J. All the affected members (IV-1) show short stature, dolichocephalic head (a), dislocation and stiffness of elbow joints (b, c, e, f), and bilateral brachydactyly of both hands (b) and feet (a,d).
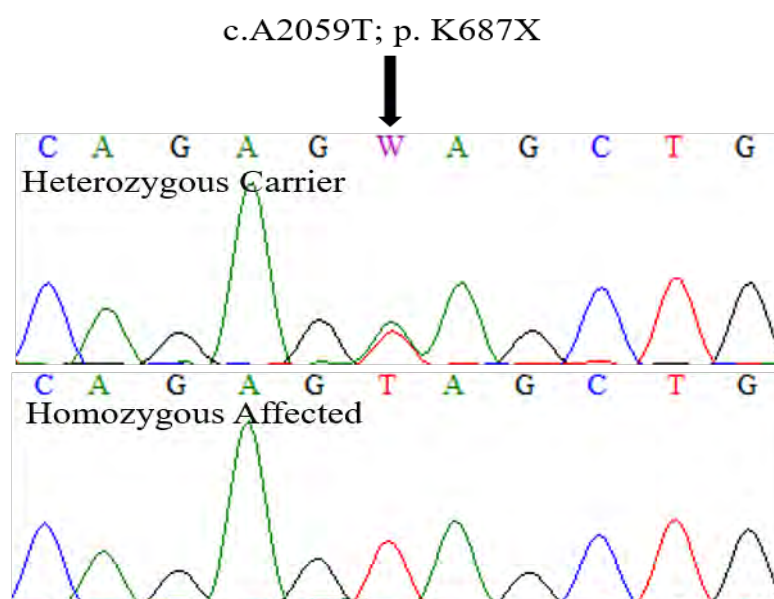
Fig. 7.6. Sanger sequencing results of family J. The upper and lower panels show heterozygous carrier and homozygous affected members
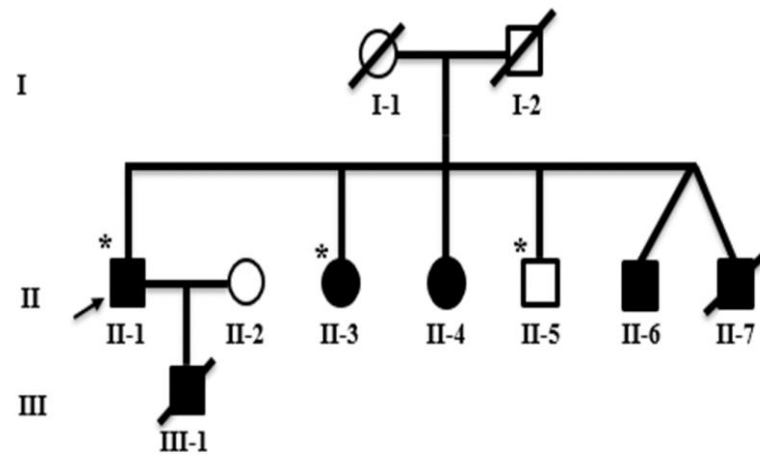
Fig. 7.7. Family K pedigree. Squares and circles indicate males and females. Empty and filled shades indicated normal and affected members. The single line indicates no consanguinity and crossed lines over each square and circle indicate deceased individuals. The asterisk sign (*) indicates members participated in the current research study, while the arrow shows a member subjected to WES.

Fig. 7.8. Clinical phenotypes of family K. Affected member (II-1) shows disproportionate short stature (a), severe bilateral brachydactyly in both hands (b) and feet (d), dislocalized elbow joints (c), bowed and short humer, fibula and patella (d,e).
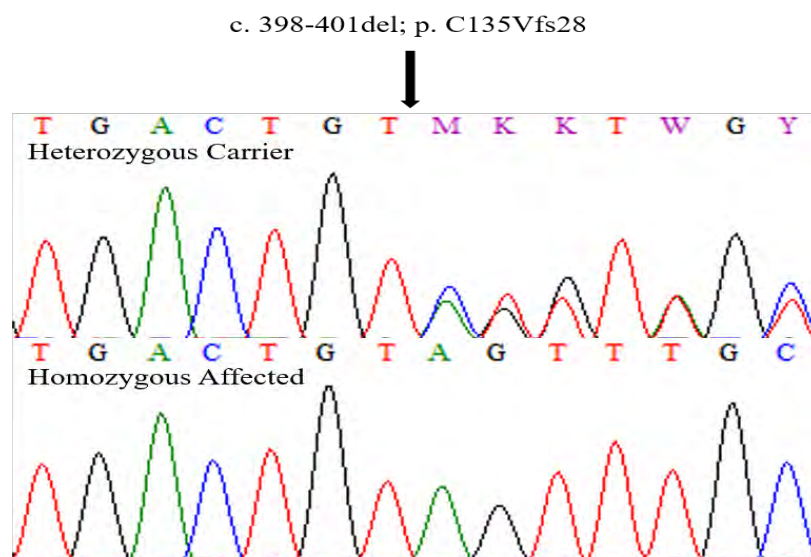
c. 398-401del; p. C135Vfs28

Fig. 7.9. Sanger sequencing chromatogram. Upper and lower panels show heterozygous carrier and homozygous affected member.
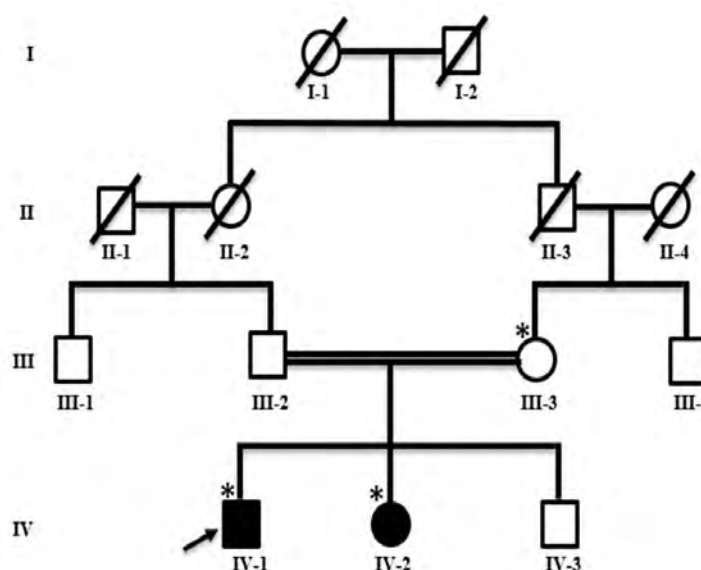
Fig. 7.10. Family L pedigree. Squares and circles indicate males and females. Empty and filled shades indicated normal and affected members. Double lines show consanguinity, while single lines indicate no consanguinity. Crossed lines over each square and circle indicate deceased individuals. The asterisk sign (*) indicates members participated in the current research study. Arrow shows member subjected to Sanger sequencing.

Fig. 7.11. Clinical phenotypes of family L. Affected member (IV-1) show short stature (a), severe bilateral brachydactyly in hands (b) and feet (c), bowed and short fibula and patella (c). Affected member (IV-2) also exhibits short stature, bilateral brachydactyly in upper and lower limbs (d,e), and bowed feet (e).
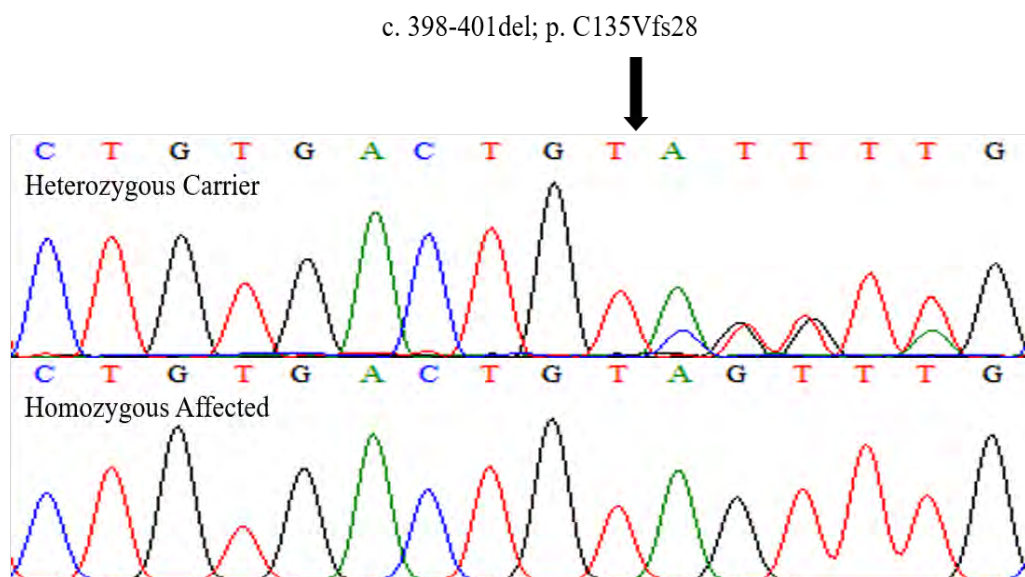
c. 398-401del; p. C135Vfs28

Fig. 7.12. Sanger sequencing chromatogram. Upper and lower panels show heterozygous carrier and homozygous affected members respectively.
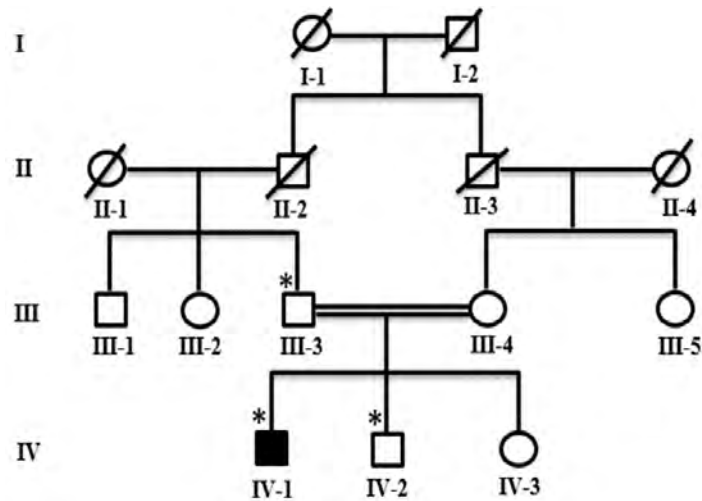
Fig. 7.13. Pedigree of Family M. Squares and circles indicate males and females. Empty and filled shades indicate normal and affected members. Double lines show consanguinity, while single lines indicate no consanguinity. Crossed lines over each square and circle indicate deceased individuals. The asterisk sign (*) indicates participated members.

Fig. 7.14. Phenotypes of Family M. Affected member (IV-1) shows disproportionate short stature (a), severe bilateral brachydactyly in hands (b) and feet (c, d), dislocalized elbow joints (c), bowed and short humer, fibula and patella (c, d).
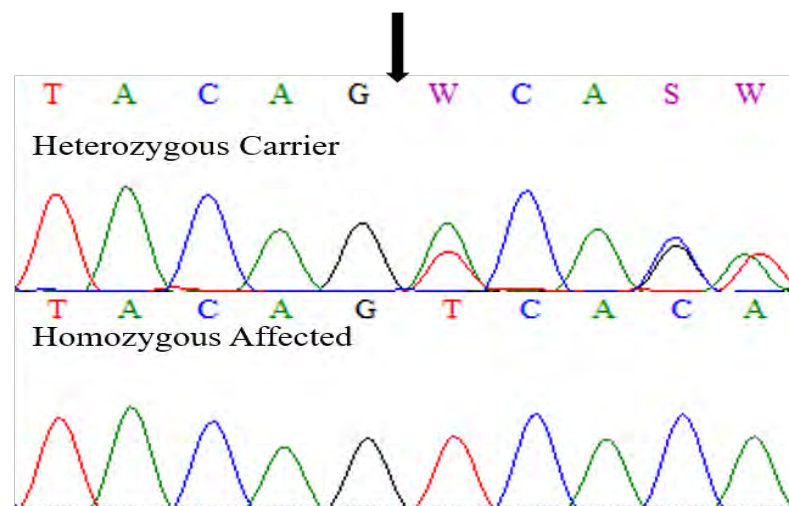
Fig. 7.15. Sanger sequencing chromatogram. Upper and lower panels show heterozygous carrier and homozygous affected member respectively.

Conclusion

Pakistan is a multi-ethnic country where people of different ethnicities live together. The most common castes are Pukhtoon, Punjabi, Sindhi, Balochi, Seraiki, Hindko and Hazara community. Besides these ethnic groups, people of different religious belives are also living. Due to these social and religious differences, most of the people tend to have cousin marriages, which is the basic cause of prevalence of congenital anomalies in Pakistan. On average estimated, more than 80% people have consanguinity. These families are more prone to have recessive diseases in their siblings. In Pakistan, most common anomalies are skeletal dysplasia, neurodevelopmental disorders, ectodermal dysplasia and others. There is dire need to diagnose these diseases both at clinical and molecular level.

With the advent of sequencing technologies (especially 3rd generation sequencing), it is now possible to characterize genetic diseases at genetic level. It facilitates disease diagnosis and clinical relevance and further help in diseases management, treatment and genetic counselling.

In the present research study, thirteen families exhibiting different congenital skeletal dysplasia either in autosomal recessive or dominant form, were sampled from different regions of district Swabi, Khyber Pakhtunkhwa, Pakistan. One affected member from each family (A-K) was subjected to whole exome sequencing, except family L & M where homozygosity mapping and linkage analysis was performed using microsatellite markers. Whole exome sequencing data analysis and Sanger sequencing confirmed segregation of identified pathogenic variants in all available family members. We have found previously reported pathogenic variants in *BBS5, EVC, CHST3, IDUA, GALNS, HOXD13, GJA1* and *NPR2* gene, while novel variants in *ROR2, GNPTG, NPR2* and *BMPR1B* genes.

References

Abbas S, Khan H, Alam Q *et al* (2023). Genetic advances in skeletal disorders: an overview. *Journal of Biochemical and Clinical Genetics* 6(1): 57-57.

Adzhubei IA, Schmidt S, Peshkin L, Ramensky VE, Gerasimova A, Bork P, ... & Sunyaev SR (2010). A method and server for predicting damaging missense mutations. *Nature methods* 7(4): 248-249.

Afzal AR & Jeffery S (2003). One gene, two phenotypes: ROR2 mutations in autosomal recessive Robinow syndrome and autosomal dominant brachydactyly type B. *Human mutation* 22(1): 1-11.

Aggarwal S, Coutinho MF, Dalal AB, Jain SJMN, Prata MJ & Alves S (2014). Prenatal skeletal dysplasia phenotype in severe MLII alpha/beta with novel GNPTAB mutation. *Gene* 542(2): 266-268.

Aguirre WE, Walker K, Gideon S (2014). Tinkering with the axial skeleton: vertebral number variation in ecologically divergent three spine stickleback populations. *Biological Journal of the Linnean Society* 113(1): 204-219.

Ahmad M, Abbas H, Wahab A & Haque S (1990). Fibular hypoplasia and complex brachydactyly (Du Pan syndrome) in an inbred Pakistani kindred. *American journal of medical genetics* 36(3): 292-296.

Akarsu A, Stoilov I, Yilmaz E, Sayli B and Sarfarazi M (1996). Genomic structure of HOXD13 gene: a nine polyalanine duplication causes synpolydactyly in two unrelated families. *Human Molecular Genetics* 5: 945-952.

Albrecht AN, Kornak U, Böddrich A, Süring K, Robinson PN, Stiege AC, Lurz R, Stricker S, Wanker EE, Mundlos SA (2004). molecular pathogenesis for transcription factor associated poly-alanine tract expansions. *Human Molecular Genetics* 13(20): 2351-2359.

Alegra T, Koppe T, Acosta A., *et* al (2014). Pitfalls in the prenatal diagnosis of mucolipidosis II alpha/beta: A case report. *Meta Gene* 2: 403-406.

Al-Fardan A & Al-Qattan MM (2017). Wide-spread cone-shaped epiphyses in two Saudi siblings with Ellis-van Creveld syndrome. *International Journal of Surgery Case Reports* 39: 212– 217.

Ali A, Abdullah, Bilal M, Mis EK, Lakhani SA, Ahmad W & Ullah I (2023). Sequence variants in different genes underlying Bardet-Biedl syndrome in four consanguineous families. *Molecular Biology Reports* 50(12): 9963-9970.

Al-Qattan MM, Al AbdulkareemI, Al Haidan Y, Al Balwi M (2012). A novel mutation in the SHH long-range regulator (ZRS) is associated with preaxial polydactyly, triphalangeal thumb and severe radial ray deficiency. *American Journal of Medical Genetics A 158A:* 2610-2615.

Alves Pereira D, Berini Aytés L & Gay Escoda C (2009). Ellis-van Creveld syndrome. Case report and literature review. *Medicina Oral, Patología Oral y Cirugia Bucal* 14(7):340-343.

AlYahyaee, S. A. S., Al- Kindi, M. N., Habbal, O., & Kumar, D. S. (2003). Clinical and molecular analysis of Grebe acromesomelic dysplasia in an Omani family. *American Journal of Medical Genetics Part A*, 121(1), 9-14.

Amano N, Mukai T, Ito Y, Narumi S, Tanaka T, Yokoya S, ... & Hasegawa T (2014). Identification and functional characterization of two novel NPR2 mutations in Japanese patients with short stature. *The Journal of Clinical Endocrinology & Metabolism* 99(4): 713-718.

Amir N, Zlotogora J & Bach G (2013). Mucolipidosis type IV: clinical spectrum and natural history. *Pediatrics* 79(6): 953-959.

Ammer LS, Muschol NM, Santer R., *et al* (2022). Anaesthesia-Relevant Disease Manifestations and Perianaesthetic Complications in Patients with Mucolipidosis—A Retrospective Analysis of 44 Anaesthetic Cases in 12 Patients. *Journal of Clinical Medicine* 11(13): 3650.

Ammer LS, Oussoren E, Muschol NM, Pohl S, Rubio-Gozalbo ME, Santer R, ... & Breyer SR. (2020). Hip morphology in mucolipidosis type II. *Journal of Clinical Medicine* 9(3): 728.

Anderson HJ, Hansen AK (1990). Tibial hypoplasia with preaxial syn-and polydactyly. *Arch Ortho Trauma Surg* 109: 231-233.

Anderson IJ, Goldberg RB, Marion RW, Upholt WB & Tsipouras P (1990). Spondyloepiphyseal dysplasia congenita: genetic linkage to type II collagen (COL2AI). *American journal of human genetics* 46(5): 896.

Anneren G, Amilon A (1994). X-linked recessive fusion of metacarpals IV and V and hypoplastic metacarpal V. *American Journal of Medical Genetics* 52: 248-250.

Attisano L, Wrana JL, Montalvo E & Massagué J (1996). Activation of signalling by the activin receptor complex. *Molecular and Cellular Biology* 1066-1073.

Aziz A, Raza SI, Ali S & Ahmad W (2016). Novel homozygous mutations in the EVC and EVC2 genes in two consanguineous families segregating autosomal recessive Ellis–van Creveld syndrome. *Clinical Dysmorphology* 25(1): 1-6.

Bach G (2001). Mucolipidosis type IV. *Molecular genetics and metabolism* 73(3): 197-203.

Baker K & Beales PL (2009, November). Making sense of cilia in disease: the human ciliopathies. *American Journal of Medical Genetics part C: Seminars in Medical Genetics* 151(4):281-295.

Baldridge D, Shchelochkov O, Kelley B, Lee B (2010). Signaling pathways in human skeletal dysplasias. *Annual Review of Genomics and Human Genetics* 11: 189-217.

Bargal R, Avidan N, Ben-Asher E *et al* (2000). Identification of the gene causing mucolipidosis type IV. *Nature Genetics* 26(1): 118-122.

Bartels CF, Bükülmez H, Padayatti P, Rhee DK, van Ravenswaaij-Arts C, Pauli RM, ... & Warman ML (2004). Mutations in the transmembrane natriuretic peptide receptor NPR-B impair skeletal growth and cause acromesomelic dysplasia, type Maroteaux. *The American Journal of Human Genetics* 75(1): 27-34.

Basit S, Naqvi SKUH, Wasif N, Ali G, Ansar M & Ahmad W (2008). A novel insertion mutation in the cartilage-derived morphogenetic protein-1 (CDMP1) gene underlies Grebe-type chondrodysplasia in a consanguineous Pakistani family. *BMC Medical Genetics* 9: 1-6.

Bassi MT, Manzoni M, Monti E, Pizzo MT, Ballabio A & Borsani G (2000). Cloning of the gene encoding a novel integral membrane protein, mucolipidin and identification of the two major founder mutations causing mucolipidosis type IV. *The American Journal of Human Genetics* 67(5): 1110-1120.

Bénazet JD, Bischofberger M, Tiecke E, Gonçalves A, Martin JF, Zuniga A, ... & Zeller R (2009). A self-regulatory system of interlinked signaling feedback loops controls mouse limb patterning. *Science* 323(5917): 1050-1053.

Bennett RL, French KS, Resta RG & Doyle DL (2008). Standardized human pedigree nomenclature: update and assessment of the recommendations of the National Society of Genetic Counselors. *Journal of Genetic Counseling* 17: 424-433.

Berman ER, Livni N, Shapira E, Merin S, Levij IS (1974). Congenital corneal clouding with abnormal systemic storage bodies: a new variant of mucolipidosis. *The Journal of Pediatrics* 84(4): 519-526.

Blottner D, Salanova M, Püttmann B, Schiffl G, Felsenberg D, Buehring B & Rittweger J (2006). Human skeletal muscle structure and function preserved by vibration muscle exercise following 55 days of bed rest. *European Journal of Applied Physiology* 97: 261-271.

Bond CS, Clements PR, Ashby SJ, Collyer CA, Harrop SJ, Hopwood JJ, Guss JM (1997). Structure of a human lysosomal sulfatase. *Structure* 5:277–289.

Bosse K, Betz RC, Lee YA, Wienker TF, Reis A, Kleen H, ... & Nöthen MM (2000). Localization of a gene for syndactyly type 1 to chromosome 2q34-q36. *The American Journal of Human Genetics* 67(2): 492-497.

Boudewyn LC & Walkley SU (2019). Current concepts in the neuropathogenesis of mucolipidosis type IV. *Journal of Neurochemistry* 148(5): 669-689.

Boyadjiev SA, Jabs EW, LaBuda M, Jamal JE, Torbergsen T, Ptáček II LJ, ... & Shapiro RE (1999). Linkage analysis narrows the critical region for oculodentodigital dysplasia to chromosome 6q22–q23. *Genomics* 58(1): 34-40.

Brison N, Debeer P, Tylzanowski P (2014). Joining the fingers: a HOXD13 Story. *Developmental Dynamics* 243(1): 37-48.

Bunn KJ, Daniel P, Rösken HS, O'Neill AC, Cameron-Christie SR, Morgan T, ... & Robertson SP (2015). Mutations in DVL1 cause an osteosclerotic form of Robinow syndrome. *The American Journal of Human Genetics* 96(4): 623-630.

Canale ST, Beaty JH, Eds (2008). Campbell's operative orthopaedics. 11th ed. Philadelphia: Mosby Elsevier vol 4: pp. 4403-4404.

Cantiello HF, Montalbetti N, Goldmann WH, Raychowdhury MK, Gonzalez-Perrett S, Timpanaro GA & Chasan B (2005). Cation channel activity of mucolipin-1: the effect of calcium. *Pflügers Archiv* 451:304-312.

Caparrós Martín JA, Valencia M, Reytor E, Pacheco M, Fernandez M, Perez-Aytes A, ... & Ruiz-Perez VL (2013). The ciliary Evc/Evc2 complex interacts with Smo and controls Hedgehog pathway activity in chondrocytes by regulating Sufu/Gli3 dissociation and Gli3 trafficking in primary cilia. *Human Molecular Genetics* 22(1): 124-139.

Capdevila J, Belmonte JCI (2001). Patterning mechanisms controlling vertebrate limb development. *Annual Review of Cell and Developmental Biology* 17(1): 87-132.

Capdevila J, Tsukui T, Esteban CR, Zappavigna V Belmonte JCI (1999). Control of vertebrate limb outgrowth by the proximal factor Meis2 and distal antagonism of BMPs by Gremlin. *Molecular Cell* 4(5): 839-849.

Castilla EE, Paz JE, Orioli-Parreiras IM (1980). Syndactyly: frequency of specific types. *American Journal of Medical Genetics* 5: 357-364.

Cathey SS, Kudo M, Tiede S, Raas-Rothschild A, Braulke T, Beck M, ... & McKusick VA (2008). Molecular order in mucolipidosis II and III nomenclature. *American Journal of Medical Genetics.* Part A 146(4): 512.

Cathey SS, Leroy JG, Wood T, Eaves K, Simensen RJ, Kudo M, ... & Friez MJ (2010). Phenotype and genotype in mucolipidoses II and III alpha/beta: a study of 61 probands. *Journal of Medical Genetics* 47(1): 38-48.

Chapel A, Kieffer-Jaquinod S, Sagne C, Verdon Q, Ivaldi C, Mellal M, ... & Journet A (2013). An extended proteome map of the lysosomal membrane reveals novel potential transporters. *Molecular & Cellular Proteomics* 12(6): 1572-1588.

Cheng JC, Chang HM, Fang L, Sun YP & Leung PC (2015). TGF- β1 up- regulates connexin43 expression: a potential mechanism for human trophoblast cell differentiation. *Journal of Cellular Physiology* 230(7): 1558-1566.

Cheng X, Shen D, Samie M & Xu H (2010). Mucolipins: intracellular TRPML1-3 channels. *FEBS letters* 584(10): 2013-2021.

Chinkers M & Garbers DL (1989). The protein kinase domain of the ANP receptor is required for signaling. *Science* 245(4924): 1392-1394.

Cho TJ, Baek GH, Lee HR, Moon HJ, Choi IH (2013). Tibial hemimelia-polydactyly-five fingered hand syndrome associated with a 404G>A mutation in a distant sonic hedgehog cis-regulator (ZRS): A case report. *Journal of Pediatric Orthopaedics B* 22: 219-221.

Chopra K, Tadisina KK, Patel KR, Singh DP (2013). Syndactyly repair. *Eplasty* 13: 51.

Costa T, Ramsby G, Cassia F, Peters KR, Soares J, Correa J, ... & Tsipouras P (1998). Grebe syndrome: clinical and radiographic findings in affected individuals and heterozygous carriers. *American Journal of Medical Genetics* 75(5): 523-529.

Costain G, Inbar-Feigenberg M, Saleh M, Yaniv-Salem S, Ryan G, Morgen E, ... & Chitayat D (2018). Challenges in diagnosing rare genetic causes of common in utero presentations: report of two patients with Mucolipidosis type II (I-cell disease). *Journal of Pediatric Genetics* 7(3): 134-137.

D'Alessio C & M Dahms N (2015). Glucosidase II and MRH-domain containing proteins in the secretory pathway. *Current Protein and Peptide Science* 16(1): 31-48.

d'Azzo A, Machado E, Annunziata I (2015). Pathogenesis, emerging therapeutic targets and treatment in sialidosis. *Expert Opinion on Orphan Drugs* 3(5): 491-504.

Dai L, Guo H, Meng H, Zhang K, Hu H, Yao H & Bai Y (2013). Confirmation of genetic homogeneity of syndactyly type IV and triphalangeal thumb–polysyndactyly syndrome in a Chinese family and review of the literature. *European Journal of Pediatrics* 172 1467-1473.

Dai L, Liu D, Song M, Xu X, Xiong G, Yang K, ... & Bai Y (2014). Mutations in the homeodomain of HOXD13 cause syndactyly type 1-c in two Chinese families. *PLoS One* 9(5): e96192.

Dai L, Liu D, Song M, Xu X, Xiong G, Yang K, Zhang K, Meng H, Guo H, Bai Y (2014). Mutations in the homeodomain of HOXD13 cause syndactyly type 1c in two Chinese families. *PLoS One* 9 (5): 96192.

D'Asdia MC, Torrente I, Consoli F, Ferese R, Magliozzi M, Bernardini L, ... & De Luca A (2013). Novel and recurrent EVC and EVC2 mutations in Ellis-van Creveld syndrome and Weyers acrofacial dyostosis. *European Journal of Medical Genetics* 56(2): 80-87.

David- Vizcarra G, Briody J, Ault J, Fietz M, Fletcher J, Savarirayan R, ... & Sillence D (2010). The natural history and osteodystrophy of mucolipidosis types II and III. *Journal of Paediatrics and Child Health* 46(6): 316-322.

Davis AP, Capecchi MR (1996). A mutational analysis of the five *HOXD* genes: dissection of genetic interactions during limb development in the mouse. *Development* 122: 1175-1185.

de Baat P, Heijboer MP, de Baat C (2005). Development, Physiology and cell activity of bone. *Nederlands Tijdschrift Tandheelkdunde* 112: 4261-4269.

De Smet L, De Beer P & Fryns JP (1996). Cenani-Lenz syndrome in father and daughter. *Genetic Counseling (Geneva, Switzerland)* 7(2): 153-157.

Debeer P, Schoenmakers EFPM, De Smet L, Van De Ven WJM, & Fryns JP (1998). Co-segregation of an apparently balanced reciprocal t (12; 22)(p11. 2; q13. 3) with a complex type of 3/3'/4 synpolydactyly associated with metacarpal, metatarsal and tarsal synostoses in three family members. *Clinical Dysmorphology* 7(3): 225-228.

Debeer P, Schoenmakers EFPM, Thoelen R, Fryns JP, Van de Ven WJM (1998). Physical mapping of the t (12; 22) translocation breakpoints in a family with a complex type of 3/3′/4 synpolydactyly. *Cytogenetics and Cell Genetics* 81(3-4): 229-234.

Debeer P, Schoenmakers EFPM, Thoelen R, Holvoet M, Kuittinen T, Fabry G, ... & Van de Ven WJM (2000). Physical map of a 1.5 mb region on 12p11. 2 harbouring a synpolydactyly associated chromosomal breakpoint. *European Journal of Human Genetics* 8(8): 561-570.

Debeer P, Schoenmakers EFPM, Twal WO, Argraves WS, De Smet L, Fryns JP & Van de Ven, WJM (2002). The fibulin-1 gene (FBLN1) is disrupted in at (12; 22) associated with a complex type of synpolydactyly. *Journal of Medical Genetics* 39(2) 98-104.

Deng H & Tan T (2015). Advances in the molecular genetics of non-syndromic syndactyly. *Current Genomics* 16(3): 183-193.

Di Fruscio G, Schulz A, De Cegli R, Savarese M, Mutarelli M, Parenti G, ... & Ballabio A (2015). Lysoplex: An efficient toolkit to detect DNA sequence variations in the autophagy-lysosomal pathway. *Autophagy* 11(6): 928-938.

Di Lorenzo G, Velho RV, Winter D, Thelen M, Ahmadi S, Schweizer M, ... & Pohl S (2018). Lysosomal proteome and secretome analysis identifies missorted enzymes and their nondegraded substrates in mucolipidosis III mouse cells. *Molecular & Cellular Proteomics* 17(8): 1612-1626.

Di Lorenzo G, Westermann LM, Yorgan TA, Stürznickel J, Ludwig NF, Ammer LS, ... & Pohl S (2021). Pathogenic variants in GNPTAB and GNPTG encoding distinct subunits of GlcNAc-1-phosphotransferase differentially impact bone resorption in patients with mucolipidosis type II and III. *Genetics in Medicine* 23(12): 2369-2377.

Díaz-González F, Wadhwa S, Rodriguez-Zabala M, Kumar S, Aza-Carmona M, Sentchordi-Montané L, ... & Heath KE (2022). Biallelic cGMP-dependent type II protein kinase gene (PRKG2) variants cause a novel acromesomelic dysplasia. *Journal of Medical Genetics* 59(1): 28-38.

Dimitrov BI, Voet T, De Smet L, Vermeesch JR, Devriendt K, Fryns JP & Debeer P (2010). Genomic rearrangements of the GREM1-FMN1 locus cause oligosyndactyly, radio-ulnar synostosis, hearing loss, renal defects syndrome and Cenani–Lenz-like non-syndromic oligosyndactyly. *Journal of Medical Genetics* 47(8): 569-574.

Dobrowolski R, Sasse P, Schrickel JW, Watkins M, Kim JS, Rackauskas M, ... & Willecke K (2008). The conditional connexin43G138R mouse mutant represents a new model of hereditary oculodentodigital dysplasia in humans. *Human Molecular Genetics* 17(4): 539-554.

Docherty B (2007). Skeletal system: part four--the appendicular skeleton. *Nursing Times* 103(8): 26-27.

Dogterom EJ, Wagenmakers MA, Wilke M, Demirdas S, Muschol NM, Pohl S, ... & Oussoren E (2021). Mucolipidosis type II and type III: a systematic review of 843 published cases. *Genetics in Medicine* 23(11): 2047-2056.

Dollé P, Dierich A, LeMeur M, Schimmang T, Schuhbaur B, Chambon P, Duboule D (1993). Disruption of *Hoxd13* gene induces localised heterochrony leading to mice with neotenic limbs. *Cell* 75: 431-441.

Dorn KV, Hughes CE & Rohatgi R (2012). A Smoothened-Evc2 complex transduces the Hedgehog signal at primary cilia. *Developmental cell* 23(4), 823-835.

Dowd CN (1896). Cleft hand: a report of a case successfully treated with the use of periosteal flaps. *Annals of Surgery* 24: 210.2-21216.

Drossopoulou G, Lewis KE, Sanz-Ezquerro JJ, Nikbakht N, McMahon AP, Hofmann C & Tickle C (2000). A model for anteroposterior patterning of the vertebrate limb based on sequential long-and short-range Shh signalling and Bmp signalling. *Development* 127(7): 1337-1348.

Duboc V, Logan MP (2011). Regulation of limb bud initiation and limb type morphology. *Developmental Dynamics* 240: 1017-1027.

Duz MB & Topak A (2020). Recurrent c. 776T> C mutation in CHST3 with four other novel mutations and a literature review. *Clinical dysmorphology* 29(4): 167-172.

Du Pan CM (1924). Absence congenitale du perone sans deformation du tibia: Curieuses deformations congenitales des mains. *Rev Orthop* 11: 227-234.

Edelmann L, Dong J, Desnick RJ & Kornreich R (2002). Carrier screening for mucolipidosis type IV in the American Ashkenazi Jewish population. *The American Journal of Human Genetics* 70(4): 1023-1027.

Eivazi AR & Modarresi M (2014). Bioinformatics analysis of BMPR1B gene in different species. *International Journal of Biosciences* 4(1): 399-406.

Elçioglu N, Atasu M, Cenani A (1997). Dermatoglyphics in patients with Cenani- Lenz type syndactyly: Studies in a new case. *American Journal of Medical Genetics* 70(4): 341-345.

Elsner J, Mensah MA, Holtgrewe M, Hertzberg J, Bigoni S, Busche A, Coutelier M, de Silva DC, Elçioglu N, Filges I, Gerkes E (2021). Genome sequencing in families with congenital limb malformations. *Human Genetics* 140 (8): 1229-1239.

Erlebacher A, Filvaroff EH, Gitelman SE, Derynck, R (1995). Toward a molecular understanding of skeletal development. *Cell* 80(3): 371-378.

Faivre L, Le Merrer M, Megarbane A, Gilbert B, Mortier G, Cusin V, ... & Cormier-Daire V (2000). Exclusion of chromosome 9 helps to identify mild variants of acromesomelic dysplasia Maroteaux type. *Journal of Medical Genetics* 37(1): 52-54.

Faiyaz- Ul- Haque M, Ahmad W, Wahab A, Haque S, Azim AC, Zaidi SH, ... & Tsui LC (2002). Frameshift mutation in the cartilage- derived morphogenetic protein 1 (CDMP1) gene and severe acromesomelic chondrodysplasia resembling Grebe-type chondrodysplasia. *American Journal of Medical Genetics* 111(1): 31-37.

Favret JM, Weinstock NI, Feltri ML & Shin D (2020). Pre-clinical mouse models of neurodegenerative lysosomal storage diseases. *Frontiers in Molecular Biosciences* 7: 57.

Flenniken AM, Osborne LR, Anderson N, Ciliberti N, Fleming C, Gittens JE, ... & Rossant J (2005). A Gja1 missense mutation in a mouse model of oculodentodigital dysplasia. *Development & Disease* 132(19): 4375-4386.

Funato Y, Michiue T, Asashima M & Miki H (2006). The thioredoxin-related redox-regulating protein nucleoredoxin inhibits Wnt–β-catenin signalling through dishevelled. *Nature Cell Biology* 8(5): 501-508.

Funato Y, Michiue T, Terabayashi T, Yukita A, Danno H, Asashima M & Miki H (2008). Nucleoredoxin regulates the Wnt/planar cell polarity pathway in Xenopus. *Genes to Cells* 13(9): 965-975.

Furniss D, Kan SH, Taylor IB, Johnson D, Critchley P, Giele HP, Wilkie AOM (2009). Genetic screening of 202 individuals with congenital limb malformations and requiring reconstructive surgery. *Journal of Medical Genetics* 46: 730-735.

Galdzicka M, Patnala S, Hirshman MG, Cai JF, Nitowsky H, Egeland JA & Ginns EI (2002). A new gene, EVC2, is mutated in Ellis–van Creveld syndrome. *Molecular Genetics and Metabolism* 77(4): 291-295.

Gedeon ÁK, Colley A, Jamieson R, Thompson EM, Rogers J, Sillence D, ... & Gécz J (1999). Identification of the gene (SEDL) causing X-linked spondyloepiphyseal dysplasia tarda. *Nature Genetics* 22(4): 400-404.

Geetha-Loganathan P, Nimmagadda S, Scaal M (2008). Wnt signaling in limb organogenesis. *Organogenesis* 4: 109-115.

Ghadami M, Majidzadeh AK, Haerian BS, Damavandi E, Yamada K, Pasallar P, ... & Niikawa N (2001). Confirmation of genetic homogeneity of syndactyly type 1 in an Iranian family. *American Journal of Medical Genetics* 104(2): 147-151.

Gilboa L, Nohe A, Geissendorfer T, Sebald W, Henis YI & Knaus P (2000). Bone morphogenetic protein receptor complexes on the surface of live cells: a new

oligomerization mode for serine/threonine kinase receptors. *Molecular Biology of the Cell* 11(3): 1023-1035.

Girisha KM, Bidchol AM, Kamath PS, Shah KH, Mortier GR, Mundlos S, Shah H (2014). A novel mutation (g. 106737G>T) in zone of polarizing activity regulatory sequence (ZRS) causes variable limb phenotypes in Werner mesomelia. *American Journal of Medical Genetics A* 164A: 898-906.

Gladwin A, Donnai D, Metcalfe K, Schrander-Stumpel C, Brueton L, Verloes A, ... & Dixon M (1997). Localization of a gene for oculodentodigital syndrome to human chromosome 6q22–q24. *Human Molecular Genetics* 6(1): 123-127.

Goodman FR, Mundlos S, Muragaki Y, Donnai D, Giovannucci- Uzielli ML, Lapi E, et al (1997). Synpolydactyly phenotypes correlate with size of expansion in *HOXD 13* polyalanine tract. *Proceedings of Natural Academy of Sciences USA* 94: 7458-7463.

Graul-Neumann LM, Deichsel A, Wille U, Kakar N, Koll R, Bassir C, ... & Seemann P (2014). Homozygous missense and nonsense mutations in BMPR1B cause acromesomelic chondrodysplasia-type Grebe. *European Journal of Human Genetics* 22(6): 726-733.

Grebe H (1955a). Chondrodysplasie. *Anal Genet* 2:300-303.

Grebe H (1952). Die Achondrogenesis: ein einfach rezessives Erbmerkmal. *Folia Hered Pathol* 2: 23-28.

Green DP, Hotchkiss RN, Pederson WC, Wolfe SW (2005). Green's operative hand surgery. 5th ed. Philadelphia, PA: Elsevier vol. 2: pp. 1381-1382.

Haas SL (1940). Bilateral complete syndactylism of all fingers. *American Journal of Surgery* 50: 363-366.

Hantash FM, Olson SC, Anderson B, Buller A, Chen R, Crossly B, ... & Strom CM (2006). Rapid one-step carrier detection assay of mucolipidosis IV mutations in the Ashkenazi Jewish population. *The Journal of Molecular Diagnostics* 8(2): 282-287.

Harpf C, Pavelka M, Hussl H (2005). A variant of Cenani-Lenz syndactyly (CLS): review of the literature and attempt of classification. *British Journal of Plastic Surgery* 58: 251-257.

Harrison RG (1918). Experiments on the development of fore limb of Amblystoma, a self-differentiating and equipotential system. *Journal of Experimental Zoology* 25: 413-461.

Helms JA, Kim CH, Eichele G, Thaller C (1996). Retinoic acid signaling is required during early chick limb development. *Development* 122:1385–1394.

Heo JS, Choi KY, Sohn SH, Kim C, Kim YJ, Shin SH, ... & Choi JH (2012). A case of mucolipidosis II presenting with prenatal skeletal dysplasia and severe secondary hyperparathyroidism at birth. *Korean Journal of Pediatrics* 55(11): 438.

HGMD Professional. Available online: http://www.hgmd.cf.ac.uk/ac/index.php (accessed on 31 May 2020).

Hoffmann B & Mayatepek E (2005). Neurological manifestations in lysosomal storage disorders-from pathology to first therapeutic possibilities. *Neuropediatrics* 36(5): 285-289.

Hogan BL (1996). Bone morphogenetic proteins: multifunctional regulators of vertebrate development. *Genes & Development* 10(13): 1580-1594.

Holmes LB, Wolf E, Miettinen OS (1972). Metacarpal 4-5 fusion with X-linked recessive inheritance. *American Journal of Human Genetics* 24: 562-568.

Hunter AG & Thompson MW (1976). Acromesomelic dwarfism: description of a patient and comparison with previously reported cases. *Human Genetics* 34: 107-113.

Hurst JA, Firth HV, Smithson S (2005). Skeletal dysplasias. *Seminars in Fetal and Neonatal Medicine* 10 (3): 233-241.

Ibrahim DM, Tayebi N, Knaus A, Stiege AC, Sahebzamani A, Hecht J, Mundlos S, Spielmann MA (2016). homozygous HOXD13 missense mutation causes a severe form of synpolydactyly with metacarpal to carpal transformation. *American Journal of Medical Genetics Part A* 170(3): 615-21.

Idol RA, Wozniak DF, Fujiwara H, Yuede CM, Ory DS, Kornfeld S & Vogel P (2014). Neurologic abnormalities in mouse models of the lysosomal storage disorders mucolipidosis II and mucolipidosis III γ. *PLoS One* 9(10): e109768.

Izumi K, Lippa AM, Wilkens A, Feret HA, McDonald- McGinn DM & Zackai EH (2013). Congenital heart defects in oculodentodigital dysplasia: report of two cases. *American Journal of Medical Genetics Part A* 161(12): 3150-3154.

Jacob M, Menon S, Botti C & Marshall I (2018). Heterozygous NPR2 mutation in two family members with short stature and skeletal dysplasia. *Case Reports in Endocrinology*.

Jamsheer A, Zemojtel T, Kolanczyk M, Stricker S, Hecht J, Krawitz P, ... & Mundlos S (2013). Whole exome sequencing identifies FGF16 nonsense mutations as the cause of X-linked recessive metacarpal 4/5 fusion. *Journal of Medical Genetics* 50(9): 579-584.

Jan AU, Ahmad S *et al* (2018). Chondroectodermal syndrome. *Journal of Ayub Medical College Abbottabad* 30(3): 473–475.

Johnston O, Kirby Jr VV (1955). Syndactyly of ring and little finger. *American Journal of Human Genetics* 7: 80-82.

Jordan D, Hindocha S, Dhital M, Saleh M & Khan W (2012). Suppl 1: The Epidemiology, Genetics and Future Management of Syndactyly. *The Open Orthopaedics Journal* 6:14.

Kalcheva N, Qu J, Sandeep N, Garcia L, Zhang J, Wang Z, ... & Fishman GI (2007). Gap junction remodeling and cardiac arrhythmogenesis in a murine model of oculodentodigital dysplasia. *Proceedings of the National Academy of Sciences* 104(51): 20512-20516.

Kamal R, Dahiya P, Kaur S, Bhardwaj R & Chaudhary K (2013). Ellis-van Creveld syndrome: a rare clinical entity. *Journal of Oral and Maxillofacial Pathology* 17(1): 132-135.

Kant SG, Polinkovsky A, Mundlos S, Zabel B, Thomeer RT, Zonderland HM, ... & Warman ML (1998). Acromesomelic dysplasia Maroteaux type maps to human chromosome 9. *The American Journal of Human Genetics* 63(1): 155-162.

Kant SG, Polinkovsky A, Mundlos S, Zabel B, Thomeer RT, Zonderland HM, ... & Warman ML (1998). Acromesomelic dysplasia Maroteaux type maps to human chromosome 9. *The American Journal of Human Genetics* 63(1): 155-162.

Karczewski KJ, Francioli LC, Tiao G, Cummings BB, Alföldi J, Wang Q, ... & MacArthur DG (2020). The mutational constraint spectrum quantified from variation in 141,456 humans. *Nature* 581(7809): 434-443.

Kausar M, Ain NU, Hayat F, Fatima H, Azim S, Ullah H, ... & Siddiqi S (2022). Biallelic variants in CHST3 cause Spondyloepiphyseal dysplasia with joint dislocations in three Pakistani kindreds. *BMC Musculoskeletal Disorders* 23(1): 818.

Kawakami Y, Capdevila J, Büscher D, Itoh T, Esteban CR & Belmonte JCI (2001). WNT signals control FGF-dependent limb initiation and AER induction in the chick embryo. *Cell* 104(6): 891-900.

Kawasaki Y, Kugimiya F, Chikuda H, Kamekura S, Ikeda T, Kawamura N, ... & Kawaguchi H (2008). Phosphorylation of GSK-3β by cGMP-dependent protein kinase II promotes hypertrophic differentiation of murine chondrocytes. *The Journal of Clinical Investigation* 118(7): 2506-2515.

Khan S, Basit S, Khan MA, Muhammad N & Ahmad W (2016). Genetics of human isolated acromesomelic dysplasia. *European Journal of Medical Genetics* 59(4): 198-203.

Kishimoto I. Rossi K & Garbers DL (2001). A genetic model provides evidence that the receptor for atrial natriuretic peptide (guanylyl cyclase-A) inhibits cardiac ventricular myocyte hypertrophy. *Proceedings of the National Academy of Sciences* 98(5): 2703-2706.

Kjaer KW, Hansen L, Eiberg H, Utkus A, Skovgaard LT, Leicht P, ... & Tommerup N (2005). A 72- year- old Danish puzzle resolved—comparative analysis of

phenotypes in families with different- sized HOXD13 polyalanine expansions. *American Journal of Medical Genetics Part A* 138(4): 328-339.

Kleinebrecht J, Selow J, Winkler W (1982). The mouse mutant limb-deformity (ld). *Anatomischer Anzeiger* 152(4): 313-324.

Klopocki E, Ott CE, Banatar N, Ullmann R, Mundlos S, Lehmann K (2008). A microduplication of the long range SHH limb regulator (ZRS) is associated with triphalangeal thumb-polysyndactyly syndrome. *Journal of Medical Genetics* 45:370-375.

Koller KJ & Goeddel DV (1992). Molecular biology of the natriuretic peptides and their receptors. *Circulation* 86(4): 1081-1088.

Kollmann K, Damme M, Markmann S, Morelle W, Schweizer M, Hermans-Borgmeyer I, ... & Braulke T(2012). Lysosomal dysfunction causes neurodegeneration in mucolipidosis II 'knock-in' mice. *Brain* 135(9): 2661-2675.

Koltes JE, Mishra BP, Kumar D, Kataria RS, Totir LR, Fernando RL, ... & Reecy JM (2009). A nonsense mutation in cGMP-dependent type II protein kinase (PRKG2) causes dwarfism in American Angus cattle. *Proceedings of the National Academy of Sciences* 106(46): 19250-19255.

Kornak U, Mundlos S (2003). Genetic disorders of the skeleton: A developmental Approach. *American Journal of Human Genetics* 73: 447-474.

Kornfeld S & Sly WS (1985). Lysosomal storage defects. *Hospital Practice* 20(8): 71-82.

Kowalski MH, Qian H, Hou Z, Rosen JD, Tapia AL, Shan Y, ... & Li Y (2019). Use of> 100,000 NHLBI Trans-Omics for Precision Medicine (TOPMed) Consortium whole genome sequences improves imputation quality and detection of rare variant associations in admixed African and Hispanic/Latino populations. *PLoS Genetics* 15(12): e1008500.

Kozin SH (2001). Syndactyly. *Journal of the American Society for Surgery of the Hand* 1(1): 1-13.

Krejci P, Masri B, Fontaine V, Mekikian PB, Weis M, Prats H & Wilcox WR (2005). Interaction of fibroblast growth factor and C-natriuretic peptide signaling in regulation of chondrocyte proliferation and extracellular matrix homeostasis. *Journal of Cell Science* 118(21): 5089-5100.

Kudo M, Bao M, D'Souza A, Ying F, Pan H, Roe BA & Canfield WM (2005). The α-and β-subunits of the human UDP-N-acetylglucosamine: lysosomal enzyme N-acetylglucosamine-1-phosphotransferase are encoded by a single cDNA. VOLUME 280 (2005) PAGES 36141-36149. *Journal of Biological Chemistry* 280(51): 42476.

Langenickel TH, Buttgereit J, Pagel-Langenickel I, Lindner M, Monti J, Beuerlein K, ... & Bader M (2006). Cardiac hypertrophy in transgenic rats expressing a dominant-negative mutant of the natriuretic peptide receptor B. *Proceedings of the National Academy of Sciences* 103(12): 4735-4740.

Langer LO & Garrett RT (1980). Acromesomelic dysplasia. *Radiology* 137(2): 349-355.

Langer LO, Cervenka J & Camargo M (1989). A severe autosomal recessive acromesomelic dysplasia, the Hunter-Thompson type, and comparison with the Grebe type. *Human Genetics* 81: 323-328.

LaPlante JM, Sun M, Falardeau J, Dai D, Brown EM, Slaugenhaupt SA & Vassilev PM (2006). Lysosomal exocytosis is impaired in mucolipidosis type IV. *Molecular Genetics and Metabolism* 89(4): 339-348.

Laufer E, Nelson CE, Johnson RL, Morgon BA, Tabin C (1994). *Sonic hedgehog* and *Fgf-4* act through a signaling cascade and feedback loop to integrate growth and patterning of developing limb bud. *Cell* 79: 993-1003.

Lauritano D, Attuati S, Besana M, Rodilosso G, Quinzi V, Marzo G & Carinci F (2019). Oral and craniofacial manifestations of Ellis-Van Creveld syndrome: A systematic review. *European Journal of Paediatric Dentistry* 20(4): 306-310.

Le Douarin NM, Creuzet S, Couly G, Dupin E (2004). Neural crest cell plasticity and its limits. *Development* 131 (19): 4637-4650.

Lee CS, Buttitta LA, May NR, Kispert A, Fan CM (2000). SHH-N regulates Sfrp2 to mediate its competitive interaction with Wnt1/4 in the somatic mesoderm. *Development* 127: 109-118.

Lee NK, Karsenty G (2008). *Trends in Endocrinology and Metabolism* 19 (5):161-166.

Lee WS, Payne BJ, Gelfman CM, Vogel P & Kornfeld S (2007). Murine UDP-GlcNAc: lysosomal enzyme N-acetylglucosamine-1-phosphotransferase lacking the γ-subunit retains substantial activity toward acid hydrolases. *Journal of Biological Chemistry* 282(37): 27198-27203.

Lerch H. (1948). Erbliche Synostosen der Ossa metacarpalia IV und V. *Z Orthop* 78: 13-16.

Leroy JG, DeMars RI (1967). Mutant enzymatic and cytological phenotypes in cultured human fibroblasts. *Science* 157(3790): 804-806.

Lettice LA, Heaney SJ, Purdie LA, Li L, De Beer P, Oostra BA, ... & de Graaff E (2003). A long-range Shh enhancer regulates expression in the developing limb and fin and is associated with preaxial polydactyly. *Human Molecular Genetics* 12(14): 1725-1735.

Lettice LA, Horikoshi T, Heaney SJ, van Baren MJ, van der Linde HC, Breedveld GJ, ... & Noji S (2002). Disruption of a long-range cis-acting regulator for Shh causes preaxial polydactyly. *Proceedings of the National Academy of Sciences* 99(11): 7548-7553.

Levin M (2002). Isolation and community: a review of the role of gap-junctional communication in embryonic patterning. *Journal of Membrane Biology* 185(3).

Li H & Durbin R (2009). Fast and accurate short read alignment with Burrows–Wheeler transform. *Bioinformatics* 25(14): 1754-1760.

Li H, Wang CY, Wang JX, Wu GS, Yu P, Yan XY, ... & Zhang YP (2009). Mutation analysis of a large Chinese pedigree with congenital preaxial polydactyly. *European Journal of Human Genetics* 17(5): 604-610.

Li Y, Pawlik B, Elcioglu N, Aglan M, Kayserili H, Yigit G, ... & Wollnik B (2010). LRP4 mutations alter Wnt/β-catenin signaling and cause limb and kidney malformations in Cenani-Lenz syndrome. *The American Journal of Human Genetics* 86(5): 696-706.

Lincoln TM & Cornwell TL (1993). Intracellular cyclic GMP receptor proteins. *The FASEB Journal* 7(2): 328-338.

Liu S, Zhang W, Shi H, Yao F, Wei M & Qiu Z (2016). Mutation analysis of 16 mucolipidosis II and III alpha/beta Chinese children revealed genotype-phenotype correlations. *PLoS One* 11(9): e0163204.

Lohan S, Spielmann M, Doelken SC, Flöttmann R, Muhammad F, Baig SM, ... & Klopocki E (2014). Microduplications encompassing the Sonic hedgehog limb enhancer ZRS are associated with Haas- type polysyndactyly and Laurin-Sandrow syndrome. *Clinical Genetics* 86(4): 318-325.

Lohmann W (1920). Beitrag zur Kenntnis des reinen Mikrophthalmus. *Arch Augenheilkd* 86: 136-141.

Lonardo F, Della Monica M, Riccardi G, Riccio I, Riccio V & Scarano G (2004). A family with X- linked recessive fusion of metacarpals IV and V. *American Journal of Medical Genetics Part A* 124(4): 407-410.

Loren DJ, Campos Y, d'Azzo A, Wyble L, Grange DK, Gilbert-Barness E, ... & Hamvas A (2005). Sialidosis presenting as severe nonimmune fetal hydrops is associated with two novel mutations in lysosomal α-neuraminidase. *Journal of Perinatology* 25(7): 491-494.

Lueken KG (1938). Uber eine Familie mit Syndaktylie. *Z Menschl Vererb Konstituts* 22: 152-159.

Lukatela G, Krauss N, Theis K, Selmer T, Gieselmann VV, Von Figura K & Saenger W (1998). Crystal structure of human arylsulfatase A: the aldehyde function and the metal ion at the active site suggest a novel mechanism for sulfate ester hydrolysis. *Biochemistry* 37(11): 3654-3664.

Lyles CR, Lunn MR, Obedin-Maliver J, Bibbins-Domingo K (2018). The new era of precision population health: insights for the All of Us Research Program and beyond. *Journal of Translational Medicine* 16:1-4.

Malik S (2012). Syndactyly: Phenotypes, genetics and current classification. *European Journal of Human Genetics* 20: 817-824.

Malik S, Abbasi AA, Ansar M, Ahmad W, Koch MC & Grzeschik KH (2006). Genetic heterogeneity of synpolydactyly: a novel locus SPD3 maps to chromosome 14q11. 2- q12. *Clinical Genetics* 69(6): 518-524.

Malik S, Ahmad W, Grzeschik KH & Koch MC (2005). A simple method for characterising syndactyly in clinical practice. *Genetic Counseling* 16(3): 229-238.

Malik S, Arshad M, Amin- ud- Din M, Oeffner F, Dempfle A, Haque S, ... & Grzeschik KH (2004). A novel type of autosomal recessive syndactyly: clinical and molecular studies in a family of Pakistani origin. *American Journal of Medical Genetics Part A* 126(1): 61-67.

Malik S, Grzeschik KH (2008). Synpolydactyly: Clinical and molecular advances. *Clinical Genetics* 73: 113-120.

Malik S, Jabeen N (2011). Zygodactyly with thumb aplasia: an unusual variant in a male subject. *Journal of the College of Physicians and Surgeons Pakistan* 21:710-712.

Malik S, Percin FE, Ahmad W, Percin S, Akarsu NA, Koch MC & Grzeschik KH (2005). Autosomal recessive mesoaxial synostotic syndactyly with phalangeal reduction maps to chromosome 17p13. 3. *American Journal of Medical Genetics Part A* 134(4): 404-408.

Malik S, Schott J, Ali SW, Oeffner F, Amin-ud-Din M, Ahmad W, ... & Koch MC (2005). Evidence for clinical and genetic heterogeneity of syndactyly type I: the phenotype of second and third toe syndactyly maps to chromosome 3p21. 31. *European Journal of Human Genetics* 13(12): 1268-1274.

Maroteaux P, Lamy M & Bernard J (1957). La dysplastie spodyloepiphysaire tardive: Description clinique et radiologique. *Presse méd* 65:1205-1208.

Maroteaux P, Martinelli B & Campailla E (1971). Acromesomelic dwarfism. *La Presse Medicale* 79(42): 1839-1842.

Martinez-Garcia M, Garcia-Canto E, Fenollar-Cortes M, Aytes AP & Trujillo-Tiebas MJ (2016). Characterization of an acromesomelic dysplasia, Grebe type case: novel mutation affecting the recognition motif at the processing site of GDF5. *Journal of Bone and Mineral Metabolism* 34: 599-603.

Massagué J, Attisano L & Wrana JL (1994). The TGF-β family and its composite receptors. *Trends in Cell Biology* 4(5): 172-178.

Masue M, Sukegawa K, Orii T, Hashimoto T (1991). N-acetylgalactosamine-6-sulfate sulfatase in human placenta: purification and characteristics. *Journal of Biochemistry* 110(6): 965-970.

Masuno M, Tomatsu S, Nakashima Y, Hori T, Fukuda S, Masue M, Sukegawa K, Orii T (1993). Mucopolysaccharidosis IV A: assignment of the human Nacetylgalactosamine-6-sulfate sulfatase (GALNS) gene to chromosome 16q24. *Genomics* 16: 777-778.

Matalon R, Arbogast B, Justice P, Brandt IK, Dorfman A (1974). Morquio's syndrome: defciency of a chondroitin sulfate N-acetyl hexosamine sulfate sulfatase. *Biochemical and Biophysical Research Communications* 61 (2):759–765.

Mazzeu JF & Brunner HG (2020). 50 years of Robinow syndrome. *American Journal of Medical Genetics. A* 182: 2005-2007

McKenna A, Hanna M, Banks E, Sivachenko A, Cibulskis K, Kernytsky A, ... & DePristo MA (2010). The Genome Analysis Toolkit: a Map Reduce framework for analyzing next-generation DNA sequencing data. *Genome Research* 20(9): 1297-1303.

Merino R, Rodriguez-Leon J, Macias D, Ganan Y, Economides AN, Hurle, J. M. (1999). The BMP antagonist Gremlin regulates outgrowth, chondrogenesis and programmed cell death in the developing limb. *Development* 126(23): 5515-5522.

Meyer-Schwickerath G (1957). Mikrophthalmussyndrome. *Klin Monatsbl Augenheilkd* 131:18-30.

Minami Y, Oishi I, Endo M & Nishita M (2010). Ror- family receptor tyrosine kinases in noncanonical Wnt signaling: Their implications in developmental morphogenesis and human diseases. *Developmental dynamics: an official publication of the American Association of Anatomists* 239(1): 1-15.

Miura K, Kim OH, Lee HR, Namba N, Michigami T, Yoo WJ, ... & Cho TJ (2014). Overgrowth syndrome associated with a gain- of- function mutation of the natriuretic peptide receptor 2 (NPR2) gene. *American Journal of Medical Genetics Part A* 164(1): 156-163.

Mondolfi PE (1983). Syndactyly of toes. *Plastic and Reconstructive Surgery* 71(2):212-217.

Montagu MFA (1953). A pedigree of syndactylism of the middle and ring fingers. *American Journal of Human Genetics* 5: 70-72.

Morrone A, Tylee KL, Al-Sayed M, Brusius-Facchin AC, Caciotti A, Church HJ (2014 a). Molecular testing of 163 patients with Morquio A (Mucopolysaccharidosis IVA) identifies 39 novel GALNS mutations. *Molecular Genetics and Metabolism* 112: 160-170.

Mortier GR (2001). The diagnosis of skeletal dysplasias: a multidisciplinary approach. *European Journal of Radiology* 40:161-167.

Munro S (2001). The MRH domain suggests a shared ancestry for the mannose 6-phosphate receptors and other N-glycan-recognising proteins. *Current Biology* 11(13): 499-501.

Muragaki Y, Mundlos S, Upton J & Olsen BR (1996). Altered growth and branching patterns in synpolydactyly caused by mutations in HOXD13. *Science* 272(5261): 548-551.

Muragaki Y, Mundlos S, Upton J, Olsen BR (1996). Altered growth and branching patterns in synpolydactyly caused by mutations in HOXD13. *Science* 272(5261): 548-5451.

Mustafa S, Akhtar Z, Latif M, Hassan M, Faisal M & Iqbal F (2020). A novel nonsense mutation in NPR2 gene causing Acromesomelic dysplasia, type Maroteaux in a consanguineous family in Southern Punjab (Pakistan). *Genes & Genomics* 42: 847-854.

Nakashima Y, Tomatsu S, Hori T, Fukuda S, Sukegawa K, Kondo N *et al* (1994). Mucopolysaccharidosis IV A: molecular cloning of the human N-acetylgalactosamine-6-sulfatase gene (GALNS) and analysis of the 5'-fanking region. *Genomics* 20:99–104.

National Institute of Neurological Disorders and Stroke. Mucolipidoses Fact Sheet. September 2015. NIH Publication No. 15-4899. Available online: https://www.ninds.nih.gov/Disorders/Patient-Caregiver-Education/Fact-Sheets/Mucolipidoses-Fact-Sheet (accessed on 29 July 2020).

Netscher DT, Baumholtz MA (2007). Treatment of congenital upper extremity problems. *Plastic and Reconstructive Surgery* 119 (5): 101-129.

Niederreither K, Subbarayan V, Dolle P, Chambon P (1999). Embryonic retinoic acid synthesis is essential for early mouse post-implantation development. *Nature Genettics* 21:444–448.

Nishimura F, Naruishi H, Naruishi K, Yamada T, Sasaki J, Peters C, ... & Murayama Y (2002). Cathepsin-L, a key molecule in the pathogenesis of drug-induced and I-cell disease-mediated gingival overgrowth: a study with cathepsin-L-deficient mice. *The American Journal of Pathology* 161(6): 2047-2052.

Niswander L, Martin GR (1992). Fgf-4 expression during gastrulation, myogenesis, limb and tooth development in the mouse. *Development* 114: 755-768.

Niswander L, Tickle C, Jeffery S, Martin GR, Tickle C (1994). A positive feedback loop coordinates growth and patterning in vertebrate limb. *Nature* 371: 609-612.

Nohe A, Hassel S, Ehrlich M, Neubauer F, Sebald W, Henis YI & Knaus P (2002). The mode of bone morphogenetic protein (BMP) receptor oligomerization determines different BMP-2 signaling pathways. *Journal of Biological Chemistry*, *277*(7), 5330-5338.

Norbnop P, Scrichomthong C, Suphapeetiporen K, Shotelersuk V (2014). ZRS 406 A>G mutation in patients with tibial hypoplasia, polydactyly and triphalangeal first fingers. *Journal of Human Genetics* 59: 467-470.

Oishi I, Suzuki H, Onishi N, Takada R, Kani S, Ohkawara B, ... & Minami Y (2003). The receptor tyrosine kinase Ror2 is involved in non- canonical Wnt5a/JNK signalling pathway. *Genes to Cells* 8(7): 645-654.

Olney RC (2006). C-type natriuretic peptide in growth: a new paradigm. *Growth Hormone & IGF Research* 16: 6-14.

Olney RC, B. külmez H, Bartels CF, Prickett TC, Espiner EA, Potter LR. & Warman ML (2006). Heterozygous mutations in natriuretic peptide receptor-B (NPR2) are associated with short stature. *The Journal of Clinical Endocrinology & Metabolism* 91(4): 1229-1232.

Olsen BR, Reginato AM, Wang W (2000). Bone development. *Annual Review of cell and Developmental Biology* 16 (1):191-220.

Orel H (1928) Kleine Beitrage zur Vererbunswissenschaft 1. *Polydaktylie Z Konstit-Lehre.* 13: 691-698.

Osebold WR, Lester EL, Remondini DJ, Spranger JW, Opitz JM & Reynolds JF (1985). An autosomal dominant syndrome of short stature with mesomelic shortness of limbs, abnormal carpal and tarsal bones, hypoplastic middle phalanges, and bipartite calcanei. *American Journal of Medical Genetics* 22(4): 791-809.

Oussoren E, van Eerd D, Murphy E, Lachmann R, van der Meijden JC, Hoefsloot LH, ... & Langeveld M (2018). Mucolipidosis type III, a series of adult patients. *Journal of Inherited Metabolic Disease* 41: 839-848.

Pagel-Langenickel I, Buttgereit J, Bader M & Langenickel TH (2007). Natriuretic peptide receptor B signaling in the cardiovascular system: protection from cardiac hypertrophy. *Journal of Molecular Medicine* 85: 797-810.

Palmieri M, Impey S, Kang H, di Ronza A, Pelz C, Sardiello M & Ballabio A (2011). Characterization of the CLEAR network reveals an integrated control of cellular clearance pathways. *Human Molecular Genetics* 20(19): 3852-3866.

Panda A, Gamanagatti S, Jana M & Gupta AK (2014). Skeletal dysplasias: a radiographic approach and review of common non-lethal skeletal dysplasias. *World Journal of Radiology* 6(10): 808.

Parenti G, Andria G & Ballabio A (2015). Lysosomal storage diseases: from pathophysiology to therapy. *Annual Review of Medicine* 66: 471-486.

Parilla BV, Leeth EA, Kambich MP, Chilis P & MacGregor SN (2003). Antenatal detection of skeletal dysplasias. *Journal of Ultrasound in Medicine* 22(3): 255-258.

Parr BA, McMahon AP (1995). Dorsalizing signal Wnt-7a required for normal polarity of d-v and a-p axes of mouse limb. *Nature* 374:350–353.

Paznekas WA, Boyadjiev SA, Shapiro RE, Daniels O, Wollnik B, Keegan CE, ... & Jabs EW (2003). Connexin 43 (GJA1) mutations cause the pleiotropic phenotype of oculodentodigital dysplasia. *The American Journal of Human Genetics* 72(2): 408-418.

Paznekas WA, Karczeski B, Vermeer S, Lowry RB, Delatycki M, Laurence F, ... & Wang Jabs E (2009). GJA1 mutations, variants, and connexin 43 dysfunction as it relates to the oculodentodigital dysplasia phenotype. *Human Mutation* 30(5): 724-733.

Pei SLC & Chung BHY (2022). Genetics and mechanism of ciliopathies. *Frontiers in Genetics* 13: 1067168.

Peña-Cardelles JF, Domínguez-Medina DA, Cano-Durán JA, Ortega-Concepción D & Cebrián JL (2019). Oral manifestations of ellis-van creveld syndrome. A rare case report. *Journal of Clinical and Experimental Dentistry* 11(3): e290.

Peracha H, Sawamoto K, Averill L, Kecskemethy H, Theroux M, Thacker M *et al* (2018). Molecular genetics and metabolism, special edition: diagnosis, diagnosis and prognosis of Mucopolysaccharidosis IVA. *Molecular Genetics and Metabolism*. 125:18–37.

Percin EF, Percin S, Egilmez H, Sezgin I, Ozbas F & Akarsu AN (1998). Mesoaxial complete syndactyly and synostosis with hypoplastic thumbs: an unusual combination or homozygous expression of syndactyly type I?. *Journal of Medical Genetics* 35(10): 868-874.

Pfeifer A, Aszodi A, Seidler U, Ruth P, Hofmann F & Fässler R (1996). Intestinal secretory defects and dwarfism in mice lacking cGMP-dependent protein kinase II. *Science* 274(5295): 2082-2086.

Pfeifer A, Ruth P, Dostmann W, Sausbier M, Klatt P & Hofmann F (2005). Structure and function of cGMP-dependent protein kinases. *Reviews of Physiology, Biochemistry and Pharmacology* 135: 105-149.

Potter LR & Hunter T (1998). Identification and characterization of the major phosphorylation sites of the B-type natriuretic peptide receptor. *Journal of Biological Chemistry* 273(25): 15533-15539.

Potter LR, Abbey-Hosch S & Dickey DM (2006). Natriuretic peptides, their receptors, and cyclic guanosine monophosphate-dependent signaling functions. *Endocrine Reviews* 27(1): 47-72.

Potter LR, Abbey-Hosch S & Dickey DM (2006). Natriuretic peptides, their receptors, and cyclic guanosine monophosphate-dependent signaling functions. *Endocrine Reviews* 27(1): 47-72.

Pshezhetsky AV & Potier M (1996). Association of N-acetylgalactosamine-6-sulfate sulfatase with the multienzyme lysosomal complex of β-galactosidase, cathepsin

A, and neuraminidase: possible implication for intralysosomal catabolism of keratan sulfate. *Journal of Biological Chemistry* 271(45): 28359-28365.

Pusapati GV, Hughes CE, Dorn KV, Zhang D, Sugianto P, Aravind L & Rohatgi R (2014). EFCAB7 and IQCE regulate hedgehog signaling by tethering the EVC-EVC2 complex to the base of primary cilia. *Developmental cell* 28(5): 483-496.

Qian Y, Lee I, Lee WS, Qian M, Kudo M, Canfield WM, ... & Kornfeld S (2010). Functions of the α, β, and γ subunits of UDP-GlcNAc: lysosomal enzyme N-acetylglucosamine-1-phosphotransferase. *Journal of Biological Chemistry* 285(5): 3360-3370.

Quadri N & Upadhyai P (2023). Primary cilia in skeletal development and disease. *Experimental Cell Research* 113751.

Raas-Rothschild A, Cormier-Daire V, Bao M, Genin E, Salomon R, Brewer K, ... & Canfield WM (2000). Molecular basis of variant pseudo-hurler polydystrophy (mucolipidosis IIIC). *The Journal of Clinical Investigation* 105(5): 673-681.

Racacho, L., Byrnes, A. M., MacDonald, H., Dranse, H. J., Nikkel, S. M., Allanson, J., ... & Bulman, D. E. (2015). Two novel disease-causing variants in BMPR1B are associated with brachydactyly type A1. *European Journal of Human Genetics*, *23*(12), 1640-1645.

Rajab A, Kunze J & Mundlos S (2004). Spondyloepiphyseal dysplasia Omani type: a new recessive type of SED with progressive spinal involvement. *American Journal of Medical Genetics Part A* 126(4): 413-419.

Rajab A, Kunze J & Mundlos S (2004). Spondyloepiphyseal dysplasia Omani type: a new recessive type of SED with progressive spinal involvement. *American Journal of Medical Genetics Part A* 126(4): 413-419.

Reaume AG, de Sousa PA, Kulkarni S, Langille BL, Zhu D, Davies TC, ... & Rossant J (1995). Cardiac malformation in neonatal mice lacking connexin 43. *Science* 267(5205): 1831-1834.

Richardson R, Donnai D, Meire F & Dixon MJ (2004). Expression of Gja1 correlates with the phenotype observed in oculodentodigital syndrome/type III syndactyly. *Journal of Medical Genetics* 41(1): 60-67.

Rivera-Colón Y, Schutsky EK, Kita AZ, Garman SC (2012). The structure of human GALNS reveals the molecular basis for mucopolysaccharidosis IV A. *Journal of Molecular Biology* 423: 736-751.

Robinow M, Johnson GF, Broock GJ & Opitz JM (1982). Syndactyly type V. *American Journal of Medical Genetics* 11(4): 475-482.

Robinow M, Silverman FN & Smith HD (1969). A newly recognized dwarfing syndrome. *American journal of diseases of children* 117(6): 645-651.

Ruiz-Perez VL, Ide SE, Strom TM, Lorenz B, Wilson D, Woods K, ... & Goodship J (2000). Mutations in a new gene in Ellis-van Creveld syndrome and Weyers acrodental dysostosis. *Nature genetics* 24(3): 283-286.

Sacher M, Kim YG, Lavie A, Oh BH & Segev N (2008). The TRAPP complex: insights into its architecture and function. *Traffic* 9(12): 2032-2042.

Sacher M, Shahrzad N, Kamel H & Milev M P (2019). TRAPPopathies: an emerging set of disorders linked to variations in the genes encoding transport protein particle (TRAPP)- associated proteins. *Traffic* 20(1) 5-26.

Sagai T, Masuya H, Tamura M, Shimizu K, Yada Y, Wakana S, ... & Shiroishi T (2004). Phylogenetic conservation of a limb-specific, cis-acting regulator of Sonic hedgehog (Shh). *Mammalian Genome 15*: 23-34.

Saito S, Ohno K, Maita N & Sakuraba H (2014). Structural and clinical implications of amino acid substitutions in α-L-iduronidase: insight into the basis of mucopolysaccharidosis type I. *Molecular Genetics and Metabolism* 111(2): 107-112.

Sargar KM., Singh AK, Kao SC (2017). Imaging of skeletal disorders caused by fibroblast growth factor receptor gene mutations. *Radiographics* 37(6): 1813-1830.

Satoh W, Gotoh T, Tsunematsus Y, Aizawa S, Shimono A (2006). Sfrp1 and Sfrp2 regulate anteroposterior axis elongation and somite segmentation during mouse embryogenesis. *Development* 133:989-999.

Satoh W, Matsuyama M, Takemura H, Aizawa S, Shimono A (2008). Sfrp1 and Sfrp2 regulate the Wnt/β-catenin and the planer cell polarity pathway during the early trunk formation in mouse. *Genesis* 41: 92-103.

Saunders JW Jr (1972). Developmental control of three dimensional polarity in the avian limb. *Annals of the New York Academy of Sciences* 193: 29-42.

Saunders JW Jr (1977). The experimental analysis of chick limb development in vertebrate limb and somite morphogenesis. *Cambridge: Cambridge University Press*. P 1-24.

Saunders JW Jr, Gasseling M (1968) In Epithelial-Mesenchymal Interaction. R Fleischmayer and RB Billingham, eds (*Baltimore: Williams and Wilkins*), pp. 78-97.

Savarirayan R and Rimoin DL (2002). The skeletal dysplasias. *Best Practice and Research. Clinical Endocrinology and Metabolism* 16 (3): 5470560.

Sayli B, Akarsu A, Sayli U, Akhan O, Ceylaner S & Sarfarazi M (1995). A Large Turkish kindred with syndactyly type II (synpolydactyly).I. Field investigation, clinical and pedigree data. *Journal of Medical Genetics* 32: 421-434.

Schiff M, Maire I, Bertrand Y, Cochat P, Guffon N (2005). Long-term follow-up of metachronous marrow-kidney transplantation in severe type II sialidosis: what does success mean? *Nephrology Dialysis Transplantation* 20(11): 2563-2565.

Schiffmann R, Mayfield J, Swift C & Nestrasil I (2014). Quantitative neuroimaging in mucolipidosis type IV. *Molecular Genetics and Metabolism* 111(2): 147-151.

Schramm T, Gloning KP, Minderer S, Daumer- Haas C, Hörtnagel K, Nerlich A & Tutschek B (2009). Prenatal sonographic diagnosis of skeletal dysplasias. *Ultrasound in Obstetrics and Gynecology: The Official Journal of the International Society of Ultrasound in Obstetrics and Gynecology* 34(2): 160-170.

Schröder B, Wrocklage C, Pan C, Jäger R, Kösters B, Schäfer H, ... & Hasilik A (2007). Integral and associated lysosomal membrane proteins. *Traffic* 8(12): 1676-1686.

Schulz S (2005). C-type natriuretic peptide and guanylyl cyclase B receptor. *Peptides* 26(6): 1024-1034.

Schulz S (2005). C-type natriuretic peptide and guanylyl cyclase B receptor. *Peptides* 26(6): 1024-1034.

Scott HS, Anson DS, Orsborn AM, Nelson PV, Clements PR, Morris CP & Hopwood JJ (1991). Human alpha-L-iduronidase: cDNA isolation and expression. *Proceedings of the National Academy of Sciences* 88(21): 9695-9699.

Scott HS, Ashton LJ, Eyre HJ, Baker E, Brooks DA, *et al* (1990). Chromosomal localization of the human α-L-Iduronidase gene (IDUA) to 4p16.3. *American Journal of Human Genetics* 47:802–807.

Scott HS, Guo XH, Hopwood JJ & Morris CP (1992). Structure and sequence of the human α-L-iduronidase gene. *Genomics* 13(4): 1311-1313.

Shibazaki T, Hirabayashi K, Saito S, Shigemura T, Nakazawa Y, Sakashita K, ... & Koike K (2016). Clinical and laboratory outcomes after umbilical cord blood transplantation in a patient with mucolipidosis II alpha/beta. *American Journal of Medical Genetics Part A* 170(5): 1278-1282.

Slaugenhaupt SA, Acierno Jr JS, Helbling LA, Bove C, Goldin E, Bach G, ... & Gusella JF (1999). Mapping of the mucolipidosis type IV gene to chromosome 19p and definition of founder haplotypes. *The American Journal of Human Genetics* 65(3): 773-778.

Sleat DE, Ding L, Wang S, Zhao C, Wang Y, Xin W, ... & Sims KB (2009). Mass spectrometry-based protein profiling to determine the cause of lysosomal storage diseases of unknown etiology. *Molecular & Cellular Proteomics* 8(7): 1708-1718.

Söhl G & Willecke K (2004). Gap junctions and the connexin protein family. *Cardiovascular Research* 62(2): 228-232.

Spranger J & Wiedemann HR (1966). Dysplasia spondyloepiphysaria congenita. *The Lancet* 288(7464): 642.

Spranger JW & Densler JR J (1970). Spondyloepiphyseal dysplasia congenita. *Radiology* 94 (2):313-322.

Spranger JW & Wiedemann HR (1970). The genetic mucolipidoses: Diagnosis and differential diagnosis. *Humangenetik* 9(2): 113-139.

Spritz, Richard A., Robert A. Doughty, Thomas J. Spackman, Mary Jo Murnane, Paul M. Coates, Otakar Koldovský, and Elaine H. Zackai (1978). Neonatal presentation of I-cell disease. *The Journal of Pediatrics* 93 (6): 954-958.

Srivastava P, Pandey H, Agarwal D, Mandal K & Phadke SR (2017). Spondyloepiphyseal dysplasia Omani type: CHST3 mutation spectrum and phenotypes in three Indian families. *American Journal of Medical Genetics Part A* 173(1): 163-168.

Stange K, Désir J, Kakar N, Mueller TD, Budde BS, Gordon CT, ... & Borck G (2015). A hypomorphic BMPR1B mutation causes du Pan acromesomelic dysplasia. *Orphanet journal of rare diseases* 10: 1-6.

Stiles KA, Hawkins (1946). The inheritance of zygodactyly. *J Hered* 37: 16-18.

Stoll C, Dott B, Roth MP & Alembik, Y (1989). Birth prevalence rates of skeletal dysplasias. *Clinical genetics* 35(2): 88-92.

Stratford T, Horton C, Maden M. (1996). Retinoic acid is required for the initiation of outgrowth in the chick limb bud. *Current Biology* 6 (9):1124–1133.

Sukegawa K, Nakamura H, Kato Z, Tomatsu S, Montaño AM, Fukao T, ... & Kondo N (2000). Biochemical and structural analysis of missense mutations in N-acetylgalactosamine-6-sulfate sulfatase causing mucopolysaccharidosis IVA phenotypes. *Human Molecular Genetics* 9 (9): 1283-1290.

Summerbell D, Lewis JH, Wolpert L (1973). Positional information in chick limb morphogenesis. *Nature* 244: 492-496.

Sun M, Ma F, Zeng X, Liu Q, Zhao XL, Wu FX, ... & Zhang X (2008). Triphalangeal thumb–polysyndactyly syndrome and syndactyly type IV are caused by genomic duplications involving the long range, limb-specific SHH enhancer. *Journal of Medical Genetics* 45(9): 589-595.

Suzuki HR, Sakamoto H, Yashida T, Sugimura T (1992). Localization of Hstl transcripts to the apical ectodermal ridge in the mouse embryo. *Developmental Biology* 150: 219-222.

Swindell EC, Thaller C, Sockanathan S, Petkovich M, Jessell TM, Eichele G (1999) Complementary domains of retinoic acid production and degradation in the early chick embryo. *Developmental Biology* 216:282–296.

Szklarczyk D, Franceschini A, Wyder S, Forslund K, Heller D, Huerta-Cepas J, ... & Von Mering C (2015). STRING v10: protein–protein interaction networks, integrated over the tree of life. *Nucleic Acids Research* 43(1): 447-452.

Szpiro-Tapia S, Sefiani A, Guilloud-Bataille M, Heuertz S, Le Marec B, Frezal J, ... & Hors-Cayla MC (1988). Spondyloepiphyseal dysplasia tarda: linkage with genetic markers from the distal short arm of the X chromosome. *Human Genetics* 81(1): 61-63.

Taichman RS (2005). Blood and bone: two tissues whose fates are intertwined to create the hematopoietic stem-cell niche. *Blood* 105(7):2631-2639.

Tamura N & Garbers DL (2003). Regulation of the guanylyl cyclase-B receptor by alternative splicing. *Journal of Biological Chemistry* 278(49): 48880-48889.

Tamura N, Doolittle LK, Hammer RE, Shelton JM, Richardson JA & Garbers DL (2004). Critical roles of the guanylyl cyclase B receptor in endochondral ossification and development of female reproductive organs. *Proceedings of the National Academy of Sciences* 101(49): 17300-17305.

Taylor JA, Gibson GJ, Brooks DA & Hopwood JJ (1991). α-l-Iduronidase in normal and mucopolysaccharidosis-type-I human skin fibroblasts. *Biochemical Journal* 274(1): 263-268.

Temtamy SA, Ismail S, Nemat A (2003). Mild facial dysmorphism and quasidominat inheritance in Cenani-Lenz syndrome. *Clinical Dysmorphology* 12:77-83.

Temtamy SA, McKusick VA (1978). Syndactyly: The genetics of hand malformation. New York: *Alan R Liss* 301-322.

Terhal PA, Nievelstein RJA, Verver EJ, Topsakal V, van Dommelen P, Hoornaert K, ... & Mortier GR (2015). A study of the clinical and radiological features in a cohort of 93 patients with a COL2A1 mutation causing spondyloepiphyseal dysplasia congenita or a related phenotype. *American Journal of Medical Genetics Part A* 167(3): 461-475.

Thaller C, Eichele G (1987). Identification and spatial distribution of retinoids in the developing chick limb bud. *Nature* 327:625–628.

Thiele H, Sakano M, Kitagawa H, Sugahara K, Rajab A, Höhne W, ... & Mundlos S (2004). Loss of chondroitin 6-O-sulfotransferase-1 function results in severe human chondrodysplasia with progressive spinal involvement. *Proceedings of the National Academy of Sciences* 101(27): 10155-10160.

Thomas JT, Kilpatrick MW, Lin K, Erlacher L, Lembessis P, Costa T, ... & Luyten F P (1997). Disruption of human limb morphogenesis by a dominant negative mutation in CDMP1. *Nature Genetics* 17(1): 58-64.

Tickle C, Eichele G (1994). Vertebrate limb development. *Annual Review of Cell Biology* 10:121-152.

Tiede S, Storch S, Lübke T, Henrissat B, Bargal R, Raas-Rothschild A & Braulke T (2005). Mucolipidosis II is caused by mutations in GNPTA encoding the α/β GlcNAc-1-phosphotransferase. *Nature Medicine* 11(10): 1109-1112.

Tomatsu S, Fukuda S, Masue M, Sukegawa K, Fukao T, Yamagishi A *et al* (1991). Morquio disease: isolation, characterization and expression of full-length cDNA for human N-acetylgalactosamine-6-sulfate sulfatase. *Biochemical and Biophysical Research Communications* 181:677–683.

Towers M & Tickle C (2009). Growing models of vertebrate limb development. *Development* 136:179-190.

Tsuchida A, Yokoi N, Namae M, Fuse M, Masuyama T, Sasaki M, ... & Komeda K (2008). Phenotypic characterization of the Komeda miniature rat Ishikawa, an animal model of dwarfism caused by a mutation in Prkg2. *Comparative Medicine* 58(6): 560-567.

Tsutsumi K, Shimakawa H, Kitagawa H, Sugahara K (1998). Functional expression and genomic structure of human chondroitin 6-sulfotransferase 1. *FEBS Lett* 441(2):235-241.

Tucker AS, Matthews KL, Sharpe PT (1998). Transformation of tooth type induced by inhibition of bmp signaling. *Science* 282:1136–1138.

Tuna EB, Koruyucu M, Kürklü E, Çifter M, Gençay K, Seymen F & Tüysüz B (2016). Oral and craniofacial manifestations of Ellis–van Creveld syndrome: Case series. *Journal of Cranio-Maxillofacial Surgery* 44(8): 919-924.

Turan MG, Orhan ME, Cevik S & Kaplan OI (2023). CiliaMiner: an integrated database for ciliopathy genes and ciliopathies. *Database* 2023: baad047.

Turgut GT, Kalelioglu IH, Karaman V, Sarac Sivrikoz T, Karaman B, Uyguner ZO & Kalayci T(2023). Fibular Agenesis and Ball-Like Toes Mimicking Preaxial Polydactyly: Prenatal Presentation of Du Pan Syndrome. *Molecular Syndromology* 14(2): 152-157.

Tüysüz B, Kasapçopur Ö, Alkaya DU, Şahin S, Sözeri B & Yeşil G (2018). Mucolipidosis type III gamma: three novel mutation and genotype-phenotype study in eleven patients. *Gene* 64(2): 398-407.

Tuysuz B, Mizumoto S, Sugahara K, Celebi A, Mundlos S & Turkmen S (2009). Omani- type spondyloepiphyseal dysplasia with cardiac involvement caused by a missense mutation in CHST3. *Clinical Genetics* 75(4): 375-383.

Tuysuz B, Mizumoto S, Sugahara K, Celebi A, Mundlos S & Turkmen S (2009). Omani- type spondyloepiphyseal dysplasia with cardiac involvement caused by a missense mutation in CHST3. *Clinical Genetics* 75(4): 375-383.

Tyl RW, Chernoff N & Rogers JM (2007). Altered axial skeletal development. *Birth Defects Research Part B: Developmental and Reproductive Toxicology* 80(6): 451-472.

Ullah A, Umair M, Muhammad D, Bilal M, Lee K, Leal SM & Ahmad W (2018). A novel homozygous variant in BMPR1B underlies acromesomelic dysplasia Hunter–Thompson type. *Annals of Human Genetics* 82(3): 129-134.

Ullah A, Umair M, Muhammad D, Bilal M, Lee K, Leal SM & Ahmad W (2018). A novel homozygous variant in BMPR1B underlies acromesomelic dysplasia Hunter–Thompson type. *Annals of HumanGgenetics* 82(3): 129-134.

Umair M, Khan S & Ahmad W (2015). Homozygous sequence variants in the NPR2 gene underlying Acromesomelic dysplasia Maroteaux type (AMDM) in consanguineous families. *Annals of Human Genetics* 79(4): 238-244.

Umair M, Rafique A, Ullah A, Ahmad F, Ali RH, Nasir A, ... & Ahmad W (2017). Novel homozygous sequence variants in the GDF5 gene underlie acromesomelic dysplasia type- grebe in consanguineous families. *Congenital Anomalies* 57(2): 45-51.

Unger S, Ferreira CR, Mortier GR, Ali H, Bertola DR, Calder A, ... & Superti- Furga A (2023). Nosology of genetic skeletal disorders: 2023 revision. *American Journal of Medical Genetics Part A* 191(5): 1164-1209.

Unger S, Lausch E, Rossi A, Mégarbané A, Sillence D, Alcausin M, ... & Superti- Furga A (2010). Phenotypic features of carbohydrate sulfotransferase 3 (CHST3) deficiency in 24 patients: congenital dislocations and vertebral changes as principal diagnostic features. *American Journal of Medical Genetics Part A* 152(10): 2543-2549.

Van Meel E, Lee WS, Liu L, Qian Y, Doray B & Kornfeld S (2016). Multiple domains of GlcNAc-1-phosphotransferase mediate recognition of lysosomal enzymes. *Journal of Biological Chemistry* 291(15): 8295-8307.

van Roij MH, Mizumoto S, Yamada S, Morgan T, Tan- Sindhunata MB, Meijers-Heijboer H, ... & Robertson SP (2008). Spondyloepiphyseal dysplasia, Omani type: further definition of the phenotype. *American Journal of Medical Genetics Part A* 146(18): 2376-2384.

Vasques G A, Arnhold IJ & Jorge AA (2014). Role of the natriuretic peptide system in normal growth and growth disorders. *Hormone Research in Paediatrics* 82(4): 222-229.

Velho RV, Harms FL, Danyukova T, Ludwig NF, Friez MJ, Cathey SS, ... & Pohl S (2019). The lysosomal storage disorders mucolipidosis type II, type III alpha/beta, and type III gamma: Update on GNPTAB and GNPTG mutations. *Human Mutation* 40(7), 842-864.

Venditti R, Scanu T, Santoro M, Di Tullio G, Spaar A, Gaibisso R, ... & De Matteis MA (2012). Sedlin controls the ER export of procollagen by regulating the Sar1 cycle. *Science* 337(6102): 1668-1672.

Vitiello C, D'adamo P, Gentile F, Vingolo EM, Gasparini PAOLO & Banfi S (2005). A novel GJA1 mutation causes oculodentodigital dysplasia without syndactyly. *American Journal of Medical Genetics Part A* 133(1): 58-60.

von Bubnoff A & Cho KW (2001). Intracellular BMP signaling regulation in vertebrates: pathway or network? *Developmental Biology* 239(1): 1-14.

Wakabayashi K, Gustafson AM, Sidransky E & Goldin E (2011). Mucolipidosis type IV: an update. *Molecular Genetics and Metabolism* 104(3): 206-213.

Waldmann L, Leyhr J, Zhang H, Allalou A, Öhman- Mägi C, Haitina T (2022). The role of Gdf5 in the development of the zebrafish fin endoskeleton. *Developmental Dynamics* 251(9): 1535-1549.

Wang K, Li M & Hakonarson H (2010). ANNOVAR: functional annotation of genetic variants from high-throughput sequencing data. *Nucleic Acids Research* 38(16): e164-e164.

Wang W, Song MH, Miura K, Fujiwara M, Nawa N, Ohata Y, ... & Cho TJ (2016). Acromesomelic dysplasia, type maroteaux caused by novel loss- of- function mutations of the NPR2 gene: Three case reports. *American Journal of Medical Genetics Part A* 170(2): 426-434.

Waryah AM, Shahzad M, Shaikh H, Sheikh SA, Channa NA, Hufnagel RB, ... & Ahmed ZM (2016). A novel CHST3 allele associated with spondyloepiphyseal dysplasia and hearing loss in Pakistani kindred. *Clinical Genetics* 90(1): 90-95.

Waters AM & Beales PL (2011). Ciliopathies: an expanding disease spectrum. *Pediatric Nephrology* 26(7): 1039-1056.

Weidenreich F (1923): Die Zygodactylie und ihre Verebung. *Z Abst Vererb*. 32: 304.

Wheway G, Mitchison HM & Genomics England Research Consortium. (2019). Opportunities and challenges for molecular understanding of ciliopathies–the 100,000 genomes project. *Frontiers in Genetics* 10: 438269.

White J, Mazzeu JF, Hoischen A, Jhangiani SN, Gambin T, Alcino MC, ... & Carvalho CM (2015). DVL1 frameshift mutations clustering in the penultimate exon cause autosomal-dominant Robinow syndrome. *The American Journal of Human Genetics* 96(4): 612-622.

White JJ, Mazzeu JF, Coban-Akdemir Z, Bayram Y, Bahrambeigi V, Hoischen A, ... & Carvalho CM (2018). WNT signaling perturbations underlie the genetic heterogeneity of Robinow syndrome. *The American Journal of Human Genetics* 102(1): 27-43.

White JJ, Mazzeu JF, Hoischen A, Bayram Y, Withers M, Gezdirici A, ... & Carvalho CM (2016). DVL3 alleles resulting in a− 1 frameshift of the last exon mediate autosomal-dominant Robinow syndrome. *The American Journal of Human Genetics* 98(3): 553-561.

Whyte MP, Gottesman GS, Eddy MC & McAlister WH (1999). X-Linked Recessive Spondyloepiphyseal Dysplasia Tarda Clinical and Radiographic Evolution in a 6-Generation Kindred and Review of the Literature. *Medicine* 78(1): 9-25.

Wieczorek D, Pawlik B, Li Y, Akarsu NA, Caliebe A, May KJ, ... & Wollnik B (2010). A specific mutation in the distant sonic hedgehog (SHH) cis- regulator (ZRS) causes Werner mesomelic syndrome (WMS) while complete ZRS duplications underlie Haas type polysyndactyly and preaxial polydactyly (PPD) with or without triphalangeal thumb. *Human Mutation* 31(1): 81-89.

Wilkinson DG, Bhatt S, M, McMahon AP (1989). Expression pattern of FGF-4 related proto-oncogene int-2 suggests multiple roles in fetal development. *Development* 105: 131-136.

Winter RM, Tickle C (1993). Syndactylies and ploydactylies: Embryological overview and suggested classifications. *European Journal of Human Genetics* 1: 96-104.

Witters I, Moerman P & Fryns JP (2008). Skeletal dysplasias: 38 prenatal cases. *Genetic Counseling* 19(3): 267-275.

Wolpert L (1969). Positional information and the spatial pattern of cellular differentiation. *Journal of Theoritical Biology* 25: 1-47.

Wu L, Liang D, Niikawa N, Ma F, Sun M, Pan Q, ... & Xia J (2009). A ZRS duplication causes syndactyly type IV with tibial hypoplasia. *American Journal of Medical Genetics A* 149(4): 816-818.

www. Hgmd.cf. ac. uk accessed May, 2022

Wynne-Davies RUTH & Gormley JESS (1985). The prevalence of skeletal dysplasias. An estimate of their minimum frequency and the number of patients requiring orthopaedic care. *The Journal of Bone & Joint Surgery British* 67(1): 133-137.

Wynne-Davies RUTH & Hall CHRISTINE (1982). Two clinical variants of spondylo-epiphysial dysplasia congenita. *The Journal of Bone & Joint Surgery British* 64(4): 435-441.

Yamaguchi TP, Bradley A, McMahon AP, Jones S (1999). A wnt5a pathway underlies outgrowth of multiple structures in the vertebrate embryo. *Development* 126:1211–1223.

Yang M, Cho SY, Park HD, Choi R, Kim YE, Kim J, ... & Jin DK (2017). Clinical, biochemical and molecular characterization of Korean patients with mucolipidosis II/III and successful prenatal diagnosis. *Orphanet Journal of Rare Diseases* 12: 1-9.

Yang Y, Drossopoulou G, Chuang PT, Duprez D, Marti E, Bumcrot D, Vargesson N, Clarke J, Niswander L, McMahon A, Tickle C. (1997). Relationship between dose, distance and time in sonic hedgehog mediated regulation of anteroposterior polarity in the chick limb. *Development* 124:4393–4404.

Yıldırım Y, Ouriachi T, Woehlbier U, Ouahioune W, Balkan M, Malik S & Tolun A (2018). Linked homozygous BMPR1B and PDHA2 variants in a consanguineous family with complex digit malformation and male infertility. *European Journal of Human Genetics* 26(6): 876-885.

You G, Cai H, Jiang L, Zheng Z, Wang B, Fu Q & Wang J (2016). A novel GJA1 mutation identified by whole exome sequencing in a Chinese family with autosomal dominant syndactyly. *Clinica chimica acta* 459: 73-78.

Yuksel A. Kayserili H & Gungor F (2007). Short femurs detected at 25 and 31 weeks of gestation diagnosed as Leroy I-cell disease in the postnatal period: a report of two cases. *Fetal Diagnosis and Therapy* 22(3): 198-202.

Zákány J, Duboule D (1996). Synpolydactyly in mice with a targeted deficiency in *HoxD* complex. *Nature* 384:69-71.

Zeller R, Lopez-Rios J, Zuniga A (2009). Vertebrate limb bud development: moving towards integrative analysis of organogenesis. *Nature Review Genetics* 10: 845-858.

Zelzer E & Olsen BR (2003). The genetic basis for skeletal diseases. *Nature* 423(6937): 343-348.

Zhang C, Jolly A, Shayota BJ, Mazzeu JF, Du H, Dawood M, ... & Genomics England Research Consortium. (2022). Novel pathogenic variants and quantitative phenotypic analyses of Robinow syndrome: WNT signaling perturbation and phenotypic variability. *Human Genetics and Genomics Advances* 3(1).

Zhang C, Mazzeu JF, Eisfeldt J, Grochowski CM, White J, Akdemir ZC, ... & Carvalho CM (2021). Novel pathogenic genomic variants leading to autosomal dominant and recessive Robinow syndrome. *American Journal of Medical Genetics Part A* 185(12): 3593-3600.

Zhao X, Sun M, Zhao J, Leyva JA, Zhu H, Yang W, ... & Zhang X (2007). Mutations in HOXD13 underlie syndactyly type V and a novel brachydactyly-syndactyly syndrome. *The American Journal of Human Genetics* 80(2): 361-371.

Zhou X, Zheng C, He B, Zhu Z, Li P, He X, Zhu S, Yang C, Lao Z, Zhu Q, Liu X (2013). A novel mutation outside homeodomain of HOXD13 causes synpolydactyly in a Chinese family. *Bone* 57: 237-241.

Zuniga A, Haramis AP, McMahon AP, Zeller R (1999). Signal relay by BMP antagonism controls the SHH/FGF4 feedback loop in vertebrate limb buds. *Nature* 401: 598-602.

Turnitin Originality Report

Clinical Investigation and Genetic Characterization of Congenital Skeletal Dysplasia   by   ✗
Amjad Ali .

From Quick Submit (Quick Submit)

- Processed on 12-Jul-2024 14:20 PKT
- ID: 2415637326
- Word Count: 21246

Similarity Index
19%
Similarity by Source

Internet Sources:
    9%
Publications:
    15%
Student Papers:
    6%

sources:

1   1% match (student papers from 29-Jun-2016)
Submitted to Higher Education Commission Pakistan on 2016-06-29

2   1% match (Asmat Ullah, Muhammad Umair, Dost Muhammad, Muhammad Bilal, Kwanghyuk Lee, Suzanne M Leal, Wasim Ahmad. " A novel homozygous variant in underlies acromesomelic dysplasia Hunter-Thompson type ", Annals of Human Genetics, 2018)
Asmat Ullah, Muhammad Umair, Dost Muhammad, Muhammad Bilal, Kwanghyuk Lee, Suzanne M Leal, Wasim Ahmad. " A novel homozygous variant in underlies acromesomelic dysplasia Hunter-Thompson type ", Annals of Human Genetics, 2018

3   < 1% match (student papers from 15-Jul-2023)
Submitted to Higher Education Commission Pakistan on 2023-07-15

4   < 1% match (student papers from 22-Mar-2024)
Submitted to Higher Education Commission Pakistan on 2024-03-22

5   < 1% match (student papers from 07-Jan-2013)
Submitted to Higher Education Commission Pakistan on 2013-01-07

6   < 1% match (student papers from 29-May-2013)
Submitted to Higher Education Commission Pakistan on 2013-05-29

7   < 1% match (student papers from 04-Jul-2012)
Submitted to Higher Education Commission Pakistan on 2012-07-04

8   < 1% match (student papers from 06-Apr-2015)
Submitted to Higher Education Commission Pakistan on 2015-04-06

9   < 1% match (student papers from 04-Oct-2012)
Submitted to Higher Education Commission Pakistan on 2012-10-04